LMH Laboratory for Hydraulic Machines

ÉCOLE POLYTECHNIQUE FÉDÉRALE DE LAUSANNE

MECHANICAL ENGINEERING
MASTER COURSE
HYDRAULIC TURBOMACHINES

HANDOUT

Prof. François AVELLAN, Dr. Eng.

Lausanne, October 2017

(This page intentionally left blank)

CONTENTS

I GLOSSARY

1 LIST OF SYMBOLS

1.1 Latin

Symbol	Unit (SI)	Definition
$\vec{e}_i$	$(-)$	i^{th} unit vector of the Cartesian system of coordinates
f	(Hz)	Frequency
g	$(\text{m}\cdot\text{s}^{-2})$	Gravity acceleration
k	$(-)$	Velocity profile shape factor
k	(m)	Roughness
$\vec{n}$	$(-)$	Normal unit vector
n	(s^{-1})	Rotating frequency
N	(min^{-1})	Rotating frequency per minute
p	(Pa)	pressure
t	(s)	Time
z	$(-)$	Number of machine components e.g. stay vanes, guide vanes, runner blades, stages, poles, unit etc.
A	(m^2)	Fluid Cross Section Area
A	$(-)$	Churchill formula coefficient
B	(m)	Span, channel height or vent opening
B	$(-)$	Churchill formula coefficient
$\vec{C}$	$(\text{m}\cdot\text{s}^{-1})$	Absolute flow velocity
Cu	$(\text{m}\cdot\text{s}^{-1})$	Tangential absolute flow velocity component
Cm	$(\text{m}\cdot\text{s}^{-1})$	Meridional absolute flow velocity component
D	(m)	Runner/impeller reference diameter
$\overline{\overline{D}}$	(s^{-1})	Strain rate tensor

Symbol	**Unit (SI)**	**Definition**
E	$\left(\mathrm{J}\cdot\mathrm{kg}^{-1}\right)$	Machine specific energy
H	(m)	Head
$\overline{\overline{I}}$	$(-)$	Unit tensor
K	$(-)$	Specific energy loss coefficient
L	(m)	Length
P	(W)	Power
$\overline{\overline{P}}$	(Pa)	Total stress tensor
Q	$\left(\mathrm{m}^3\cdot\mathrm{s}^{-1}\right)$	Discharge
$\vec{R}^0$	$(-)$	Radial unit vector of the cylindrical frame of reference
R	(m)	Radial cylindrical coordinate
R	(m)	Runner/impeller reference radius
$\vec{T}$	$(\mathrm{N}\cdot\mathrm{m})$	Resulting moment of forces
$\vec{U}$	$\left(\mathrm{m}\cdot\mathrm{s}^{-1}\right)$	Rotating velocity
V	$\left(\mathrm{m}^3\right)$	Volume
$\vec{W}$	$\left(\mathrm{m}\cdot\mathrm{s}^{-1}\right)$	Relative velocity
$\vec{X}$	(m)	Position vector
Z	(m)	Axial cylindrical coordinate
$\vec{Z}^0$	$(-)$	Axial unit vector of the cylindrical frame of reference
Z	(m)	Elevation
gH	$\left(\mathrm{J}\cdot\mathrm{kg}^{-1}\right)$	Specific energy of a fluid section
$NPSE$	$\left(\mathrm{J}\cdot\mathrm{kg}^{-1}\right)$	Net positive suction specific energy
$NPSH$	(m)	Net positive suction head

1.2 Greek

Symbol	Unit (SI)	Definition
α	$(-)$	Absolute flow angle
α	$(-)$	Exponent
β	$(-)$	Relative flow angle
β	$(-)$	Exponent
γ	$(\mathrm{N}\cdot\mathrm{m}^{-1})$	Surface tension
γ	$(-)$	Exponent
η	$(-)$	Efficiency
θ	$(-)$	Angular cylindrical coordinate
$\vec{\theta}^0$	$(-)$	Tangential unit vector of the cylindrical frame of reference
λ	$(-)$	Local coefficient of regular specific energy losses
μ	$(\mathrm{Pa}\cdot\mathrm{s})$	Dynamic viscosity
ν	$(\mathrm{m}^2\cdot\mathrm{s}^{-1})$	Kinematic viscosity
ρ	$(\mathrm{kg}\cdot\mathrm{m}^{-3})$	Mass Density
$\overline{\overline{\tau}}$	(Pa)	Stress tensor
ω	(s^{-1})	Angular speed
Π	$(\mathrm{Watt}\cdot\mathrm{kg}^{-1})$	Turbulence specific energy production rate
Φ	$(\mathrm{Watt}\cdot\mathrm{kg}^{-1})$	Viscous specific energy dissipation rate
Σ	(m^2)	Material surface area

1.3 Mathematical Operators

Symbol	Definition
$D\circ$	Material derivative operator
$\partial\circ$	Partial derivative operator
$\partial\circ$	Boundary of a set in topology, e.g. ∂V is the closed boundary area of the volume V
$\vec{\nabla}\circ$	Nabla operator
$\cdot$	Scalar product
$\times$	Cross product
$\tilde{\circ}$	Instantaneous components in the Reynolds decomposition of turbulent flow variables
$\circ'$	Fluctuating components in the Reynolds decomposition of turbulent flow variables
$\overline{\circ}$	Averaging operator in the Reynolds decomposition of turbulent flow variables
$\vec{\circ}$	Vector
$\overline{\overline{\circ}}$	Tensor

2 DIMENSIONLESS NUMBERS

2.1 Flow Coefficients

The flow velocity C_{ref} at a given reference location is used as reference velocity to define the flow coefficients listed in the table hereafter. Both reference diameter D and length L are used.

Symbol	Definition
$C_p = \dfrac{p - p_{ref}}{\dfrac{C_{ref}^2}{2}}$	Pressure coefficient with respect to reference conditions
$Fr = \dfrac{C}{\sqrt{2gL}}$	Froude number
$Re = \dfrac{C \times D}{\nu}$	Reynolds number
$We = \sqrt{\dfrac{\rho L C^2}{2\gamma}}$	Weber Number
$\lambda = \dfrac{gH_r}{\dfrac{L}{D} \times \dfrac{C^2}{2}}$	Local Energy Loss Coefficient
$\sigma = \dfrac{p_{ref} - p_v}{\rho \dfrac{C_{ref}^2}{2}}$	Cavitation coefficient with respect to reference conditions

2.2 Hydraulic Machine Coefficients

The rotation velocity $U = \pi n D$ at a given reference diameter D is used as reference velocity to define the machine coefficients listed in the table hereafter.

Symbol	Definition	Factor conversion to coefficient
$\varphi = \dfrac{Q}{A \times U} = \dfrac{4}{\pi^2} \times \dfrac{Q}{nD^3}$	Discharge coefficient	$\varphi = \dfrac{k_{Cm}}{k_U}$
$\psi = \dfrac{E}{\dfrac{U^2}{2}} = \dfrac{2}{\pi^2} \times \dfrac{E}{n^2 D^2}$	Specific energy coefficient	$\psi = \dfrac{1}{k_U^2}$

Symbol	**Definition**	**Factor conversion to coefficient**
$\nu = 2^{\frac{1}{4}}\pi^{\frac{1}{2}} \times n \times \frac{Q^{\frac{1}{2}}}{E^{\frac{3}{4}}}$	Specific speed	$\nu = \frac{\varphi^{\frac{1}{2}}}{\psi^{\frac{3}{4}}} = k_U \times \sqrt{k_{Cm}}$
$\nu_o = \frac{\nu}{z_o^{\frac{1}{2}}}$	Pelton Injector Specific Speed	
$\nu_s = z_s^{\frac{3}{4}} \times \nu$	Stage specific speed	
$\tau = \frac{2T_m}{\rho \times \frac{A \times U^3}{2\pi n}} = \frac{16}{\pi^3} \times \frac{T_m}{\rho n^2 D^5} = \eta_m \times \varphi \times \psi$	Torque coefficient	$\tau = \frac{k_T}{k_U^2} = \eta_m \times \frac{k_{Cm}}{k_U^3}$
$\lambda = \frac{2P_m}{\rho \times A \times U^3} = \frac{8}{\pi^4} \times \frac{P_m}{\rho n^3 D^5} = \eta_m \times \varphi \times \psi$	Power coefficient	$\lambda = \frac{k_P}{k_U^3} = \eta_m \times \frac{k_{Cm}}{k_U^3}$
$Re = \frac{U \times D}{\nu} = \frac{\pi n D^2}{\nu}$	Reynolds number	
$Cp_U = \frac{p - p_{ref}}{\rho \frac{U^2}{2}} = \frac{2 \times \left(p - p_{ref}\right)}{\rho \pi^2 n^2 D^2}$	Static pressure coefficient with respect to reference pressure	$Cp_U = \frac{Cp_E}{k_U^2}$
$\chi_U = \frac{p_{ref} - p_v}{\rho \frac{U^2}{2}} = \frac{2 \times \left(p_{ref} - p_v\right)}{\rho \pi^2 n^2 D^2}$	Local reference cavitation coefficient	$\chi_U = \frac{\chi_E}{k_U^2}$
$\psi_c = \frac{NPSE}{\frac{U^2}{2}} = \frac{2}{\pi^2} \times \frac{NPSE}{n^2 D^2}$	Cavitation coefficient	$\psi_c = \frac{\sigma}{k_U^2}$

2.3 Hydraulic Machine Factors

The specific energy E and machine runner/impeller diameter reference E are used to define the machine factors listed in the table hereafter.

Symbol	**Definition**	**Factor conversion to coefficient**
$Fr = \sqrt{\frac{E}{gD}} = \sqrt{\frac{H}{D}}$	Froude number	
$k_{Cm} = \frac{Q}{A \times \sqrt{2E}} = \frac{4 \times Q}{\pi D^2 \sqrt{2E}}$	Discharge factor	$k_{Cm} = \frac{\varphi}{\sqrt{\psi}}$

Symbol	Definition	Factor conversion to coefficient
$k_u = \frac{U}{\sqrt{2E}}$	Speed factor	$k_u = \frac{1}{\sqrt{\psi}}$
$\nu = k_U \sqrt{k_{Cm}}$	Specific speed	$\nu = \frac{\varphi^{\frac{1}{2}}}{\psi^{\frac{3}{4}}}$
$k_T = \frac{8}{\pi} \frac{T_m}{\rho D^3 E}$	Torque factor	$k_T = \frac{\tau}{\psi}$
$k_P = \frac{8}{\pi} \frac{P_m}{\rho D^2 (2E)^{\frac{3}{2}}}$	Power factor	$k_P = \frac{\lambda}{\psi^{\frac{3}{2}}}$
$\sigma = \frac{NPSE}{E}$	Thoma number	$\sigma = \frac{\psi_c}{\psi}$
$\chi_E = \frac{p_{ref} - p_v}{\rho E}$	Local reference cavitation factor	$\chi_E = \frac{\chi_U}{\psi}$
$Cp_E = \frac{p - p_{ref}}{\rho E}$	Static pressure factor with respect to reference pressure	$Cp_E = \frac{Cp_U}{\psi}$

2.4 IEC Hydraulic Machine Coefficients

The IEC Technical Committee 4 defines in (IEC, 1999) international standard the hydraulic machine coefficients listed in the table hereafter:

Symbol	Definition	Factor conversion to coefficient
$Q_{nD} = \frac{Q}{nD^3}$	IEC discharge coefficient	$Q_{nD} = \frac{Q_{ED}}{n_{ED}}$
$E_{nD} = \frac{E}{n^2 D^2}$	IEC specific energy coefficient.	$E_{nD} = \frac{1}{n_{ED}^2}$
$n_{QE} = n \times \frac{Q^{\frac{1}{2}}}{E^{\frac{3}{4}}} = n \times \frac{Q_{nD}^{\frac{1}{2}}}{E_{nD}^{\frac{3}{4}}}$	IEC Specific Speed	$n_{QE} = n_{ED} \times \sqrt{Q_{ED}}$
$T_{nD} = \frac{T_m}{\rho n^2 D^5}$	IEC torque coefficient	
$P_{nD} = \frac{P_m}{\rho n^3 D^5}$	IEC power coefficient	
$Re = \frac{\pi n D^2}{\nu}$	IEC Reynolds Number	

2.5 IEC Machine Factors

The IEC Technical Committee 4 defines in (IEC, 1999) international standard the hydraulic machine factors listed in the table hereafter:

Symbol	Definition	Factor conversion to coefficient
$n_{ED} = \frac{nD}{\sqrt{E}}$	IEC speed factor	
$Q_{ED} = \frac{Q}{D^2\sqrt{E}}$	IEC discharge factor	
$n_{QE} = n_{ED}\sqrt{Q_{ED}}$	IEC Specific Speed	
$T_{ED} = \frac{T_m}{\rho D^3 E}$	IEC torque factor	
$P_{ED} = \frac{P_m}{\rho D^2 E^{1.5}}$	IEC power factor	
$\sigma = \frac{NPSE}{E}$	Thoma number	$\sigma = \frac{\psi_c}{\psi}$
$Fr = \sqrt{\frac{E}{gD}} = \sqrt{\frac{H}{D}}$	Froude number	

2.6 Customary Unit Factors

Customary *"Unit Factors"* are <u>not</u> dimensionless and, therefore, depend on the choice of units. This is why they are called *"unit"* factors, meaning, for instance, that n_{11} is the speed value expressed in min^{-1} of a runner featuring a diameter of 1 unit under a head of 1 unit. Throughout the document the International System of Units, SI units and their derived units, are used, (Bureau International des Poids et Mesures, 2006), (Thompson and Taylor, 2008).

Symbol	Unit*)	Definition
$n_{11} = \frac{ND}{\sqrt{H}}$	(SI)	Unit speed factor
$Q_{11} = \frac{Q}{D^2\sqrt{H}}$	(SI)	Unit discharge factor
$n_q = N\frac{Q^{\frac{1}{2}}}{H^{\frac{3}{4}}}$	(SI)	Unit specific speed

Symbol	Unit*)	Definition
$n_q = n_{11}\sqrt{Q_{11}}$	(SI)	-id-
$n_{qs} = z_s^{\frac{3}{4}} \times n_q$	(SI)	Stage unit specific speed
$T_{11} = \dfrac{T}{D^3\sqrt{H}}$	(SI)	Unit torque factor
$P_{11} = \dfrac{P}{D^2 H^{3/2}}$	(SI)	Unit power factor
$n_s = N\dfrac{P^{\frac{1}{2}}}{H^{\frac{5}{4}}}$	(SI)	Unit specific speed based on power P
$n_{ss} = z_s^{\frac{5}{4}} \times n_s$	(SI)	Stage unit specific speed based on power P

*) *the following units are used* $D\ (\mathrm{m})$, $H\ (\mathrm{m})$, $N\ \left(\mathrm{min}^{-1}\right)$, $P\ (\mathrm{kW})$, $Q\ \left(\mathrm{m}^3 \cdot \mathrm{s}^{-1}\right)$.

3 SUBSCRIPTS

3.1 Installation Reference Sections and Components

Symbol	Definition[1]
$_{grid}$	Grid
$_{unit}$	Power units
$_{B}$	Headwater reservoir free surface
$_{A}$	Headwater intake/outlet reference section
$_{I}$	Machine high specific energy reference section
$_{\bar{I}}$	Machine unit low specific energy reference section
$_{\bar{A}}$	Tailwater outlet/intake reference section
$_{\bar{B}}$	Tailwater reservoir free surface section

[1] *See Figure 19*

3.2 Machine Reference Sections and Components

Symbol	Definition[2]
p	Poles of the synchronous machine
s	Stage of the hydraulic machine
sc	Spiral case
5	Stay vanes cascade high specific energy reference section
v	Stay vanes
4	Stay vanes cascade low specific energy reference section
3	Guide vanes cascade high specific energy reference section
o	Guide vanes cascade
2	Guide vanes cascade low specific energy reference section
1	Runner high specific energy reference section
b	Runner/impeller including blades, hub and band
e	Outer, external streamline
i	Inner, internal streamline
$\bar{1}$	Runner low specific energy reference section
$\bar{2}$	Draft tube cone high specific energy reference section
d	Draft tube

3.3 Miscellaneous

Symbol	Definition
e	Energy
i	Incipient cavitation
i	i^{th} component of the Cartesian coordinate system
j	j^{th} component of the Cartesian coordinate system
h	Hydraulic
m	Mechanical

[2] *See Figure 20*

Symbol	Definition
$_{opt}$	Optimum
$_{q}$	Volumetric
$_{r}$	Losses
$_{ref}$	Reference
$_{runaway}$	Runaway
$_{s}$	Sand
$_{t}$	Transformed
$_{t}$	Turbulent
$_{v}$	Singular losses
$_{v}$	Vapor
$_{0}$	Initial value
$_{0}$	Swirl free operating condition

4 SUPERSCRIPTS

Symbol	Definition
^{BEP}	Best efficiency operating point
^{M}	Reduced scale
^{P}	Prototype scale
^{P}	Pumping operating mode
^{T}	Generating operating mode
$^{\wedge}$	Peak efficiency operating point

5 ACRONYMS

Acronym	Definition
BEP	Best Efficiency Point
BIPM	Bureau international des poids et mesures
BPF	Blade Passing Frequency
EPFL	Ecole polytechnique fédérale de Lausanne
IEC	International Electrotechnical Commission
LMH	Laboratory for Hydraulic Machine
NIST	National Institute of Standards
RANS	Reynolds-Averaged Navier-Stokes

II FLUID MECHANICS

1 EQUATIONS OF FLOW MOTION

1.1 Navier-Stokes Equations

The fluid is considered incompressible with a constant temperature and viscosity. The instantaneous values of absolute pressure $\tilde{p}$ and absolute velocity $\vec{\tilde{C}}$ are driven by the continuity equation for incompressible flows (Panton, 2013), (White, 2009),

$$\vec{\nabla} \cdot \vec{\tilde{C}} = 0$$

and the linear momentum balance equation

$$\frac{\partial \vec{\tilde{C}}}{\partial t} + \left(\vec{\tilde{C}} \cdot \vec{\nabla}\right)\vec{\tilde{C}} = -\vec{\nabla}\left(\frac{\tilde{p}}{\rho} + gZ\right) + \vec{\nabla} \cdot \left(2\nu \overline{\overline{\tilde{D}}}\right)$$

where t is the time, ν the kinematic viscosity and $\overline{\overline{\tilde{D}}}$ the instantaneous strain rate tensor defined as the symmetric tensor of $\vec{\nabla} \otimes \vec{\tilde{C}}$ the velocity gradient tensor

$$\overline{\overline{\tilde{D}}} = \frac{1}{2}\left[\left(\vec{\nabla} \otimes \vec{\tilde{C}}\right) + \left(\vec{\nabla} \otimes \vec{\tilde{C}}\right)^T\right]$$

or in tensor notations

$$\tilde{D}_{ij} = \frac{1}{2}\left[\frac{\partial \tilde{C}_j}{\partial X_i} + \frac{\partial \tilde{C}_i}{\partial X_j}\right]$$

1.2 Reynolds-Averaged Navier-Stokes Equations

The Reynolds-Averaged Navier-Stokes (RANS) equations (Tennekes and Lumley, 1972) are derived from the instantaneous Navier-Stokes equations according to the Reynolds-Averaged decomposition of the instantaneous turbulent quantities into mean and fluctuating parts, see Figure 1.

$$\vec{\tilde{C}} = \vec{C} + \vec{c}' \quad \text{and} \quad \tilde{p} = p + p'$$

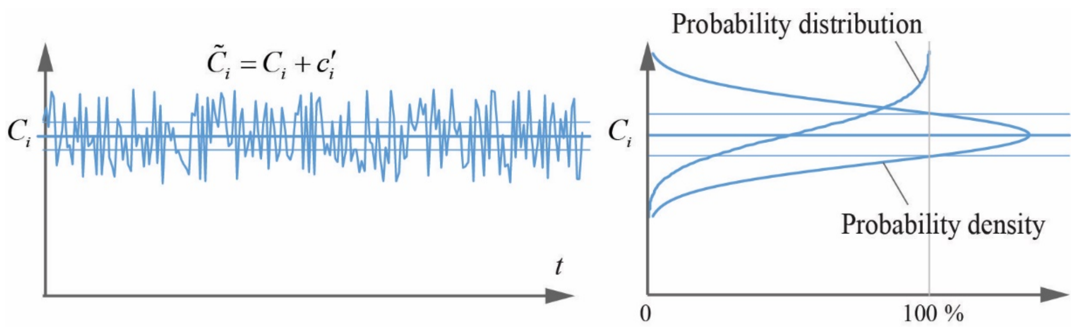

Figure 1 – Time history and statistics of a component of the turbulent velocity

The Reynolds average operator $\overline{\circ}$ is a linear operator applied to both $\tilde{\vec{C}}$ and $\tilde{p}$, instantaneous velocity and pressure fields yields, respectively.

$$\begin{aligned} &\overline{\tilde{\vec{C}}} = \vec{C} \quad \text{and} \quad \overline{\vec{c}'} = 0 \\ &\overline{\tilde{p}} = p \ \text{ and } \ \overline{p'} = 0 \end{aligned} \tag{1}$$

RANS equations are obtained by applying the Reynolds average operator to the Navier-Stokes equations reading:

$$\vec{\nabla} \cdot \vec{C} = 0 \tag{2}$$

for the continuity equation of the incompressible mean flows and

$$\frac{\partial \vec{C}}{\partial t} + \left(\vec{C} \cdot \vec{\nabla}\right)\vec{C} = -\vec{\nabla}\left(\frac{p}{\rho} + gZ\right) + \vec{\nabla} \cdot \left(2\nu \overline{\overline{D}} + \frac{\overline{\overline{\tau}}_t}{\rho}\right) \tag{3}$$

for the axial momentum balance equation of the viscous incompressible mean flows

where $\overline{\overline{\tau}}_t$ is the symmetric turbulent stress tensor defined by

$$\overline{\overline{\tau}}_t = -\rho\left(\overline{\vec{c}' \otimes \vec{c}'}\right)$$

Then, the equations driving the fluctuating motion are obtained by substituting the average components from the Navier Stokes equations:

$$\vec{\nabla} \cdot \vec{c}' = 0,$$

for the incompressibility condition and

$$\frac{\partial \vec{c}'}{\partial t} + \left(\vec{c}' \cdot \vec{\nabla}\right)\vec{c}' = -\vec{\nabla}\left(\frac{p'}{\rho}\right) + \vec{\nabla} \cdot \left(2\nu \overline{\overline{d'}}\right) + \vec{\nabla} \cdot \left(\frac{\overline{\overline{\tau}}_t}{\rho}\right) - \left(\vec{C} \cdot \vec{\nabla}\right)\vec{c}' - \left(\vec{c}' \cdot \vec{\nabla}\right)\vec{C} \tag{4}$$

for the axial fluctuating momentum.

The fluctuating motion can be considered as incompressible but momentum advection non-linearity yields three additional terms to the axial momentum equation (4).

2 MEAN DISCHARGE

2.1 Incompressible Mean Flow Continuity

The continuity equation for the incompressible mean flow reads

$$\frac{-1}{\rho}\frac{D\rho}{Dt} = \vec{\nabla} \cdot \vec{C} = 0 \tag{5}$$

where $\vec{C}$ is the absolute mean flow velocity.

Therefore, the mean mass balance for any volume V of fluid is performed by integrating the continuity equation (5) in volume V.

$$\int_V \vec{\nabla} \cdot \vec{C}\, dV = 0 \tag{6}$$

Therefore, divergence theorem applied to the volume integral yields

$$\int_{\partial V} \vec{C} \cdot \vec{n} dA = 0 \tag{7}$$

where $\vec{n}$ is the normal vector to ∂V, the closing area of the volume V, outward oriented, dA being the elementary area of ∂V.

2.2 Mean Discharge Conservation

For the flow bounded by a pipe, $\partial V = A_1 \cup \Sigma \cup A_2$ the surface boundary of the volume V is including 2 fluid sections, A_1, A_2 respectively and Σ, the pipe inner wall surface.

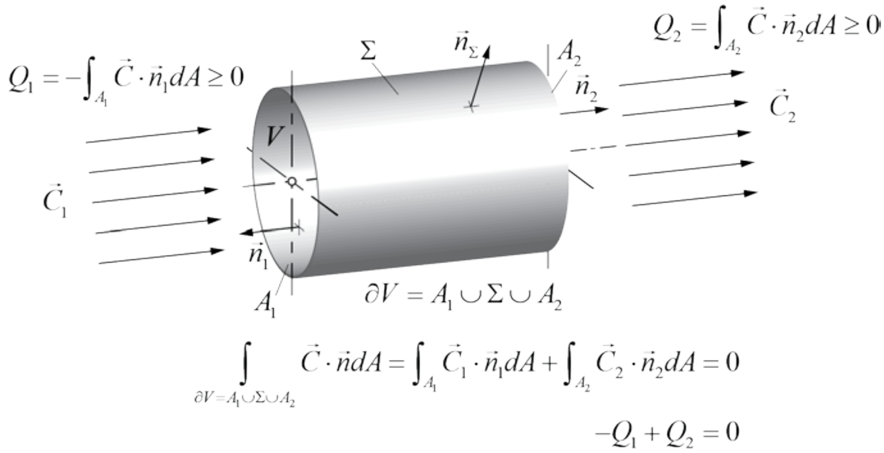

Figure 2 - Discharge balance for a pipe

Therefore, the flow balance (7) applied to V, the pipe control volume, yields:

$$\int_{\partial V = A_1 \cup \Sigma \cup A_2} \vec{C} \cdot \vec{n} dA = \int_{A_1} \vec{C}_1 \cdot \vec{n}_1 dA + \int_{\Sigma} \underbrace{\vec{C} \cdot \vec{n}_\Sigma}_{=0} d\Sigma + \int_{A_2} \vec{C}_2 \cdot \vec{n}_2 dA \tag{8)(9}$$

By assuming that Σ, the pipe inner wall, is a material surface, the kinematic condition $\vec{C} \cdot \vec{n}_\Sigma = 0$ hold on Σ therefore (9) is reduced to.

$$\int_{\partial V = A_1 \cup \Sigma \cup A_2} \vec{C} \cdot \vec{n} dA = \underbrace{\int_{A_1} \vec{C}_1 \cdot \vec{n}_1 dA}_{-Q_1} + \underbrace{\int_{A_2} \vec{C}_2 \cdot \vec{n}_2 dA}_{+Q_2} = 0$$

The mean discharge Q is defined as a positive value

$$Q_1 = -\int_{A_1} \vec{C} \cdot \vec{n}_1 dA \geq 0 \text{ and } Q_2 = \int_{A_2} \vec{C} \cdot \vec{n}_2 dA \geq 0 \qquad \left(\mathrm{m}^3 \cdot \mathrm{s}^{-1}\right) \tag{10}$$

and so, the discharge balance yields

$$\int_{A_2} \vec{C} \cdot \vec{n}_2 dA = -\int_{A_1} \vec{C} \cdot \vec{n}_1 dA = Q > 0 \tag{11}$$

2.3 Discharge Velocity

The discharge velocity for the given section 2 is defined as

$$C_2 = \frac{Q}{A_2} = \frac{1}{A_2} \int_{A_2} \vec{C} \cdot \vec{n} dA \qquad \left(\mathrm{m} \cdot \mathrm{s}^{-1}\right) \tag{12}$$

Consequently, the discharge balance between sections 1 and 2 reads

$$C_1 A_1 = C_2 A_2 = Q$$

Or alternatively

$$C_2 = \frac{A_1}{A_2} C_1 = \frac{Q}{A_2} \qquad (13)$$

In the case of an accelerating flow in a convergent pipe the mean discharge velocity is increasing and is close to the reduced fluid cross section velocity field. However, in the case of a diffuser flow, the flow may experience a flow separation and the velocity field is departing a uniform flow distribution, see Figure 3.

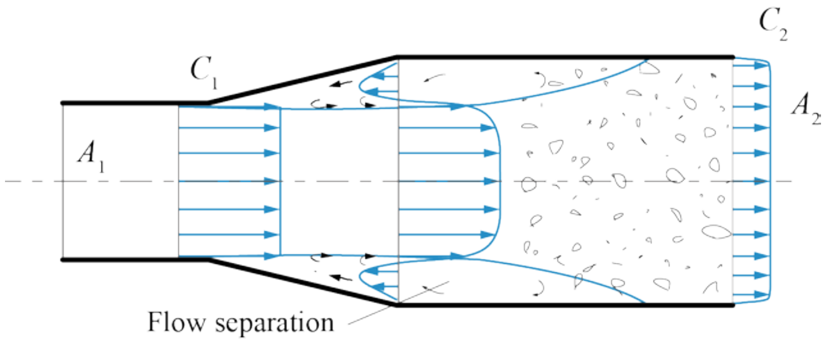

Figure 3 – Flow separation experienced by a diffuser.

2.4 Combining or Dividing T Junctions

In the case of a dividing "T" junctions, the discharge Q_1 of the flow at the inlet section A_1 is balanced between the discharge Q_2 and the discharge Q_3 at the 2 outlet sections A_2 and A_3, respectively, see Figure 4.

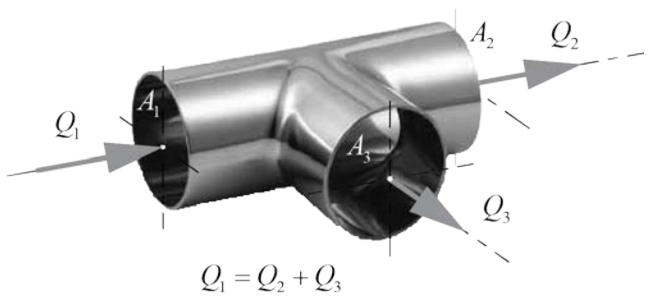

Figure 4 – Tri-junction discharge balance

Therefore, the discharge budget between the 3 sections yields

$$Q_1 = Q_2 + Q_3 \qquad \left(\mathrm{m^3 \cdot s^{-1}}\right) \quad (14)$$

Or by introducing the corresponding discharge velocities

$$C_1 = \frac{A_2}{A_1} C_2 + \frac{A_3}{A_1} C_3 \qquad \left(\mathrm{m \cdot s^{-1}}\right) \quad (15)$$

3 MEAN FLOW SPECIFIC ENERGY

3.1 Local Mean Flow Specific Kinetic Energy

If the total stress tensor $\overline{\overline{P}}$ is defined as:

$$\overline{\overline{P}} = -\left(p + \rho g Z\right)\overline{\overline{I}} + 2\mu\overline{\overline{D}} + \overline{\overline{\tau}}_t \tag{16}$$

the RANS linear momentum balance equation (3) can be cast in a compact form as

$$\frac{D\vec{C}}{Dt} = \vec{\nabla}\cdot\frac{\overline{\overline{P}}}{\rho} \tag{17}$$

Therefore, by applying the $\vec{C}$ scalar product to the RANS linear momentum balance equation (17) yields the local equation of the specific kinetic energy balance.

$$\vec{C}\cdot\frac{D\vec{C}}{Dt} = \frac{D}{Dt}\frac{\vec{C}^2}{2} \qquad \left(\mathrm{W}\cdot\mathrm{kg}^{-1}\right) \tag{18}$$

and, then (18) reads,

$$\frac{D}{Dt}\frac{\vec{C}^2}{2} = \vec{C}\cdot\left[\vec{\nabla}\cdot\frac{\overline{\overline{P}}}{\rho}\right] \qquad \left(\mathrm{W}\cdot\mathrm{kg}^{-1}\right) \tag{19}$$

According to the rule of product derivatives, (Aris, 1989), the right hand side of (19) can be written in tensor notations

$$\frac{\partial P_{ij}}{\partial X_j}C_i = \frac{\partial P_{ij}C_i}{\partial X_j} - P_{ij}\frac{\partial C_i}{\partial X_j} \tag{20}$$

Since $\overline{\overline{P}}$ is a symmetrical tensor, p Owing the symmetry properties of $\overline{\overline{P}}$, transposition of the scalar equation (20) yields

$$-P_{ij}\frac{\partial C_i}{\partial X_j} = -P_{ji}\frac{\partial C_j}{\partial X_i} = -P_{ij}\frac{\partial C_j}{\partial X_i} = -P_{ij}\underbrace{\frac{1}{2}\left(\frac{\partial C_j}{\partial X_i} + \frac{\partial C_j}{\partial X_i}\right)}_{=D_{ij}} \tag{21}$$

Then, the time change of the specific kinetic energy can be expressed as the sum of external, divergence term, and internal contributions

$$\underbrace{\frac{D}{Dt}\left(\frac{\vec{C}^2}{2}\right)}_{\text{Change of the specific kinetic energy}} = \underbrace{\vec{\nabla}\cdot\left(\frac{\overline{\overline{P}}}{\rho}\cdot\vec{C}\right)}_{\text{External contribution}} - \underbrace{\left(\overline{\overline{D}}:\frac{\overline{\overline{P}}}{\rho}\right)}_{\text{Internal contribution}} \qquad \left(\mathrm{W}\cdot\mathrm{kg}^{-1}\right) \tag{22}$$

Substituting (16), definition of $\overline{\overline{P}}$, into (22) yields

$$\frac{\partial}{\partial t}\frac{\vec{C}^2}{2} + \underbrace{\vec{\nabla}\cdot\left[\left\{\frac{p}{\rho} + gZ + \frac{\vec{C}^2}{2}\right\}\vec{C}\right]}_{\text{Flux of specific hydraulic energy}} = \underbrace{\vec{\nabla}\cdot\left[\left\{2\nu\overline{\overline{D}} + \frac{\overline{\overline{\tau}}_t}{\rho}\right\}\cdot\vec{C}\right]}_{\text{Net specific power of both viscous and turbulent stresses}} - \left(\frac{p}{\rho} + gZ\right)\underbrace{\overline{\overline{I}}:\overline{\overline{D}}}_{=\vec{\nabla}\cdot\vec{C}=0} \qquad \left(\mathrm{W}\cdot\mathrm{kg}^{-1}\right) \tag{23}$$

$$- \underbrace{2\nu\overline{\overline{D}}:\overline{\overline{D}}}_{\Phi:\ \text{viscous dissipation rate}} - \underbrace{\frac{1}{\rho}\overline{\overline{\tau}}_t:\overline{\overline{D}}}_{\Pi:\ \text{turbulence production rate}}$$

where the flux of mean flow specific hydraulic energy has been made apparent.

However, the following identity stands $\overline{\overline{I}} : \overline{\overline{D}} = \vec{\nabla} \cdot \vec{C}$ which can be easily derived by using tensor components $\delta_{ij} D_{ij} = D_{ii}$. Therefore, the flow being assumed incompressible, it can be concluded that the pressure does not contribute to internal power dissipation.

For simplification, the rates of viscous specific dissipation Φ and specific production of turbulence Π are defined

$$\Phi = 2\nu \overline{\overline{D}} : \overline{\overline{D}} \text{ and } \Pi = \frac{1}{\rho} \overline{\overline{\tau_t}} : \overline{\overline{D}} \qquad \left(\mathrm{W \cdot kg^{-1}}\right) \qquad (24)$$

With the use of tensor notations the viscous specific energy dissipation rate Φ reads

$$\begin{aligned} \Phi &= 2\nu \overline{\overline{D}} : \overline{\overline{D}} = 2\nu D_{ij} D_{ij} \\ &= 2\nu \left[\left(\frac{\partial C_1}{\partial X_1} \right)^2 + \left(\frac{\partial C_2}{\partial X_2} \right)^2 + \left(\frac{\partial C_3}{\partial X_3} \right)^2 \right] \\ &+ \nu \left[\left(\frac{\partial C_1}{\partial X_3} + \frac{\partial C_3}{\partial X_1} \right)^2 + \left(\frac{\partial C_2}{\partial X_1} + \frac{\partial C_1}{\partial X_2} \right)^2 + \left(\frac{\partial C_3}{\partial X_2} + \frac{\partial C_2}{\partial X_3} \right)^2 \right] \end{aligned} \qquad \left(\mathrm{W \cdot kg^{-1}}\right) \qquad (25)$$

and the turbulent specific energy production rate Π reads

$$\begin{aligned} \Pi &= \frac{\overline{\overline{\tau_t}}}{\rho} : \overline{\overline{D}} \\ &= \frac{-\rho}{2} \overline{c'_i c'_j} \left(\frac{\partial C_j}{\partial X_i} + \frac{\partial C_i}{\partial X_j} \right) \end{aligned} \qquad \left(\mathrm{W \cdot kg^{-1}}\right) \qquad (26)$$

Finally (23) reads

$$\frac{\partial}{\partial t} \frac{\vec{C}^2}{2} + \vec{\nabla} \cdot \left[\left\{ \frac{p}{\rho} + gZ + \frac{\vec{C}^2}{2} \right\} \vec{C} \right] = \vec{\nabla} \cdot \left[\left\{ 2\nu \overline{\overline{D}} + \frac{\overline{\overline{\tau_t}}}{\rho} \right\} \cdot \vec{C} \right] - \Phi - \Pi \qquad \left(\mathrm{W \cdot kg^{-1}}\right) \qquad (27)$$

Equation (27) expresses the flux balance of specific total enthalpy aka total specific mechanical energy

$$h_t = \frac{p}{\rho} + gZ + \frac{\vec{C}^2}{2} \qquad \left(\mathrm{W \cdot kg^{-1}}\right)$$

balanced by the time derivative of the specific kinetic energy, the net flux of viscous and turbulent stresses and the viscous dissipation and turbulence production specific power.

3.2 Mean Flow Power Balance

Integration of equation (27) in the inner pipe volume V, see Figure 3, bounded by 2 fluid sections A_1 and A_2 and by the material surface Σ corresponding to the pipe inner wall, yields

$$\begin{aligned} \int_V \frac{\partial}{\partial t} \frac{\vec{C}^2}{2} \rho dV + \int_V \vec{\nabla} \cdot \left[\left\{ \frac{p}{\rho} + gZ + \frac{\vec{C}^2}{2} \right\} \vec{C} \right] \rho dV = \int_V \vec{\nabla} \cdot \left(\left\{ 2\nu \overline{\overline{D}} + \frac{\overline{\overline{\tau_t}}}{\rho} \right\} \cdot \vec{C} \right) \rho dV \\ - \int_V \Phi \rho dV - \int_V \Pi \rho dV \end{aligned} \qquad \left(\mathrm{W}\right) (28)$$

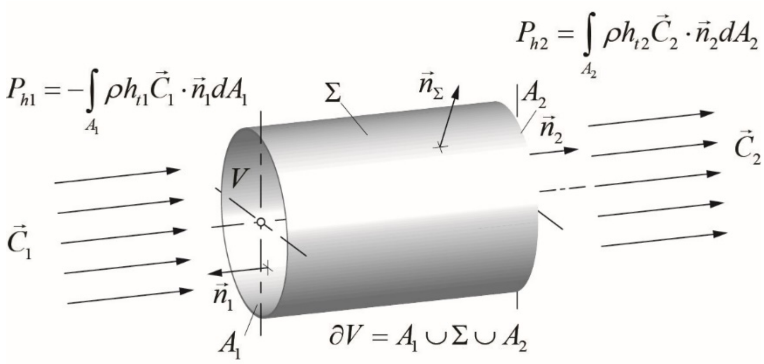

Figure 5 – Hydraulic power balance for a pipe

According to the divergence theorem, (Panton, 2013), (Charle Pusterle, 1991), volume integrals are transferred to surface integrals

$$\int_V \frac{\partial}{\partial t}\frac{\vec C^2}{2}\rho dV + \int_{\partial V}\left\{\frac{p}{\rho}+gZ+\frac{\vec C^2}{2}\right\}\rho\cdot\vec C\cdot\vec n dA = \int_{\partial V}\left[\rho\left\{2\nu\overline{\overline{D}}+\frac{\overline{\overline{\tau}}_t}{\rho}\right\}\cdot\vec C\right]\cdot\vec n dA - \int_V \rho\cdot\Phi dV - \int_V \rho\cdot\Pi dV \qquad (\mathrm{W}) \quad (29)$$

For the material surface Σ corresponding to the pipe inner wall, there is any flow transfer $\vec C\cdot\vec n_\Sigma = 0$ and the viscous wall condition applies $\vec C_\Sigma = 0$, therefore (29) reduces to

$$\underbrace{\int_{A_1\cup A_2}\left\{\frac{p}{\rho}+gZ+\frac{\vec C^2}{2}\right\}\rho\cdot\vec C\cdot\vec n dA}_{\text{Change of hydraulic power}} = -\underbrace{\int_V \rho\cdot\Phi dV}_{\text{Viscous power dissipation}} - \underbrace{\int_V \rho\cdot\Pi dV}_{\text{Production of turbulent power}}$$
$$\underbrace{\int_{A_1\cup A_2}\left[\rho\left\{2\nu\overline{\overline{D}}+\frac{\overline{\overline{\tau}}_t}{\rho}\right\}\cdot\vec C\right]\cdot\vec n dA}_{\text{Net power of viscous and turbulent stresses}} \qquad (\mathrm{W}) \quad (30)$$
$$-\underbrace{\int_V \frac{\partial}{\partial t}\frac{\vec C^2}{2}\rho dV}_{\text{Time change of mean flow kinetic energy}}$$

The change of hydraulic power of the mean flow through the pipe flow volume is due to:

1. power dissipation by both viscosity and turbulent production terms;
2. net power balance of both viscous and turbulent stresses;
3. change with time of mean flow kinetic energy of the control volume.

Therefore, by introducing h_t the glow total specific enthalpy the hydraulic power balance reads

$$\underbrace{-\int_{A_1} h_t\rho\cdot\vec C\cdot\vec n dA}_{A_1\text{ Section mean flow power}} = \underbrace{\int_{A_2}\left\{\frac{p}{\rho}+gZ+\frac{\vec C^2}{2}\right\}\rho\cdot\vec C\cdot\vec n dA}_{A_2\text{ Section mean flow power}}$$
$$+\underbrace{\int_V \rho\cdot\Phi dV}_{\text{Viscous power dissipation}} + \underbrace{\int_V \rho\cdot\Pi dV}_{\text{Production of turbulent power}} \qquad (\mathrm{W}) \quad (31)$$
$$-\underbrace{\int_{A_1\cup A_2}\left[\rho\left\{2\nu\overline{\overline{D}}+\frac{\overline{\overline{\tau}}_t}{\rho}\right\}\cdot\vec C\right]\cdot\vec n dA}_{\text{Net power of viscous and turbulent stresses}} + \underbrace{\int_V \frac{\partial}{\partial t}\frac{\vec C^2}{2}\rho dV}_{\substack{\text{Time change of}\\ \text{mean flow kinetic energy}}}$$

The mean flow power balance (31) for a pipe flow volume V bounded by A_1 and A_2 fluid sections reads:

"The mean flow power entering the pipe by A_1 is the mean flow power leaving the pipe by A_2 added to the power dissipation by both viscosity and turbulent production in the pipe control volume, the net power between A_1 and A_2 of both viscous and turbulent stresses and the time change of mean flow kinetic energy in the pipe control volume.

$$P_{h1} = P_{h2} + \int_V (\Phi + \Pi)\rho \cdot dV - \int_{A_1 \cup A_2} \left[\rho \left\{ 2\nu \overline{\overline{D}} + \frac{\overline{\overline{\tau}}_t}{\rho} \right\} \cdot \vec{C} \right] \cdot \vec{n} dA + \int_V \frac{\partial}{\partial t} \frac{\vec{C}^2}{2} \rho dV \quad (\mathrm{W}) \quad (32)$$

3.3 Mean Flow Power Balance for stationary flow in a long (infinite) pipe

In the case of a stationary flow in a long pipe, it can be assumed that both the average and the turbulent flow fields are homogenous so the distributions of the mean and fluctuating velocities are invariant by translation along the pipe axis which yields

$$\int_{A_1 \cup A_2} \left(\left(2\nu \overline{\overline{D}} + \frac{\overline{\overline{\tau}}_t}{\rho} \right) \cdot \rho \cdot \vec{C} \right) \cdot \vec{n} dA = 0 \, .$$

Therefore, in this case, the power balance (30) is simply expressed as

$$\int_{A_1 \cup A_2} \left(\frac{p}{\rho} + gZ + \frac{\vec{C}^2}{2} \right) \rho \cdot \vec{C} \cdot \vec{n} dA = -\int_V (\Phi + \Pi) \rho dV \quad (33)$$

Or by introducing the power flow of the hydraulic energy in A_1 and A_2 sections, respectively

$$P_{h1} = -\int_{A_1} \left(\frac{p}{\rho} + gZ + \frac{\vec{C}^2}{2} \right) \rho \cdot \vec{C}_1 \cdot \vec{n}_1 dA_1 = -\int_{A_1} \rho h_{t1} \vec{C}_1 \cdot \vec{n}_1 dA_1 \quad (\mathrm{W}) \quad (34)$$

and

$$P_{h2} = \int_{A_2} \left(\frac{p}{\rho} + gZ + \frac{\vec{C}^2}{2} \right) \rho \cdot \vec{C}_2 \cdot \vec{n}_2 dA_2 = \int_{A_2} \rho h_{t2} \vec{C}_2 \cdot \vec{n}_2 dA_2 \quad (\mathrm{W}) \quad (35)$$

the power balance (31) of the mean flow simply reads

$$P_{h1} = P_{h_2} + \int_V \rho (\Phi + \Pi) dV \quad (\mathrm{W}) \quad (36)$$

According to (4), the discharge definition, and since the mass flow $\rho Q_1 = \rho Q_2$ remains constant, the balance of average specific energy between the 2 section A_1 and A_2 can be obtained from

$$\frac{P_{h1}}{\rho Q_1} = gH_1 = gH_2 + gH_{r1 \div 2} \quad (\mathrm{J \cdot kg^{-1}}) \quad (37)$$

by introducing the mean hydraulic specific energy gH_1 and gH_2 for fluid sections A_1 and A_2 respectively

$$gH_1 = -\int_{A_1} \left(\frac{p}{\rho} + gZ + \frac{\vec{C}^2}{2} \right) \frac{\vec{C}_1 \cdot \vec{n}_1 dA_1}{Q} = -\int_{A_1} h_{t1} \times \frac{\vec{C}_1 \cdot \vec{n}_1 dA_1}{Q} \quad (\mathrm{J \cdot kg^{-1}}) \quad (38)$$

and

$$gH_2 = \int_{A_2} \left(\frac{p}{\rho} + gZ + \frac{\vec{C}^2}{2} \right) \frac{\vec{C}_2 \cdot \vec{n}_2 dA_2}{Q} = \int_{A_2} h_{t2} \frac{\vec{C}_2 \cdot \vec{n}_2 dA_2}{Q} \qquad \left(\mathrm{J \cdot kg^{-1}}\right) \qquad (39)$$

Therefore, both viscous dissipation and turbulence production yield the specific energy losses $gH_{r1\div2}$ in the fluid volume V .

$$gH_{r1\div2} = \int_V (\Phi + \Pi) \frac{dV}{Q} = \frac{1}{Q} \int_V \left(2\nu \overline{\overline{D}}^2 + \overline{\overline{D}} : \frac{\overline{\overline{\tau}}_t}{\rho} \right) dV \qquad \left(\mathrm{J \cdot kg^{-1}}\right) \qquad (40)$$

3.4 Specific Energy Balance

In the general case, the flow cannot be considered homogenous, e.g. in a diffuser and/or an elbow, and the flow unsteadiness cannot be neglected, therefore the specific budget for the average specific hydraulic energy in a flow volume V of pipe limited by fluid sections A_1 and A_2 , see respectively reads

$$-\int_{A_1} h_{t1} \times \frac{\vec{C}_1 \cdot \vec{n}_1 dA_1}{Q} = \int_{A_2} h_{t2} \times \frac{\vec{C}_2 \cdot \vec{n}_2 dA_2}{Q} + \underbrace{\frac{1}{Q} \int_V (\Phi + \Pi) dV}_{\substack{\text{Specific Energy Loss} \\ \text{by Viscous Dissipation} \\ \text{and Turbulence Production}}}$$

$$+ \underbrace{\frac{1}{Q} \int_V \frac{\partial}{\partial t} \frac{\vec{C}^2}{2} dV}_{\substack{\text{Change of Flow Volume} \\ \text{Specific Kinetic Energy}}} \underbrace{- \frac{1}{Q} \int_{A_1 \cup A_2} \left[\left\{ 2\nu \overline{\overline{D}} + \frac{\overline{\overline{\tau}}_t}{\rho} \right\} \cdot \vec{C} \right] \cdot \vec{n} dA}_{\substack{\text{Net Specific Energy Flux of Viscous} \\ \text{and Turbulent Stresses}}} \qquad \left(\mathrm{J \cdot kg^{-1}}\right) \qquad (41)$$

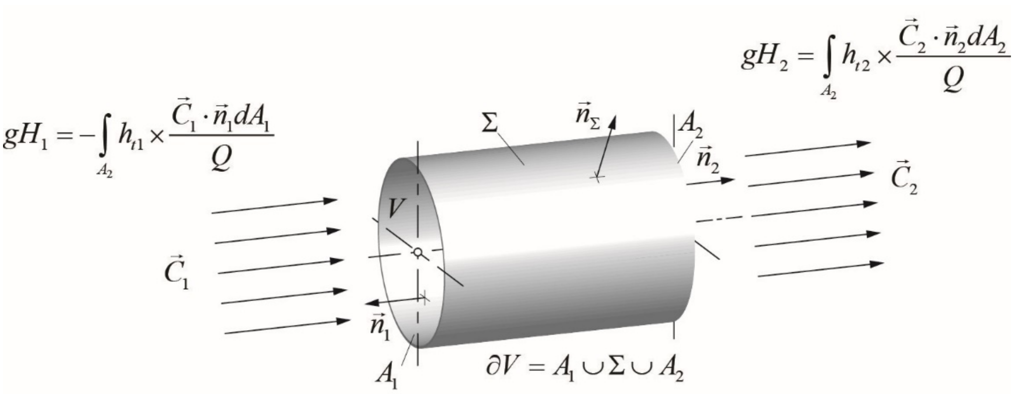

Figure 6 – Specific hydraulic energy balance

With the definition (39) for the mean hydraulic specific energy gH_1 and gH_2 for fluid sections A_1 and A_2 , respectively and the relation (40) for the specific energy loss $gH_{r1\div2}$ between fluid sections A_1 and A_2 the specific energy budget reads

$$gH_1 = gH_2 + gH_{r1\div2} \underbrace{- \frac{1}{Q} \int_{A_1 \cup A_2} \left[\left\{ 2\nu \overline{\overline{D}} + \frac{\overline{\overline{\tau}}_t}{\rho} \right\} \cdot \vec{C} \right] \cdot \vec{n} dA}_{\substack{\text{Net Specific Energy Flux of Viscous} \\ \text{and Turbulent Stresses}}} + \underbrace{\frac{1}{Q} \int_V \frac{\partial}{\partial t} \frac{\vec{C}^2}{2} dV}_{\substack{\text{Change of Flow Volume} \\ \text{Specific Kinetic Energy}}} \qquad \left(\mathrm{J \cdot kg^{-1}}\right) \qquad (42)$$

III SPECIFIC ENERGY LOSSES

1 REGULAR SPECIFIC ENERGY LOSSES

1.1 Formula

The regular specific energy loss formula is given by

$$gH_{r1\div2}=\lambda\times\frac{L_{1\div2}}{D}\times\frac{C^2}{2}=K_v\times\frac{C^2}{2} \tag{43}$$

with

- λ local energy loss coefficient;
- $L_{1\div2}=\int_{1\div2}dl$ pipe length;
- $K_v=\lambda\times L/D$ total friction loss coefficient of the pipe.

The local energy loss coefficient depends on the Reynolds and Mach numbers for accounting both viscous, compressibility effects, if any, and the pipe inner wall roughness.

1.2 Local energy loss coefficient

In the case of a constant diameter pipe, the local energy loss coefficient of regular specific energy losses depends only on the Reynolds number and the ratio between the sand roughness k_s and the pipe inner diameter, D. The original Moody diagram for local energy loss coefficient as a function of the pipe Reynolds number and the relative sand roughness is given in Figure 7, (Moody, 1944).

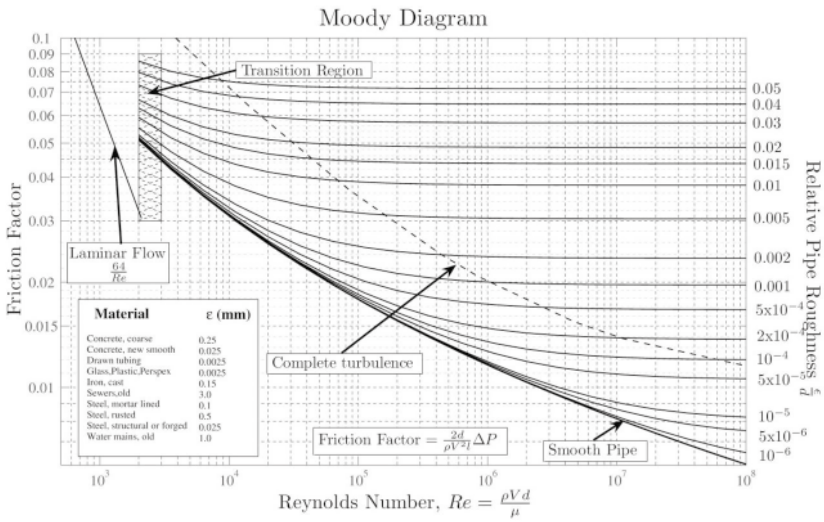

Figure 7 - Moody diagram of local energy loss coefficient for pipes

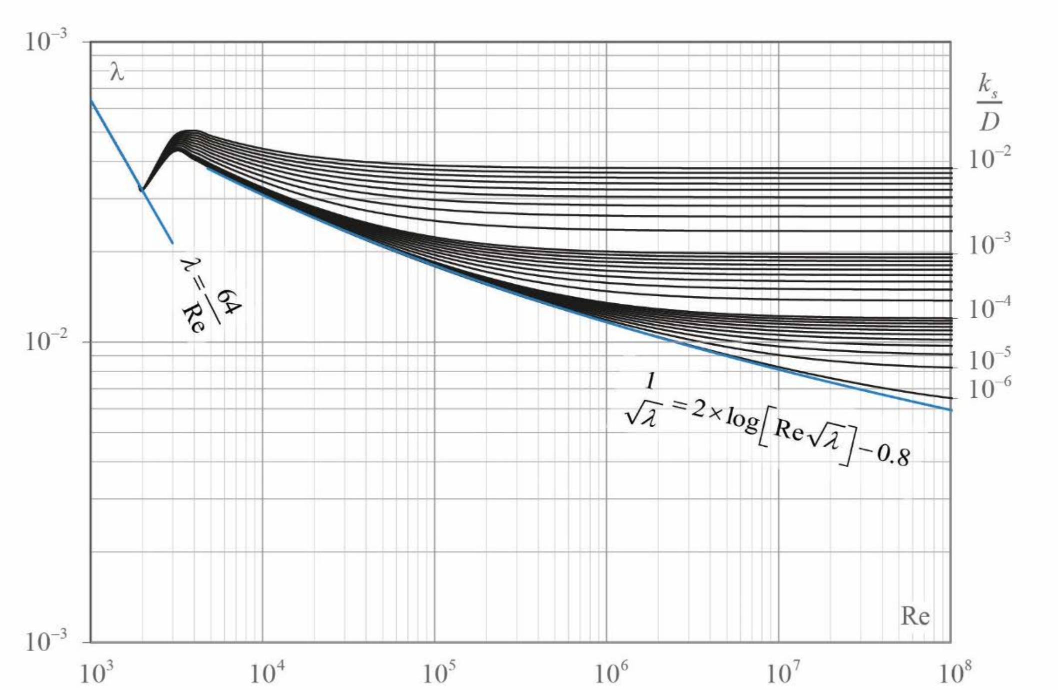

Figure 8 - Local energy loss coefficient for pipe flow as a function of the Reynolds number and for different relative sand roughness values.

The following 3 different asymptotic regimes, with transition zones in between, are made apparent:

- Laminar flow regime for $\mathrm{Re} \leq 2'000$ corresponding to Poiseuille flow for which λ is given by :

$$\lambda = \frac{64}{\mathrm{Re}}; \tag{44}$$

- Smooth turbulent flow regime for which wall roughness remains confined in the flow viscous sublayer and, then, does not influence the local energy loss coefficient. Prandtl developed the following implicit formula corresponding to a value of $\kappa = 0.407$ for the Karman constant of the constant turbulent stress layer, (Schlichting and Gersten, 2000) (Prandtl, 1933).

$$\frac{1}{\sqrt{\lambda}} = 2 \cdot \log\left[\mathrm{Re}\sqrt{\lambda}\right] - 0.8 \tag{45}$$

By assuming a 7 exponent law for the mean velocity profile, Blasius derived a closed form for the local energy loss coefficient.

$$\lambda = \frac{0.364}{\mathrm{Re}^{\frac{1}{4}}} \tag{46}$$

- Rough fully turbulent flow regime for which only the inner wall roughness influences the local energy loss coefficient. For this flow regime, wall roughness is high enough to prevent the viscous sublayer development.

(Churchill, 1977) developed a very convenient closed form for computing the local energy loss coefficient all over the range of flow regimes, see Figure 8.

$$\lambda = 8\left[\left(\frac{8}{\mathrm{Re}}\right)^{12} + \frac{1}{(A+B)^{\frac{3}{2}}}\right]^{\frac{1}{12}} \tag{47}$$

$$\text{with } A = \left[2.457 \cdot \ln \frac{1}{\left(\frac{7}{\text{Re}}\right)^{0.9} + 0.27 \cdot \frac{k_s}{D}} \right]^{16} \text{ and } B = \left[\frac{37'530}{\text{Re}} \right]^{16}$$

Pipe with non-circular section and open channels

The local energy loss coefficient formula can also be applied for both cases of pipes with non-circular section or open channels by substituting the hydraulic diameter D_h to the diameter *D*. The hydraulic diameter D_h, see Figure 9, is defined as,

$$D_h = 4 \times \frac{\text{Cross section area}}{\text{Wet perimeter}} \tag{48}$$

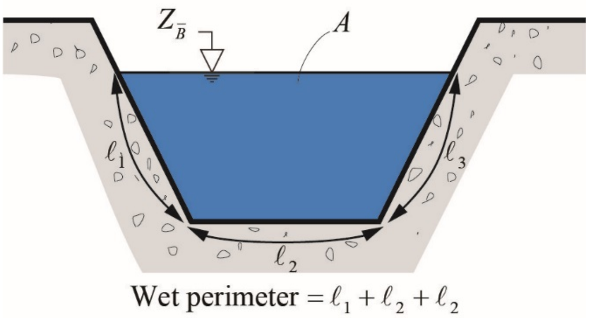

Figure 9 – Open channel

Therefore, the Reynolds number and the relative roughness coefficient used to compute the local energy loss coefficient are defined as:

$$\text{Re}_{D_h} = \frac{C \times D_h}{\nu} \text{ and } \frac{k_s}{D_h}, \text{ respectively}$$

For a pipe featuring a circular cross section of inner diameter *D*, (48) yields:

$$D_h = 4 \times \frac{\pi \cdot D^2}{4 \cdot \pi \cdot D} = D \text{ and, then, } D_h = D$$

1.3 Roughness

Definition

Surface roughness is the characteristic quality of the surface due to small departures from its general form such as those produced by the cutting action of tool edges, abrasive grains, feed of the machine, coating and painting or originally produced by the fabrication process.

The arithmetic mean deviation of the assessment profile, R_a as defined in ISO 4287:1997, characterizes the roughness, see Figure 10. For a sample of length L, R_a is defined as

$$R_a = \frac{1}{L} \int_0^L |y - \bar{y}| \, dx \tag{49}$$

where y and $\bar{y}$ are the height of the surface and the average surface, respectively.

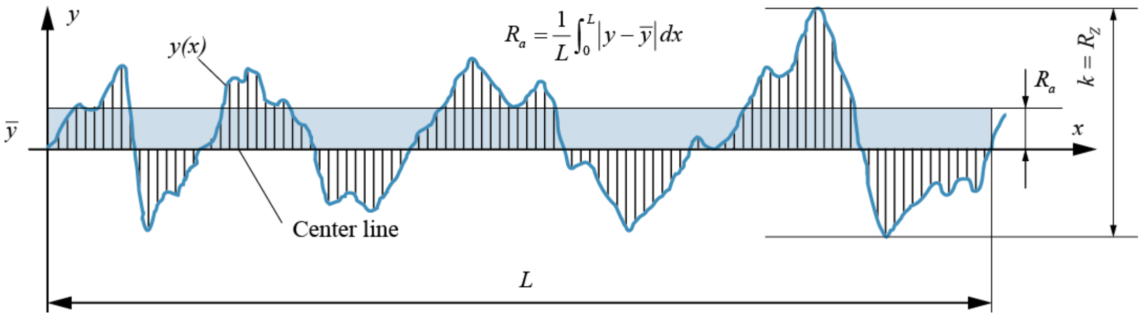

Figure 10 – Surface roughness definitions

Systematic measurements of energy loss coefficients for smooth turbulent flow regime provided the following empirical relation between R_a and the sand roughness k_s used in formula (47)

$$R_a \approx 0.43 k_s \tag{50}$$

The so-called technical roughness k corresponding to R_Z the maximum peak-to-peak value of the roughness profile for a given length is also used, see Figure 10. $R_{\max}$ to R_a ratio value is close to 6.

$$k = R_Z \approx 6 \times R_a \tag{51}$$

The Churchill formula parameter A from (47) can be expressed as a function of R_a roughness,

$$a = \left[2.457 \ln \frac{1}{\left(\frac{7}{\mathrm{Re}}\right)^{0.9} + \frac{0.63 Ra}{D_H}} \right]^{16} \tag{52}$$

Maximum roughness for smooth turbulent flow regime

Condition for smooth turbulent flow regime is given by the condition for the viscous sublayer development in the turbulent boundary layer:

$$k^+ = \frac{kC_\tau}{\nu} = \frac{k}{\nu}\sqrt{\frac{\tau_p}{\rho}} < 5 \tag{53}$$

Pipe axial momentum balance yields the following relation between c_f the friction factor and λ the local energy loss coefficient:

$$\sqrt{\frac{\tau_p}{\rho}} = \sqrt{c_f} \times C = \sqrt{\frac{\lambda}{8}} \times C$$

Substituting the local energy loss coefficient λ in condition (53) yields:

$k^+ = \sqrt{\frac{\lambda}{8}}\frac{k_s \times C}{\nu}$ where the wall friction velocity C_τ is defined as $\tau_p = \rho C_\tau^2$.

Or by making apparent Re, the pipe Reynolds number:

$$k^+ = \sqrt{\frac{\lambda}{8}}\frac{k_s}{D}\frac{CD}{\nu} = \sqrt{\frac{\lambda}{8}}\frac{k_s}{D}\mathrm{Re} < 5 \tag{54}$$

Therefore, the maximum value of relative sand roughness to hold a smooth turbulent flow regime is given by

$$\frac{k_s}{D} < 10\sqrt{\frac{2}{\lambda}}\frac{1}{\mathrm{Re}} \quad \frac{k_s}{D} \tag{55}$$

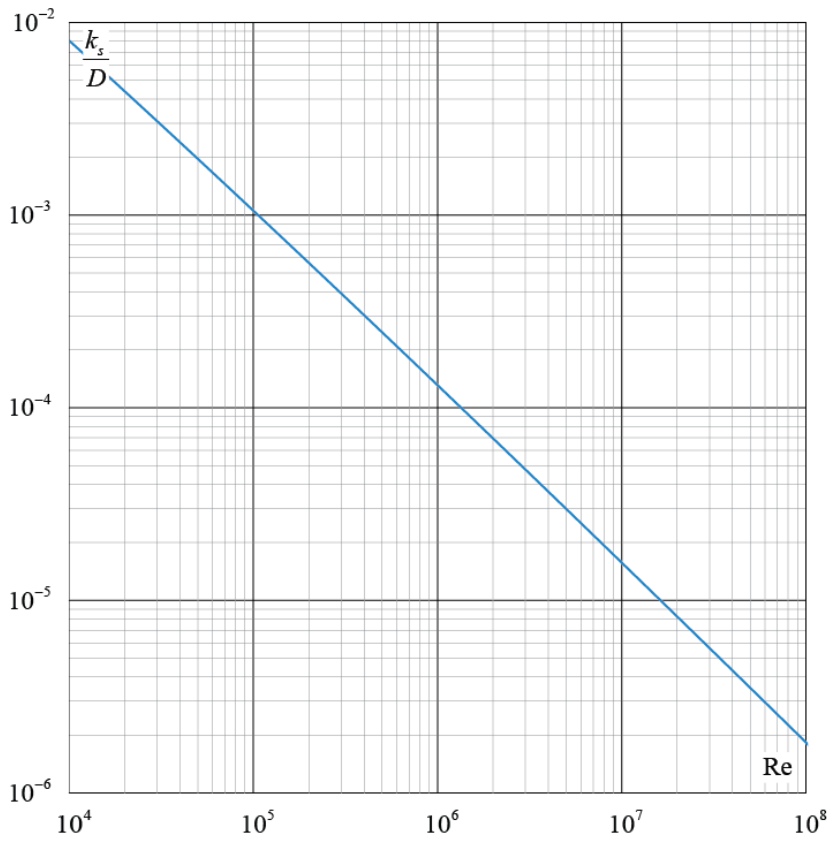

Figure 11 – Influence of the Reynolds number on the maximum relative sand roughness to hold a smooth turbulent flow regime.

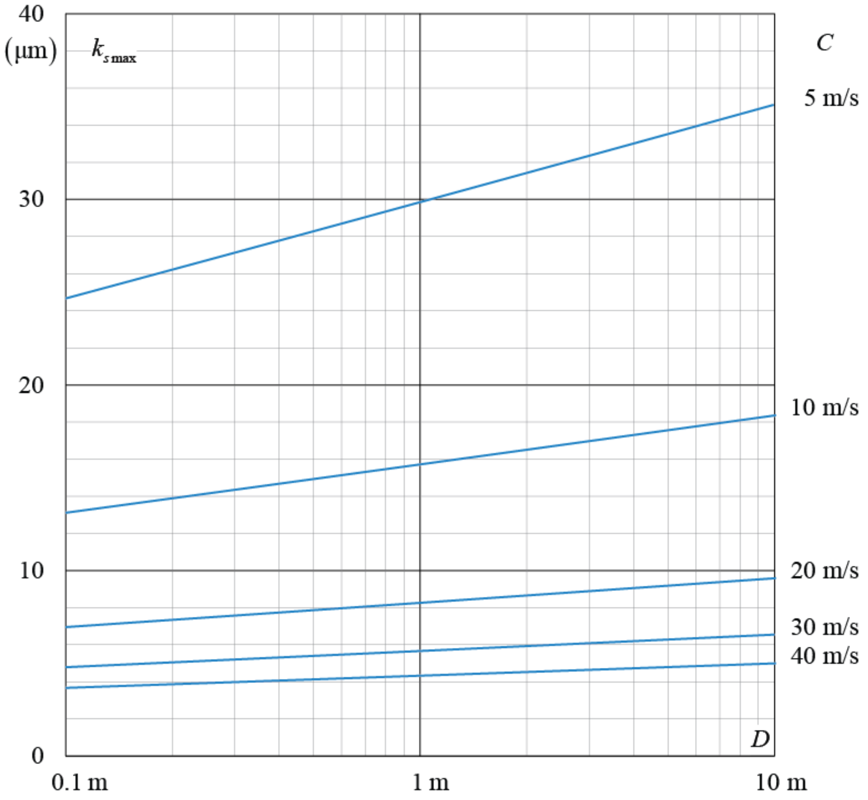

Figure 12 – Influence of discharge velocity C in a pipe of diameter D on maximum admissible sand roughness k_s to achieve a smooth turbulent flow regime.

Relation (55) is plotted as a function of the Reynolds number in Figure 11. Therefore, the maximum sand roughness compatible with a smooth turbulent flow regime can be computed by for a given discharge velocity C in a pipe of diameter D, see Figure 12.

$$k_s < 10\sqrt{\frac{2}{\lambda}}\frac{\nu}{CD} \ \left(\mathrm{m}\right) \tag{56}$$

Results in Figure 12 emphasize the inner wall roughness conditions to achieve smooth turbulent flow or minimum flow friction. The higher the discharge or alternatively the Reynolds number is the lower the maximum roughness should be.

Equivalent sand roughness

All the available experimental results of energy losses in pipes were obtained by varying the sand roughness values and so the formula to compute the local energy loss coefficient such as the Churchill formula (47), are based on sand roughness values. In Table 1; the corresponding sand roughness are provided for different common industrial pipe materials.

Table 1 – Equivalent sand roughness for common industrial pipes (Comolet 1994)

Material	**State**	**Equivalent Sand Roughness** k_s
Drawn glass, plastic, copper, brass, stainless steel	n/a	$<10^{-6}$ m
Industrial PVC	n/a	from $10\cdot10^{-6}$ m to $20\cdot10^{-6}$ m
Industrial painted pipe	n/a	$20\cdot10^{-6}$ m
Industrial brass	n/a	$25\cdot10^{-6}$ m
Rolled steel	New	$50\cdot10^{-6}$ m
	Rusted	from $150\cdot10^{-6}$ m to $250\cdot10^{-6}$ m
	Incrusted	from $1.5\cdot10^{-3}$ m to $3\cdot10^{-3}$ m
Welded steel	New	from $30\cdot10^{-6}$ m to $100\cdot10^{-6}$ m
	Rusted	$400\cdot10^{-6}$ m
Cast iron	New	$250\cdot10^{-6}$ m
	Rusted	from $1\cdot10^{-3}$ m to $1.5\cdot10^{-3}$m
Centrifuged concrete	Smooth	$300\cdot10^{-6}$ m
Concrete	Smooth	from $300\cdot10^{-6}$ m to $800\cdot10^{-6}$ m
	Rough	up to $3\cdot10^{-3}$ m
Riveted steel	n/a	from $900\cdot10^{-6}$ m to $9\cdot10^{-3}$ m
Rock tunnel	n/a	from $90\cdot10^{-3}$ m to $600\cdot10^{-3}$ m

1.2 Economical specification for the diameter of a pipe

For a given rated discharge Q, the specific energy loss gH_r of a long circular pipe of length L and diameter D is given by:

$$gH_r = \lambda\times\frac{L}{D}\times\frac{C^2}{2} = \frac{8}{\pi^2}\times\frac{\lambda\times L\times Q^2}{D^5} \tag{57}$$

In (57) the exponent -5 of the pipe diameter D should be emphasized. A small change of the diameter value greatly influences the energy losses. The corresponding power loss dissipation in the pipe can be computed as

$$P_r = \rho \times Q \times gH_r = \frac{8 \times \rho \times \lambda \times L \times Q^3}{\pi^2 \times D^5} \tag{58}$$

As an example, the following pipe featuring $D = 2.500\ \mathrm{m}$ diameter, $L = 5'400\ \mathrm{m}$ length and $\Delta Z = 915\ \mathrm{m}$ elevation difference between headwater and tailwater free surface levels is considered.

The rated discharge value is $Q = 50\ \mathrm{m^3/s}$ which yields $C = 10.2\ \mathrm{m/s}$ and $\mathrm{Re} = 25.5 \times 10^6$ corresponding discharge velocity and Reynolds values, respectively. By assuming a smooth turbulent flow regime, (47) yields $\lambda = 1 \times 10^{-2}$ local energy loss coefficient value. In this case, condition (56) for the maximum sand roughness yields $k_s \approx 17\ \mu\mathrm{m}$, see Figure 12

Therefore, the Churchill formula (47) and equation (58) yields the value of dissipated power, $P_{hr} = 57.9\ \mathrm{MW}$, corresponding to $12.9\ \%$ of the available potential hydraulic power, $P_{pot.} = \rho \times Q \times g \times \Delta Z$, i.e. $448.7\ \mathrm{MW}$.

The expected turnover of electricity sale generated by the hydropower plant is depending of the price A per kWh and of the amount of energy generated over a given time T. The following formula defines this turnover

$$A \times q \times T \times \eta \times \left(P_{pot.} - P_r\right) = A \times q \times T \times \eta \times \rho \times Q \times \left(g\Delta Z - \frac{8}{\pi^2} \times \frac{\lambda \times L \times Q^2}{D^5} \right)$$

Which yields $77.0\ \mathrm{Mio\ CHF}$ yearly sale by assuming a capacity factor $q = 50\ \%$, a generation efficiency $\eta = 90\ \%$ and $A = 0.05\ \mathrm{CHF \cdot kWh^{-1}}$ average electricity price.

If the same computation is performed for a diameter value increased to $D = 3.000\ \mathrm{m}$ to reduce the discharge velocity to $C = 7.1\ \mathrm{m/s}$ leading to $\mathrm{Re} = 21.2 \times 10^6$, in this case the local energy loss coefficient is almost unchanged $\lambda = 1 \times 10^{-2}$ and the dissipated power is lowered to $P_{hr} = 22.7\ \mathrm{MW}$, which represents $5.1\ \%$ of the available potential hydraulic power for an annual sale of $84.0\ \mathrm{Mio\ CHF}$, corresponding to an increase of $7.0\ \mathrm{Mio\ CHF}$ sale with respect to the previous case.

However, the annual interest and amortization for the capital expenditure required for the pipe or tunnel steel liner construction need to be taken into account. The capital expenditure is directly linked to the material quantity, i.e. mass M, used for the construction. Let consider the case of a circular pipe or tunnel steel liner, therefore the steel mass M is given by :

$$M = \rho_{Steel} \cdot \frac{\pi}{4} \int_L \left[\left(D + 2e\right)^2 - D^2 \right] dL = \rho_{Steel} \cdot \frac{\pi D^2}{4} \int_L \left[\frac{4e^2}{D^2} + 2\frac{2e}{D} \right] dL \tag{59}$$

where ρ_{steel} is the steel density and e is the steel pipe thickness.

The steel pipe thickness is specified as a function of the allowable stress limit σ_{adm} in the pipe according to the following condition of static hydrostatic pressure balance

$$\delta p \times D = \sigma_{adm} \times 2e \tag{60}$$

By assuming a constant pressure gradient all along the pipe, the gauge pressure δp will follow a linear law of the current distance l, therefore (60) yields.

$$\frac{2e}{D} = \frac{\delta p}{\sigma_{adm}} \approx \frac{\rho \cdot \left(g\Delta Z - gH_r - \dfrac{C^2}{2} \right)}{\sigma_{adm}} \times \frac{\ell}{L} \tag{61}$$

By introducing the maximum thickness $e_{\max}$

$$\frac{2e_{\max}}{D}=\frac{\delta p_{\max}}{\sigma_{adm}}=\frac{\rho\cdot\left(g\Delta Z-gH_r-\dfrac{C^2}{2}\right)}{\sigma_{adm}} \qquad (62)$$

and substituting (62) in (59) yields

$$M=\rho_{Steel}\times\frac{\pi D^2}{4}\int_L\left[\left(\frac{2e_{\max}}{D}\right)^2\frac{\ell^2}{L^2}+2\times\frac{2e_{\max}}{D}\times\frac{\ell}{L}\right]d\ell \qquad (63)$$

The integration of the (63) right hand side yields

$$M=\rho_{Steel}\times\left(\frac{1}{3}\left(\frac{2e_{\max}}{D}\right)^2+\frac{2e_{\max}}{D}\right)\times\frac{\pi D^2 L}{4} \qquad (64)$$

Therefore, the annual interest and amortization cost for the capital expenditure required for the pipe construction reads

$$n\times B\times M=n\times B\times\rho_{Steel}\times\frac{2e_{\max}}{D}\times\left(1+\frac{1}{3}\times\frac{2e_{\max}}{D}\right)\times\frac{\pi D^2 L}{4} \qquad (65)$$

where B is the price per unit of mass of steel taking into account all the other construction costs for the pipe and tunnel construction, n the annual rate including both interest and amortization.

By assuming that $\sigma_{adm}=200\ \text{MPa}$, $\rho_{Steel}=5'000\ \text{kg/m}^3$, $B=12\ \text{CHF/kg}$ and $n=5\ \%$, the cost of construction for a pipe of $D=2.500\ \text{m}$ diameter corresponding to $C=10.2\ \text{m}\cdot\text{s}^{-1}$ discharge velocity is $68.5\ \text{Mio CHF}$ yielding $3.4\ \text{Mio CHF}$ annual interest and amortization expenses and $73.6\ \text{Mio CHF}=77.0\ \text{Mio CHF}-3.4\ \text{Mio CHF}$ annual payback.

For $D=3.000\ \text{m}$ diameter corresponding to $C=7.1\ \text{m}\cdot\text{s}^{-1}$ discharge velocity the cost of construction is $108.4\ \text{Mio CHF}$ yielding $5.4\ \text{Mio CHF}$ annual interest and amortization expenses and $78.6\ \text{Mio CHF}=84.0\ \text{Mio CHF}-5.4\ \text{Mio CHF}$ annual payback. In this case the annual payback is increased by $5\ \text{Mio CHF}$ with respect to the previous $D=2.500\ \text{m}$ diameter.

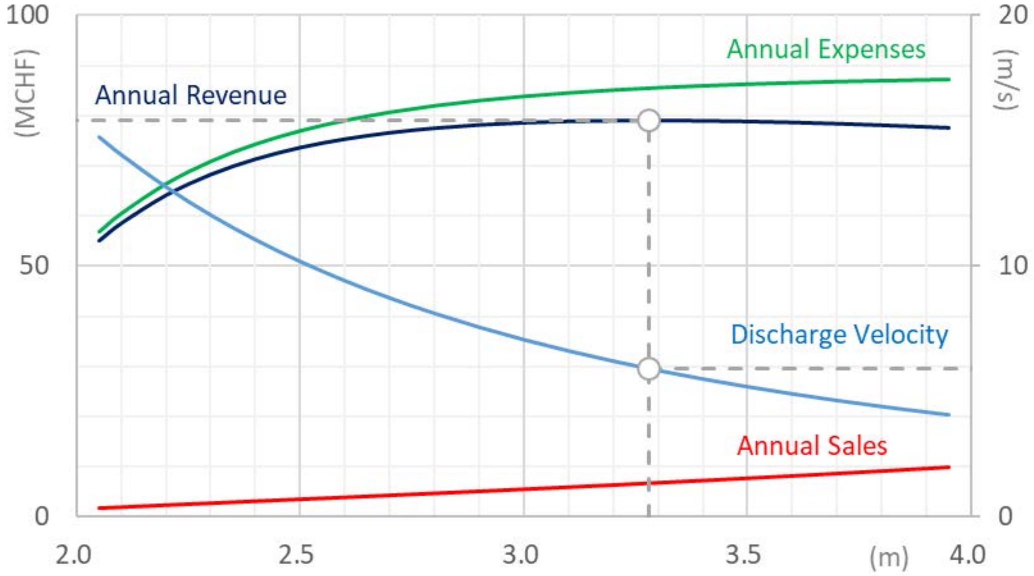

Figure 13 – Optimum diameter

This evaluation can been further performed for different values of steel pipe diameter to define the optimum diameter which yields the best payback see Figure 13.

The $D = 3.281\ \mathrm{m}$ optimum diameter value is corresponding to $C = 5.9\ \mathrm{m \cdot s^{-1}}$ discharge velocity and yielding, $132.4\ \mathrm{Mio\,CHF}$ total cost of construction, $6.6\ \mathrm{Mio\,CHF}$ annual interest and amortization expenses, $85.6\ \mathrm{Mio\,CHF}$ energy sales and $79.0\ \mathrm{Mio\,CHF}$ annual payback. The energy dissipated in the installation is $3.2\ \%$ of the hydraulic potential energy.

It is important to notice that the previous case is a very simplified example to demonstrate the methodology for specifying the optimum diameter of the hydropower project waterways.

However, the resulting discharge velocity value of about $C \approx 6\ \mathrm{m \cdot s^{-1}}$ is typical of the values specified for existing projects.

1.3 Economical specification for an oil pipe-line

The oil industry uses the following empirical formula for specifying the diameter D of an oil pipe-line as a function of the rated discharge Q.

$$D = \sqrt{\frac{Q}{500}} \qquad (\mathrm{in}) \tag{66}$$

where the units of the US Customary System (USCS) are used, inch (in) for diameter D and oil barrel per day $\left(\mathrm{bll \cdot d^{-1}}\right)$ for discharge Q.

Formula (66) transforms to:

$$\frac{Q}{D^2} = 500 \times \frac{1\ \mathrm{bbl}}{1\ \mathrm{d}} \times \frac{1}{1\ \mathrm{in}^2}$$

To be converted in SI units

$$\begin{aligned}
\frac{Q}{D^2} &= 500 \times 1\ \cancel{\mathrm{bbl}} \times \frac{42\ \cancel{\mathrm{gal}}}{1\ \cancel{\mathrm{bbl}}} \frac{231\ \cancel{\mathrm{in}^3}}{1\ \cancel{\mathrm{gal}}} \times \frac{\left(25.4\times10^{-3}\right)^3\ \mathrm{m}^3}{1\ \cancel{\mathrm{in}^3}} \times \frac{1}{1\ \cancel{\mathrm{d}}} \times \frac{1\ \cancel{\mathrm{d}}}{24\times3600\ \mathrm{s}} \times \frac{1}{1\ \cancel{\mathrm{in}^2}} \frac{1\ \cancel{\mathrm{in}^2}}{\left(25.4\times10^{-3}\right)^2\ \mathrm{m}^2} \\
&= \frac{500\times42\times231}{24\times3600} \times 25.4\times10^{-3}\ \frac{\mathrm{m}}{\mathrm{s}} \\
&= 1.426\ \frac{\mathrm{m}^3}{\mathrm{m}^2\mathrm{s}}
\end{aligned}$$

with the following conversion factors, (Thompson and Taylor, 2008)

$$\begin{aligned}
1\ \mathrm{bbl} &= 42\ \mathrm{gal} \\
1\ \mathrm{gal} &= 231\times\mathrm{in}^3 \\
1\ \mathrm{in} &= 25.4\times10^{-3}\ \mathrm{m} \\
1\ \mathrm{d} &= 24\times3600\ \mathrm{s}
\end{aligned}.$$

In SI units, the formula (66) reads

$$\frac{Q}{D^2} \approx 1.426\ \mathrm{m \cdot s^{-1}} \tag{67}$$

However, (67) can be adapted to make apparent C the pipeline discharge velocity expressed as.

$$C = \frac{Q}{\pi \frac{D^2}{4}}$$

which yields

$$C = \frac{4}{\pi} \times \frac{Q}{D} = \frac{4}{\pi} \times 1.426\ \mathrm{m/s}\ = 1.816\ \mathrm{m/s} \tag{68}$$

Therefore, a $C = 1.8\ \text{m/s}$ discharge velocity is recommended for oil transported in standard pipeline.

2 SINGULAR SPECIFIC ENERGY LOSSES

2.1 General Remarks

Derivation and details of the empirical formulas made available hereafter can be found in (Miller, 1978), (Idel'cik, 1999), (Comolet, 1994), (Pont-à-Mousson, 1989) and (White, 2009).

Otherwise mentioned, C is the discharge velocity at the inlet fluid section A_1

$$C = \frac{Q}{A_1} \ \left(\text{m} \cdot \text{s}^{-1}\right) \tag{69}$$

2.2 Long pipe

The regular specific energy losses formula is given by (43)

$$gH_{rv} = K_v \times \frac{C^2}{2} \tag{70}$$

with K_v the total pipe energy loss coefficient, defined as $K_v = \lambda \times L/D$ were λ the local energy loss coefficient given by formula (47)

$$\lambda = 8\left[\left(\frac{8}{\text{Re}}\right)^{12} + \frac{1}{\left(A+B\right)^{\frac{3}{2}}}\right]^{\frac{1}{12}} \tag{71}$$

$$\text{with } A = \left[2.457 \cdot \ln \frac{1}{\left(\frac{7}{\text{Re}}\right)^{0.9} + 0.27 \cdot \frac{k_s}{D}}\right]^{16} \text{ and } B = \left[\frac{37'530}{\text{Re}}\right]^{16}$$

2.3 Sudden Enlargement:

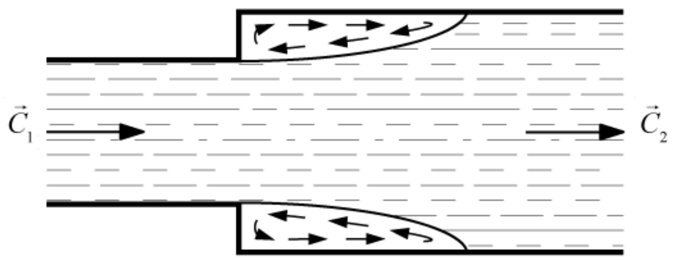

Figure 14 - Sudden enlargement flow pattern

$$gH_{rv} = K_v \times \frac{C_1^2}{2} \text{ with } K_v = \left[1 - \frac{A_1}{A_2}\right]^2 \tag{72}$$

2.4 Sudden Contraction:

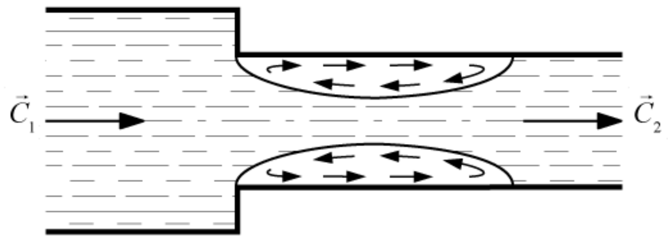

Figure 15 - Sudden contraction flow pattern

$$gH_{rv} = K_v \times \frac{C_1^2}{2} \text{ with } K_v = \frac{1}{2}\left[1 - \frac{A_2}{A_1}\right] \tag{73}$$

2.5 Intake:

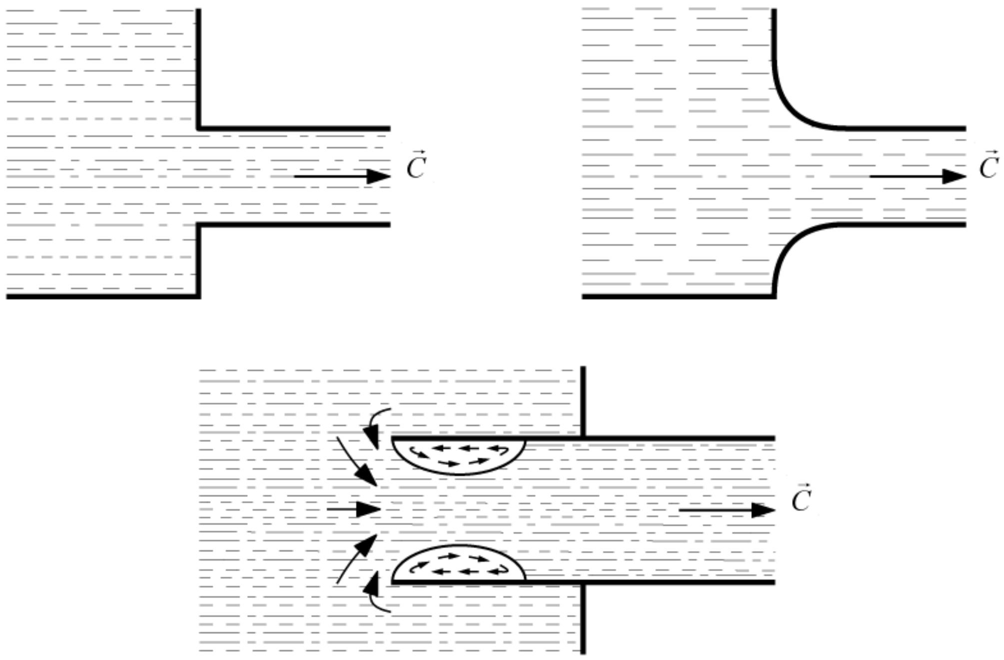

Figure 16 - Water intake with sharp (upper left), smooth (upper right) and re-entrant pipe (lower) connections

$$gH_{rv} = K_v \times \frac{C^2}{2} \text{ with } \begin{cases} K_v = 0.5 & \text{for a sharp connection} \\ K_v = 0.05 & \text{for a smooth connection} \\ K_v = 1 & \text{for a re-entrant pipe connection} \end{cases} \quad (74)$$

2.6 Outflow:

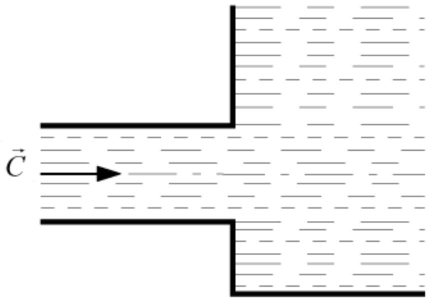

Figure 17 - Outflow with sharp connection

$$gH_{rv} = K_v \times \frac{C^2}{2} \text{ with } K_v = 1 \quad (75)$$

2.7 Elbow:

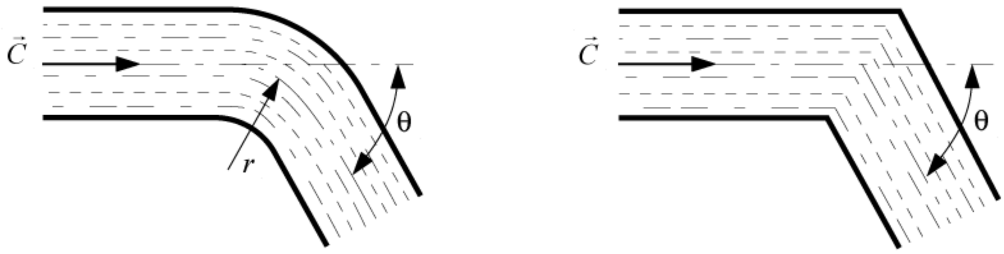

Figure 18 - Smooth (left) and sharp (right) elbows

For a smooth elbow

$$gH_{rv} = K_v \times \frac{C^2}{2} \text{ with } K_v = \left[0.131 + 1.847\left(\frac{D}{2r}\right)^{3.5}\right]\frac{\theta}{90} \tag{76}$$

For a sharp elbow, the loss coefficient K_v is given in Table 2.

Table 2 – Loss coefficient for a sharp elbow

θ °	22.5	30	45	60	90
K_v	0.07	0.11	0.24	0.47	1.13

2.8 Valve:

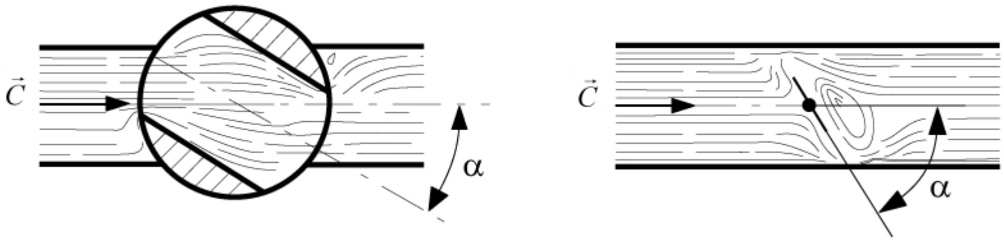

Figure 19 - Spherical (left) and butterfly (right) valves

$$gH_{rv} = K_v \times \frac{C^2}{2} \text{ with the loss coefficient } K_v \text{ given in the tables below.} \tag{77}$$

Table 3 – Loss coefficient for a spherical valve

θ °	5	10	15	25	35	45	55	65
K_v	0.05	0.29	0.75	3.1	9.7	31	110	490

Table 4 – Loss coefficient for a butterfly valve

θ °	5	10	15	20	30	40	45	50	60	70
K_v	0.24	0.52	0.90	1.5	3.9	11	19	33	120	750

IV HYDRAULIC MACHINES: CLASSIFICATION

1 DISPLACEMENT MACHINES

1.1 Reciprocating Pumps or Drives

Piston Plunger

Steam Double Acting
- Simplex
- Duplex

Power

Single Acting
- Simplex
- Duplex
- Triplex
- Multiplex

Double Acting
- Simplex
- Duplex
- Triplex
- Multiplex

Diaphragm

Simplex
- Fluid operated
- Mechanically operated

Multiplex
- Fluid operated
- Mechanically operated

1.2 Rotary

Single rotor

Vane

Piston

Flexible Member

Screw

Peristaltic

Multiple rotors

Gear

Lobe

Flexible Member

Circumferential Piston

Screw

2 TURBOMACHINES: INDUSTRIAL CENTRIFUGAL PUMPS

2.1 Axial Flow Pumps

Single stage

Closed Impeller

Open Impeller
- Fixed Pitch
- Variable Pitch

2.2 Mixed / Radial Flow Pumps

Single suction

Self-Priming
- Open Impeller
- Semi Open Impeller
- Closed Impeller

Non-Priming
- Open Impeller
- Semi Open Impeller
- Closed Impeller

Single Stage
- Open Impeller
- Semi Open Impeller
- Closed Impeller

Multistage
- Open Impeller
- Semi Open Impeller
- Closed Impeller

Double suction

Self-Priming
- Open Impeller
- Semi Open Impeller
- Closed Impeller

Non-Priming
- Open Impeller
- Semi Open Impeller
- Closed Impeller

Single Stage
- Open Impeller
- Semi Open Impeller
- Closed Impeller

Multistage
- Open Impeller
- Semi Open Impeller
- Closed Impeller

2.3 Peripheral Flow Pumps

Single Stage
- Self-Priming
- Non-Priming

Multistage
- Self-Priming
- Non-Priming

3 TURBOMACHINES: SPECIAL EFFECT PUMPS

3.1 Jet (Eductor)

3.2 Gas Lift

3.3 Hydraulic Ram

3.4 Electromagnetic

4 HYDRAULIC TURBINES

4.1 Impulse Turbine

Definition

Impulse (action) turbine is a turbine in which the available hydraulic energy is fully converted into kinetic energy at the outlet of the nozzle. Flow regulation is by means of one or more nozzles.

Pelton Turbine

Pelton turbine is an impulse turbine in which the runner has double bowl buckets and the nozzle axes are located in the plane of symmetry of the buckets.

Inclined-jet turbine

Impulse turbine is an impulse turbine in which the runner has single bowl buckets. Nozzle axes are inclined to the plane of the runner. This type of machine includes the Turgo turbine

Crossflow Turbine

Cross-flow turbine or Michell-Banki-turbine is an impulse turbine with a very small degree of reaction. The flow crosses the runner twice perpendicularly to its axis of rotation and the runner blades are arranged cylindrically.

4.2 Reaction Turbine

Radial Turbine, Francis Turbine

Reaction turbine with meridional flow which is approximately radial between usually adjustable opening of radial guide vanes and changes gradually direction inside the fixed runner blades so that the flow approaches axial flow at the outlet of the runner. (CEI TR 61364)

Diagonal Turbine, Mixed Flow Turbine, Semi-Axial Turbine

Definition

Reaction turbine with radial or diagonal flow to guide vanes and diagonal inflow to the runner.

Single-regulated machine:

Opening of guide vanes is adjustable

Double regulated machine: Dériaz Turbine

The Dériaz turbine features a diagonal flow between the stay vanes, guide vanes and runner blade and opening of both guide vanes and runner blades are adjustable.

Axial Turbines: Kaplan or Propeller Turbines

Definition

Reaction axial turbine with radial inflow to the guide vanes having approximately axial meridional flow between the runner blades, usually with vertical shaft and elbow draft tube.

Single-regulated machine: Propeller Turbine

In a propeller turbine, only opening of guide vanes is adjustable and the pitch of the runner blades is constant.

Double regulated machine: Kaplan Turbine

The Kaplan turbines feature adjustable guide vanes and adjustable runner blades.

Tubular Turbines

Definition

Axial turbine with axial or diagonal inflow to the guide vanes, usually with horizontal or inclined shaft. The unit may be double, single or non-regulated.

Bulb Unit

The unit generator is housed in a bulb in the water passage. The generator may be directly driven or equipped with a gearbox. The term "Bulb unit" includes units with bevel gear and shaft which drive the generator externally mounted outside the water passage.

Pit Unit

The generator is housed in a pit in the water passage. The generator is most frequently connected to the turbine shaft through a gearbox. The pit allows direct dismantling of the generator and the gearbox from above.

Rim Generator Unit

The generator rotor is directly attached to the runner periphery. Straflo turbine is a trademark of this type of unit

S-Type Unit

The S-type unit is an axial turbine with an S shaped water passage. The turbine drives an externally mounted generator coupled directly to the turbine shaft or through a gearbox. The S-type turbine may features either downstream or upstream S-type configurations.

5 STORAGE PUMPS

5.1 Radial Pump

A radial pump (centrifugal) is a pump having axial inflow to and radial outflow from the impeller featuring fixed pitch blades bounded by a crown and band. Discharge from the impeller is to a diffuser and/or spiral case.

5.2 Diagonal pump, mixed-flow or semi-axial

Definition

Diagonal pump features axial or diagonal meridional inflow to diagonal meridional outflow from the impeller. Discharge may be to a diffuser and/or spiral case or in an axial direction.

Non-regulated machine

Non-regulated diagonal pump features diffuser with constant opening of the guide vanes and/or spiral case or in an axial direction.

Single-regulated machine

Single-regulated diagonal pump features fixed pitch impeller blades and diffuser adjustable guide vanes.

Double-regulated machine

Double-regulated diagonal pump features adjustable pitch impeller blades and diffuser adjustable guide vanes.

5.3 Axial pump

Axial pump is a pump having axial inflow to and axial outflow from the impeller with fixed or adjustable blades.

5.4 Booster

Booster pump is a pump of any type delivering a part of the specific hydraulic energy, installed on the low pressure side of the main storage pump.

Pelton Turbine

Pelton turbine is an impulse turbine in which the runner has double bowl buckets and the nozzle axes are located in the plane of symmetry of the buckets.

Inclined-jet turbine

Impulse turbine is an impulse turbine in which the runner has single bowl buckets. Nozzle axes are inclined to the plane of the runner. This type of machine includes the Turgo turbine

V HYDRAULIC TURBOMACHINES

1 MAIN COMPONENTS

1.1 Hydraulic Layout of Hydropower Station

The hydropower station is connected by a hydraulic circuit to both headwater and tailwater reservoirs to generate (turbine mode) and/or store (pump mode) energy.

A typical hydraulic layout for hydropower station is sketched in Figure 20 with the definitions of the main components and reference sections.

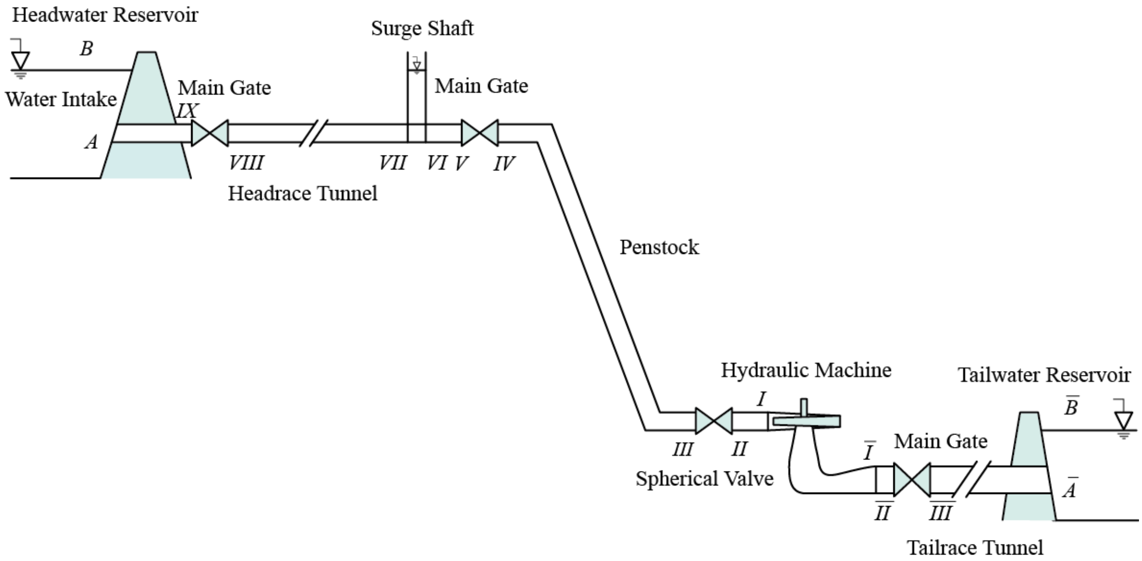

Figure 20 – Typical layout of a hydropower plant layout

1.2 Hydraulic Machine

The hydraulic machine, pump or turbine, is defined between section I and $\bar{I}$ of the hydraulic circuit. The components and reference sections for a radial-axial turbomachine are defined in Figure 21 and .

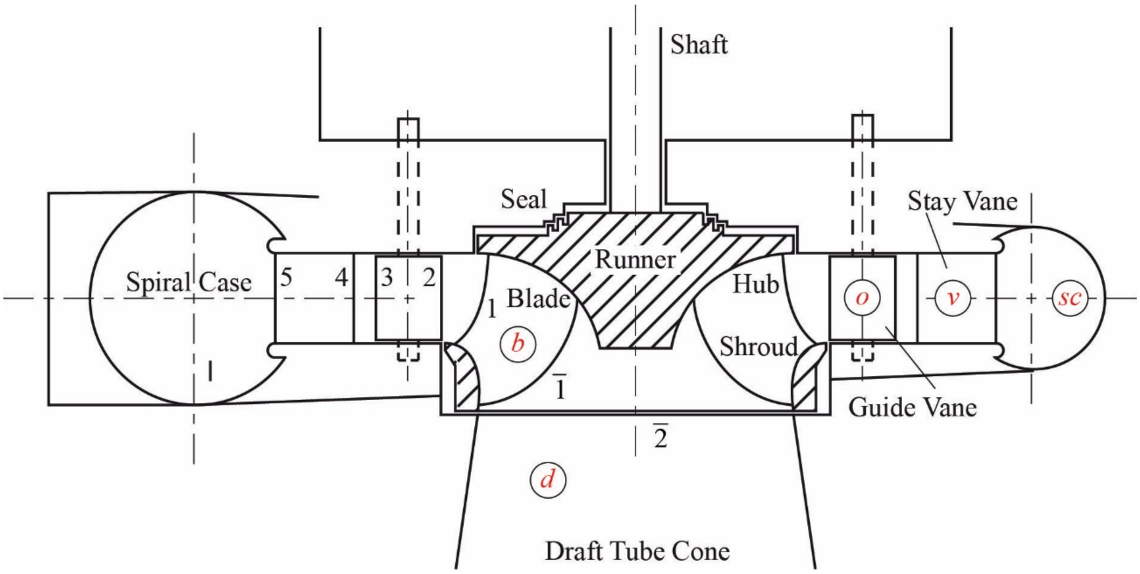

Figure 21 – Components and reference sections for a typical Francis Turbine

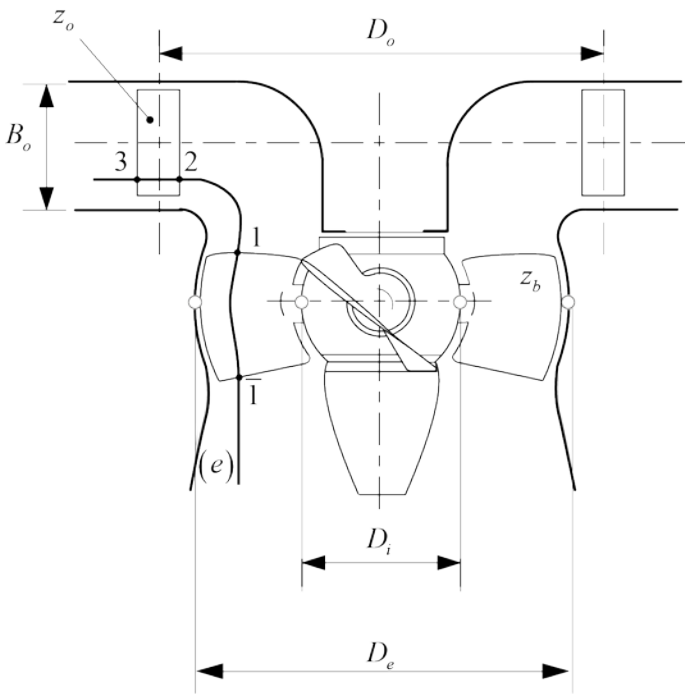

Figure 22 – Components and reference sections for a typical Kaplan Turbine

1.3 Spiral Case, Stay Ring and Stay Vanes

The spiral case (sc) is a spiral shaped converging water passage, usually with steel lined circular cross-sections which surrounds the distributor to ensure a uniform flow to the cascade of guide vanes and to the diffuser in the case of a pump. The spiral case connects the high pressure connecting pipe to the stay (diffuser) ring.

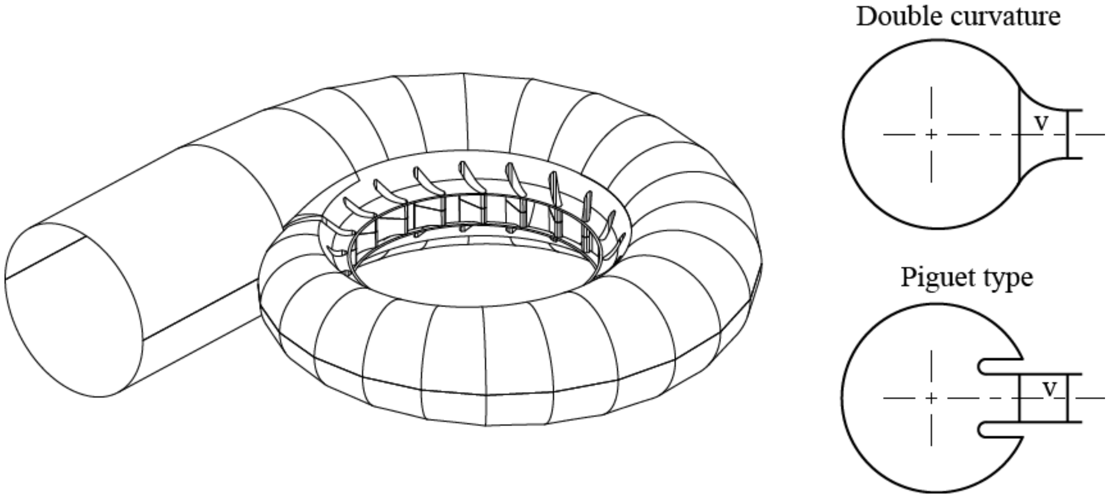

Figure 23 - Spiral case water passages and double curvature and Piguet types stay rings.

The stay ring is a structural component of the spiral case located upstream the guide vanes, usually having two annular shrouds connected by a number of fixed stay vanes in the water passages to provide support and structural continuity and to guide the flow from the spiral case to the guide vanes. Two common designs for stay ring are sketched in Figure 23. The double curvature is a historical design type, which yields quite a complex stay ring distribution of stresses. The Piguet type is a more recent design, which is more appropriate for engineering large machines. The stay vanes (v) are *"streamlined"* structural members of the stay ring which guides the flow to the guide vanes.

Guide Vanes

The guide vanes (o) or wicket gates are used to control the flow angular momentum feeding the runner. The guide vane opening is controlled by the governor ring as represented in

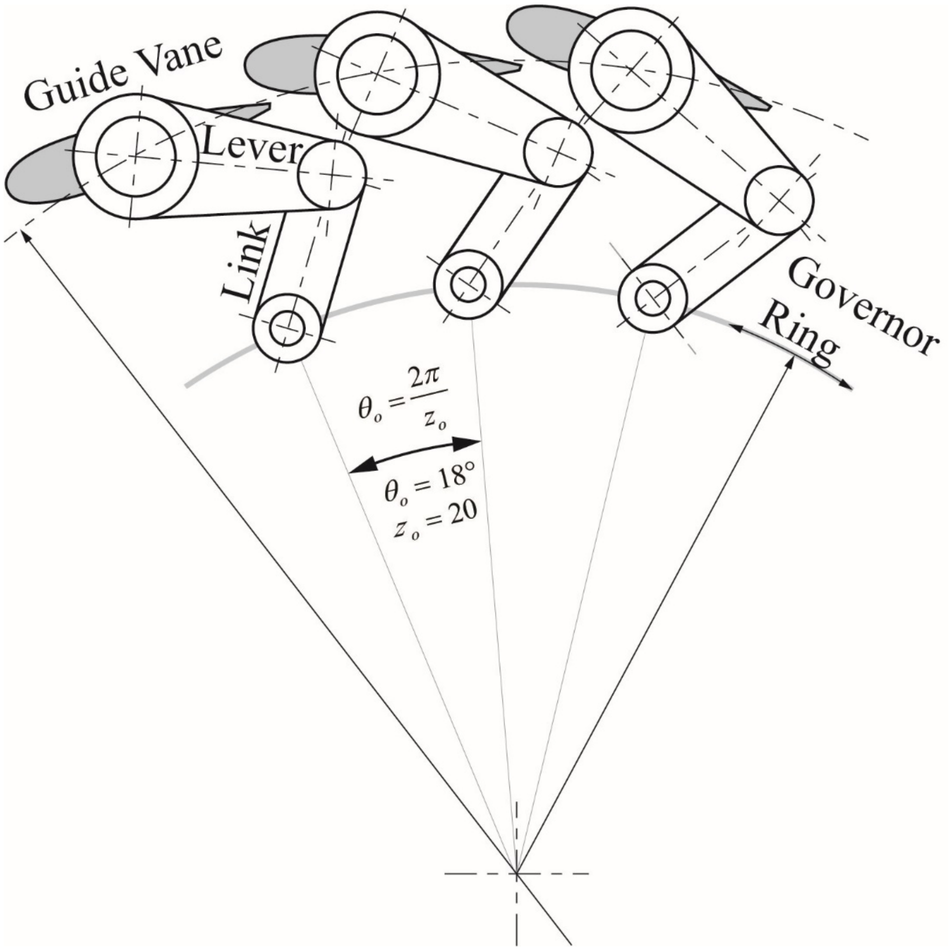

Figure 24 – Guide vanes (z_o = 20) controlled by the governor ring

The runner flow incidence angle is, then, controlled by the guide vane opening angle α_o. The different relations related to the guide vanes position are given in Figure 25.

$$R_2 = R_o\sqrt{\left(\frac{\ell}{R_o} - \sin\alpha_o\right)^2 + \cos^2\alpha_o}$$

$$\cos\alpha_{20} = \frac{R_o}{R_2}\cos\alpha_o$$

$$\theta_0 = \frac{2\pi}{z_o}$$

$$z_o = 24$$

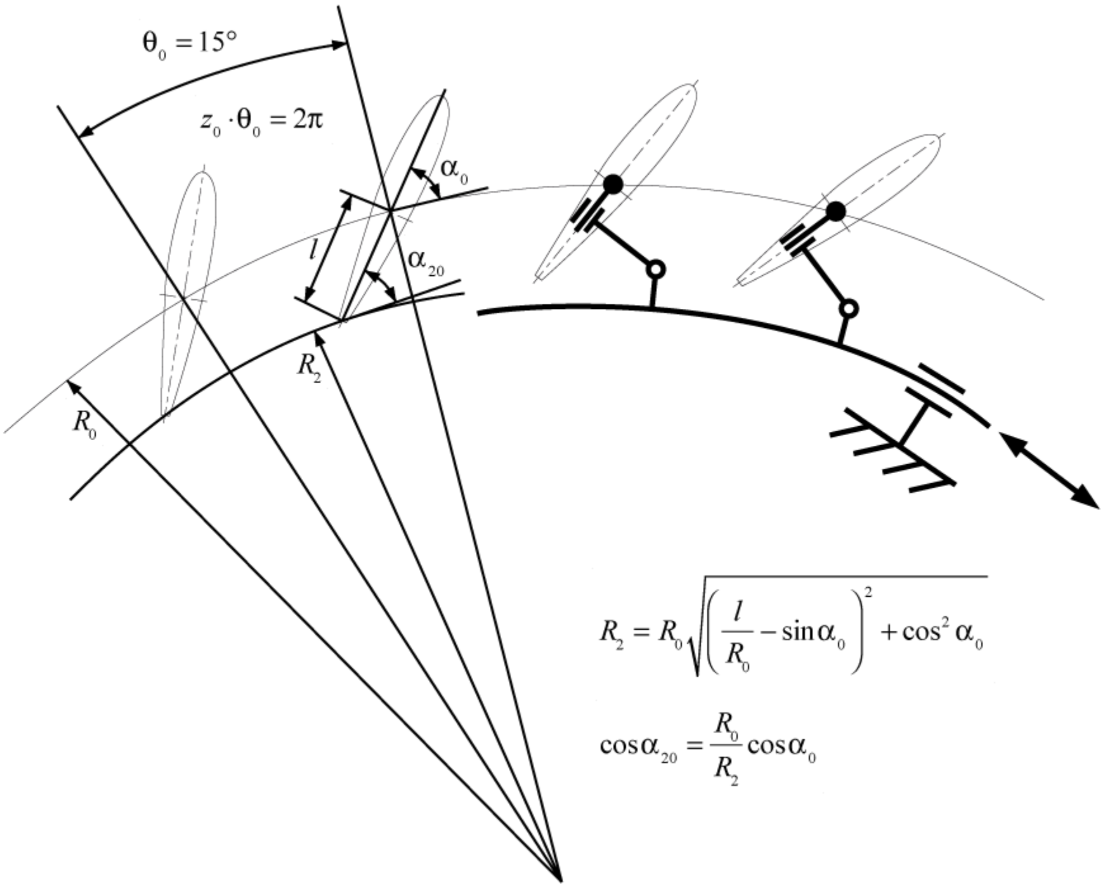

Figure 25 - Guide vanes (z_o = 24) geometrical relations

At closed position, the guide vane opening angle α_o is offset.

1.4 Runner and Impeller

The power conversion takes place in the runner (impeller in the case of a pump). Indeed, the change of angular momentum when the flow passing through the runner generates a resulting torque on the runner. This torque is appied to the generator by the shaft.

To convert efficiently the available hydropower resources, the units of large hydraulic power plants are engineered to fit the specific hydraulic conditions of the site, *i.e.* head and yearly flow duration curves. The type of units is strongly dependent on the values of the head of the power plant ranging, from Pelton, Francis, Kaplan to Bulb Turbines for large, medium, low and small head value respectively, see Figure 26 .

The appropriate operating range of a runner type is charted in this figure as a function of head H and specific speed ν , which is defined as

$$\nu = \frac{\omega \cdot \sqrt{Q}}{\sqrt{\pi}\left(2E\right)^{\frac{3}{4}}} \tag{78}$$

with

- ω runner (impeller) angular speed;
- $E = gH_I - gH_{\bar{I}}$ the available (turbine) or supplied (pump) specific energy.

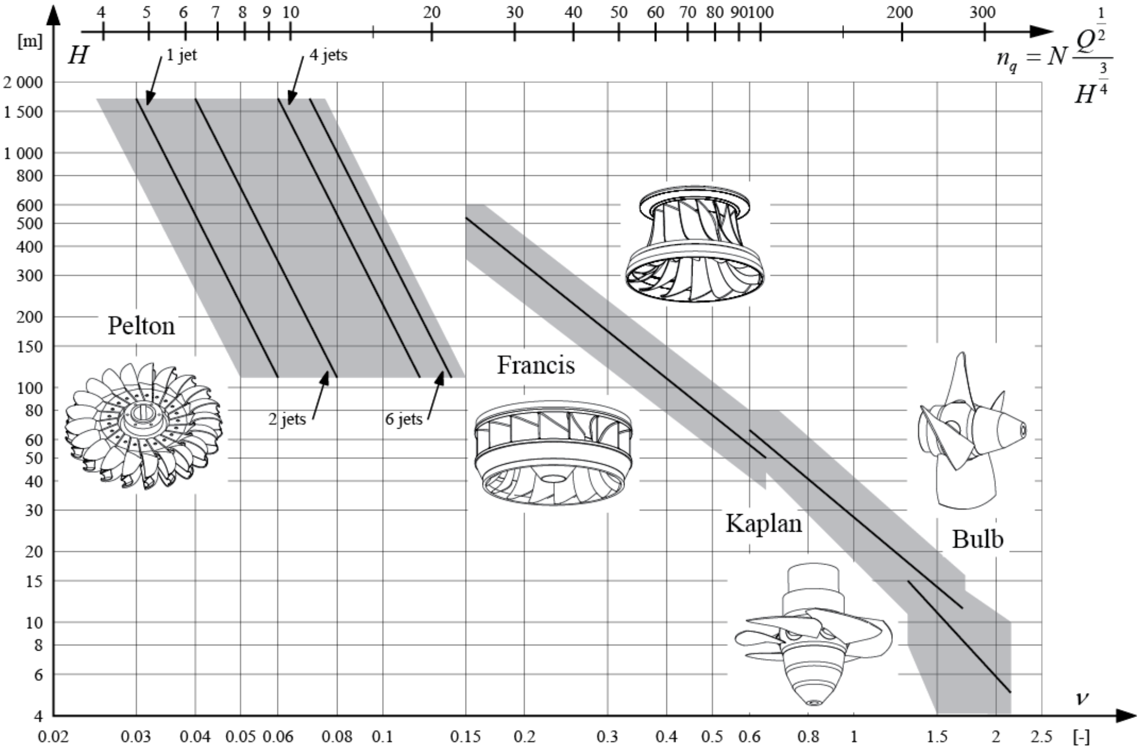

Figure 26 - Appropriate operating range for the different turbine runner types

The impeller converts the mechanical power into a pressure increase. However, an impeller may be also used as a turbine in the particular case of pump-turbine power unit.

The usual operating range of a pump-turbine as function of the head H and specific speed ν is shown in Figure 27.

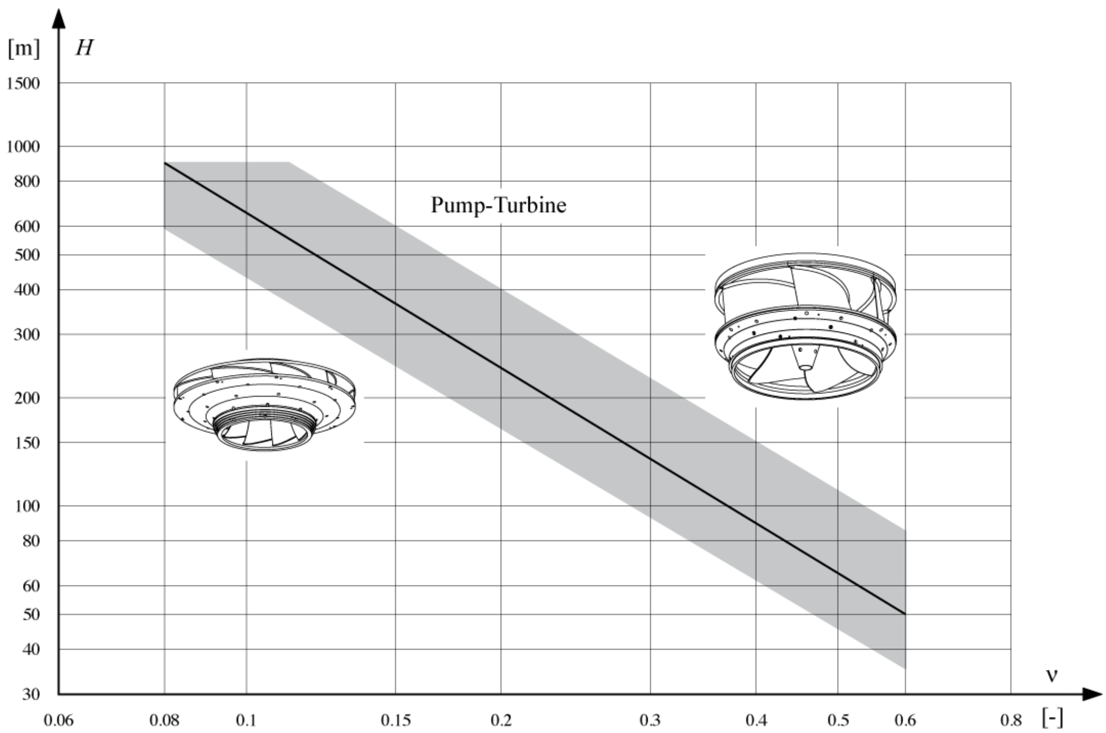

Figure 27 - Appropriate operating range for storage pump impeller

1.5 Draft Tube

As shown in Figure 28, the elbow draft tube is made of a cone, an elbow and a diffuser. The aim of the draft tube is to recover the flow kinetic energy and convert into static pressure.

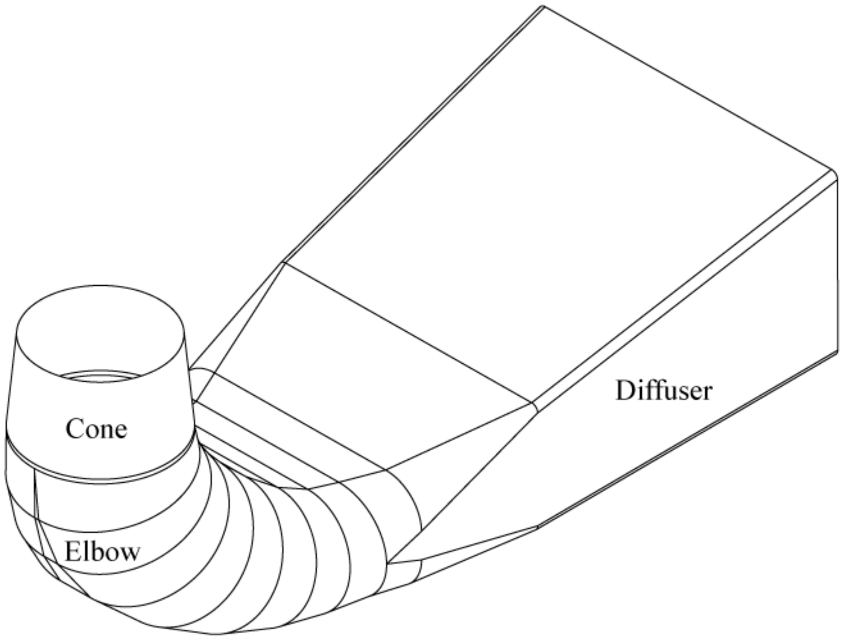

Figure 28 – Elbow draft tube components

2 OPERATING PRINCIPLES

2.1 Turbine Mode

In turbine mode, the specific energy balance between the headwater and tailwater reservoirs and and the limits of the turbine yields

$$E \doteq gH_I - gH_{\bar{I}} = \left(gH_B - gH_{\bar{B}}\right) - \sum gH_{rB \div \bar{B}} \tag{79}$$

and the transferred specific energy is expressed as

$$E_t = E - \sum E_{rI \div \bar{I}} \tag{80}$$

Specific energy distribution along the hydraulic circuit of the installation in generating mode is represented in Figure 29.

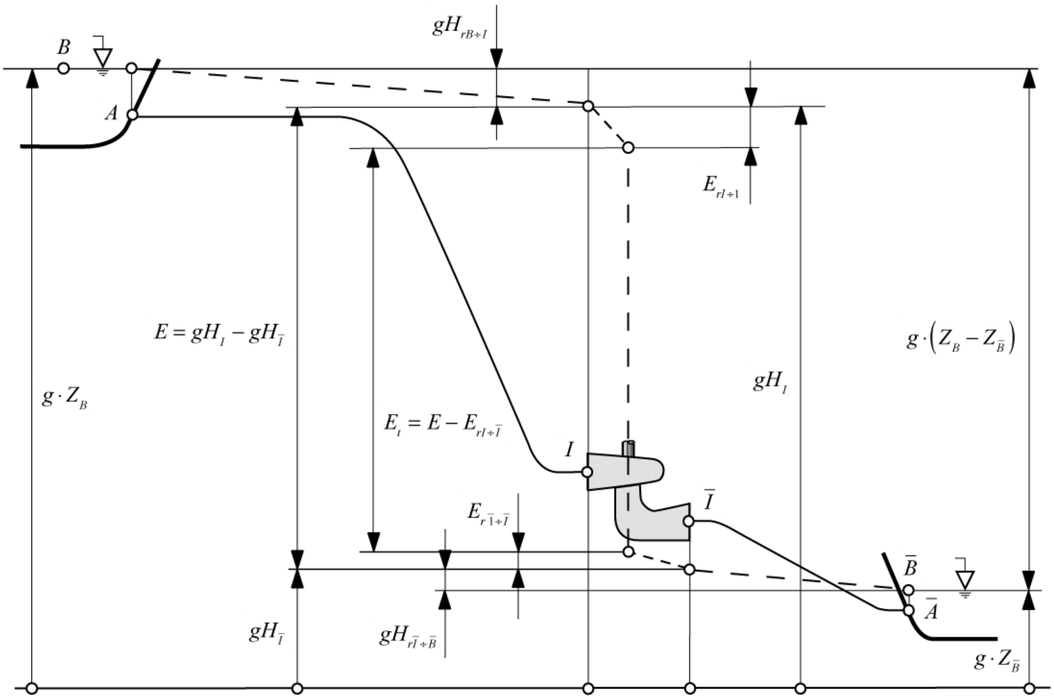

Figure 29 - Specific energy evolution in generating mode

2.2 Pump Mode

In pump mode, the supplied specific energy E is derived from the specific energy balance between the headwater and tailwater reservoirs and the limits of the pump, yielding

$$E = gH_I - gH_{\bar{I}} = \left(gH_B - gH_{\bar{B}}\right) + \sum gH_{rB \div \bar{B}} \tag{81}$$

and the transferred specific energy is expressed as

$$E_t = E + \sum E_{rI \div \bar{I}} \tag{82}$$

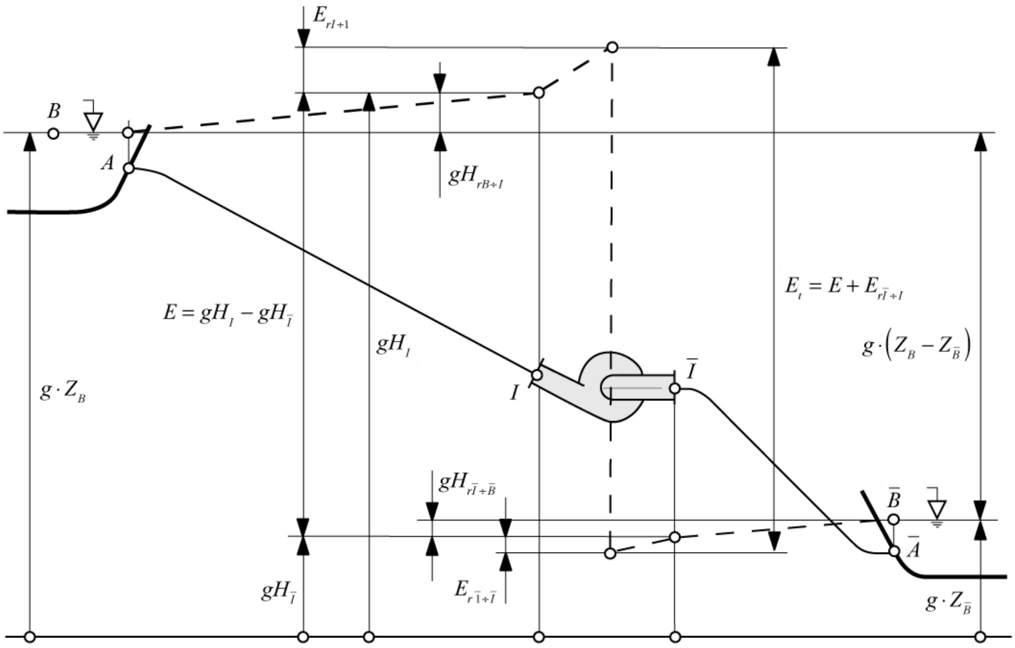

Figure 30 - Specific energy evolution in pumping mode

Specific energy distribution along the hydraulic circuit of the installation in pumping mode is represented in Figure 30.

2.3 Power and Efficiency

The hydraulic power of the unit is defined as

$$P_h = \rho \times Q \times E \quad \text{with} \begin{cases} P_h > 0 & \text{in turbine mode} \\ P_h < 0 & \text{in pump mode} \end{cases} \tag{83}$$

Therefore, the transferred power is

$$P_t = \rho \cdot Q_t \cdot E_t \quad \text{with} \begin{cases} P_t > 0 & \text{in turbine mode} \\ P_t < 0 & \text{in pump mode} \end{cases} \tag{84}$$

with Q_t the part of the discharge, which goes through the runner. Finally, the available or supplied power is defined as

$$P = \omega \cdot T \quad \text{where } T \text{ is the torque at the shaft with} \begin{cases} P > 0 & \text{in turbine mode} \\ P < 0 & \text{in pump mode} \end{cases} \tag{85}$$

As the specific energy is always defined positive, the negative discharge value in pump mode is due to the negative definition of the power. In the same way the torque is always defined positive, and so, the rotational speed is negative in pump mode.

The global efficiency of the power unit is given by

$$\eta = \eta_h \cdot \eta_m = \begin{cases} \dfrac{P}{P_h} & \text{in turbine mode} \\ \dfrac{P_h}{P} & \text{in pump mode} \end{cases} \tag{86}$$

where η_m is efficiency of the bearing and η_h the hydraulic efficiency defined by

$$\eta_h = \eta_e \cdot \eta_q \cdot \eta_{rm} \tag{87}$$

with the efficiency of the disc friction η_{rm}, the volumetric efficiency η_q and the energetic efficiency η_e. The volumetric efficiency is given by

$$\eta_q = \begin{cases} \dfrac{Q_t}{Q} & \text{in turbine mode} \\ \dfrac{Q}{Q_t} & \text{in pump mode} \end{cases} \tag{88}$$

and the energetic efficiency by

$$\eta_e = \begin{cases} \dfrac{E_t}{E} & \text{in turbine mode} \\ \dfrac{E}{E_t} & \text{in pump mode} \end{cases} \tag{89}$$

The outline of the power flow through a turbine and a pump is given in Figure 31.

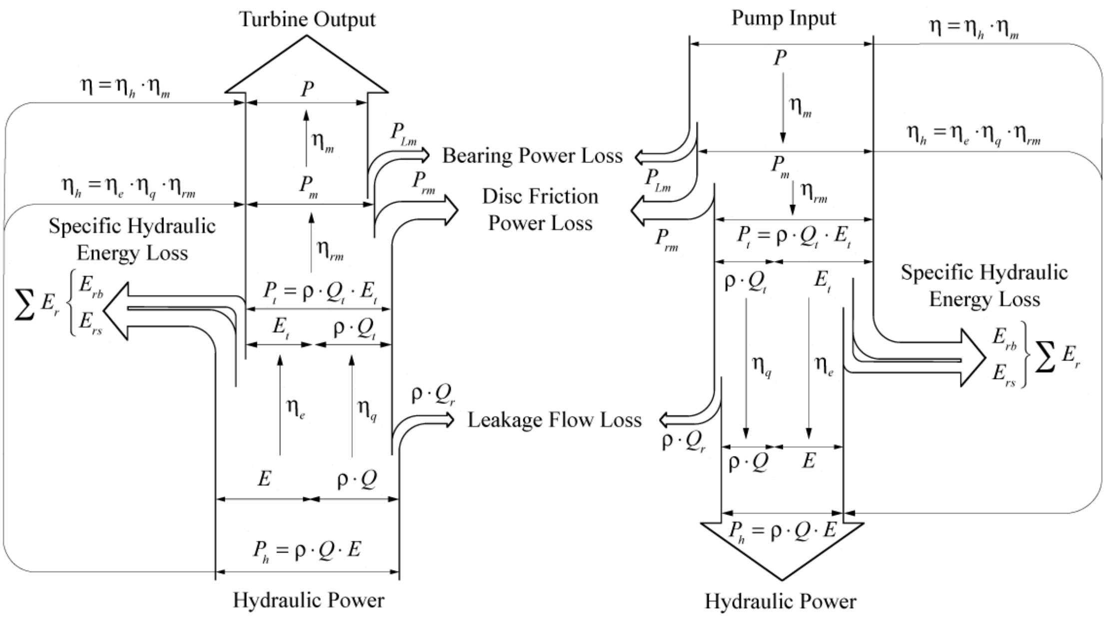

Figure 31 - Power flow through either a turbine or a pump

3 CAVITATION

3.1 Basics

The cavitation phenomenon may appear when the flow static pressure is lower than the vapor pressure p_v; the local cavitation coefficient σ being defined as

$$\sigma = \frac{p_{ref} - p_v}{\frac{1}{2}\rho C_{ref}^2} \tag{91}$$

and the pressure coefficient as

$$Cp = \frac{p - p_{ref}}{\frac{1}{2}\rho C_{ref}^2} \tag{92}$$

The condition of cavitation onset can be expressed as

$$p \le p_v \Leftrightarrow Cp \le -\sigma \tag{93}$$

Cavitation onset condition is represented in Figure 32 for the case of a typical hydraulic 2D blade.

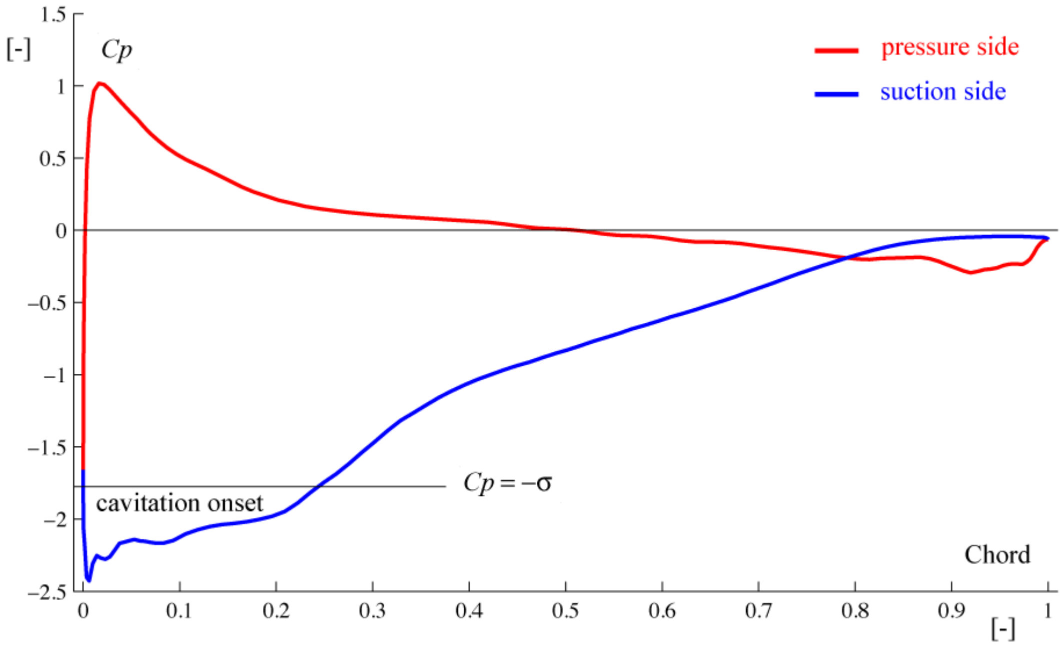

Figure 32 – Pressure coefficient distribution and cavitation onset condition for a hydraulic 2D blade.

3.2 NPSE Net Positive Suction Specific Energy

General definition

In the case of hydraulic machines, there is no reference pressure directly set. Alternatively, IEC Standard defines the $NPSE$ Net Positive Suction Specific Energy value with respect to Z_{ref} the reference elevation of the machine, see Figure 33.

$$NPSE \doteq gH_{\bar{I}} - \frac{p_v}{\rho} - gZ_{ref} \quad \left(\mathrm{J \cdot kg^{-1}}\right) \tag{94}$$

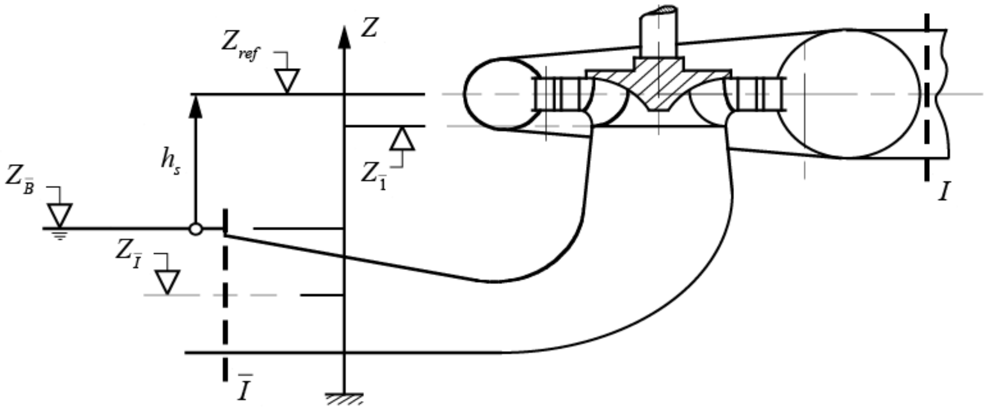

Figure 33 – Vertical hydraulic machine outline and definitions of reference elevation

Furthermore, the Thoma number σ, non dimensional cavitation factor, is introduced as

$$\sigma = \frac{NPSE}{E} \tag{95}$$

The $NPSH$, Net Positive Suction Head is also introduced as

$$NPSH \doteq \frac{NPSE}{g} \quad (\mathrm{m}) \tag{96}$$

Turbine Setting Level

In the case of a hydraulic turbine the $NPSE$ is evaluated with respect to the turbine setting level by expressing the specific hydraulic energy balance between the low energy side $A_{\bar{I}}$ of the hydraulic machine and the tailwater reservoir, yielding

$$gH_{\bar{I}} = gH_{\bar{B}} + gH_{r\bar{I} \div \bar{B}} \tag{97}$$

By assuming that the specific energy loss corresponds to the specific kinetic energy at the low energy side of the turbine

$$gH_{r\bar{I} \div \bar{B}} \approx \frac{C_{\bar{I}}^2}{2} \tag{98}$$

Then, $NPSE$ can be evaluated with respect to the turbine setting as defined in Figure 33

$$NPSE = \frac{p_{atm}}{\rho} - \frac{p_v}{\rho} - g\left(Z_{ref} - Z_{\bar{B}}\right) + \frac{C_{\bar{I}}^2}{2}$$

By introducing $h_s = Z_{ref} - Z_{\bar{B}}$ the setting level of the turbine, see Figure 33, the $NPSE$ definition (94) finally reads

$$NPSE = \frac{p_{atm}}{\rho} - \frac{p_v}{\rho} - gh_s + \frac{C_{\bar{I}}^2}{2} \tag{99}$$

In the case of a Francis turbine, the condition of cavity onset is given by

$$Cp < -\chi_E \tag{100}$$

with

- $Cp = \dfrac{p - p_{\bar{1}}}{\rho E}$ Static Pressure Factor
- $\chi_E = \dfrac{p_{\bar{1}} - p_v}{\rho E} = \sigma - \dfrac{1}{Fr^2}\left(\dfrac{Z_{\bar{1}} - Z_{ref}}{D_{\bar{1}e}}\right) - \dfrac{C_{\bar{1}}^2}{2E} + \dfrac{\sum gH_{r\bar{1}\div\bar{I}}}{E}$ Local Cavitation Factor
- $Fr = \sqrt{\dfrac{E}{gD}}$ Froude Number

Pump Setting Level

In the case of a pump, the $NPSE$ is evaluated with respect to the pump setting level by expressing the specific hydraulic energy balance between the tailwater reservoirt and the low energy side $A_{\bar{I}}$ of the pump, yielding

$$gH_{\bar{B}} = gH_{\bar{I}} + gH_{r\bar{I}\div\bar{B}} \tag{101}$$

By neglecting $gH_{r\bar{I}\div\bar{B}}$, the specific energy loss at the pump intake, is very small the $NPSE$ can be evaluated with respect to the turbine setting as defined in Figure 33

$$NPSE = \frac{p_{atm}}{\rho} - \frac{p_v}{\rho} - g\left(Z_{ref} - Z_{\bar{B}}\right).$$

By introducing $h_s = Z_{ref} - Z_{\bar{B}}$ the setting level of the pump, see Figure 33, the $NPSE$ definition (94) finally reads

$$NPSE = \frac{p_{atm}}{\rho} - \frac{p_v}{\rho} - gh_s \tag{102}$$

VI POWER BALANCE

1 TURBOMACHINERY EQUATIONS

1.1 Rotating Frame of Reference

To describe the flow inside the rotating zone of the hydraulic turbomachine, an appropriate reference frame should be defined. The Cartesian coordinate system is used to represent absolute velocity $\vec{C}$ and the cylindrical coordinate system represents the relative flow velocity $\vec{W}$.

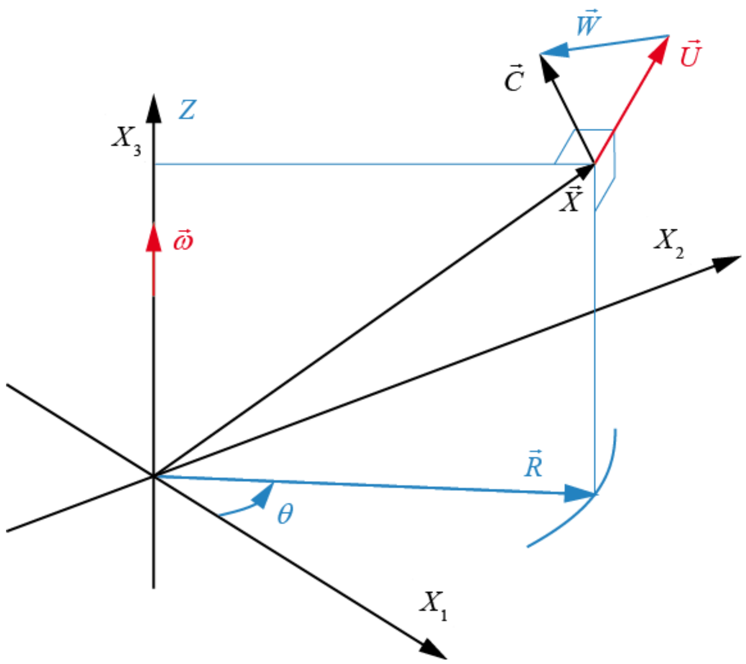

Figure 34 - Cartesian and cylindrical frames of reference

The rotating velocity is computed as

$$\vec{U} = \vec{\omega} \times \vec{X} = \omega R \cdot \vec{\theta}^0 \text{ or in Cartesian coordinates } U_i = \varepsilon_{ijk} \omega_j X_k \quad (103)$$

Consequently, the relation between the absolute and relative flow is given by

$$\vec{C} = \vec{U} + \vec{W} \quad \text{or} \quad \vec{W} = \vec{C} - \vec{U} \quad (104)$$

1.2 The Total Specific Rothalpy Conservation

Relative specific kinetic energy

The Reynolds equation in the relative reference frame is expressed as

$$\frac{D\vec{W}}{Dt} = -\vec{\nabla}\left(\frac{p}{\rho} + gZ - \frac{\vec{U}^2}{2}\right) + 2\vec{\omega} \times \vec{W} + \vec{\nabla} \cdot \left(2\nu \overline{\overline{D}} + \frac{\overline{\overline{\tau}}_t}{\rho}\right) \quad \left(\mathrm{m} \cdot \mathrm{s}^{-2}\right) \quad (105)$$

The $\vec{W}$ scalar product with equation (105) yields the relative specific kinetic energy change with time

$$\vec{W}\cdot\frac{D\vec{W}}{Dt}=\frac{D}{Dt}\left(\frac{\vec{W}^{2}}{2}\right) \qquad \left(\mathrm{W}\cdot\mathrm{kg}^{-1}\right) \quad (106)$$

Therefore, it can be written

$$\frac{D}{Dt}\left(\frac{\vec{W}^{2}}{2}\right)=\vec{W}\cdot\left[-\vec{\nabla}\left(\frac{p}{\rho}+gZ-\frac{\vec{U}^{2}}{2}\right)\right]+\underbrace{\vec{W}\cdot\left(2\vec{\omega}\times\vec{W}\right)}_{=0}+\vec{W}\cdot\vec{\nabla}\cdot\left(2\nu\overline{\overline{D}}+\frac{\overline{\overline{\tau}}_{t}}{\rho}\right) \qquad \left(\mathrm{W}\cdot\mathrm{kg}^{-1}\right) \quad (107)$$

However the Coriolis acceleration $2\vec{\omega}\times\vec{W}$ being orthogonal to the relative flow velocity $\vec{W}$ does not contribute to the relative specific kinetic energy change.

By introducing $\overline{\overline{P}}$ the total stress tensor defined as

$$\frac{\overline{\overline{P}}}{\rho}=-\left(\frac{p}{\rho}+gZ-\frac{\vec{U}^{2}}{2}\right)\overline{\overline{I}}+2\nu\overline{\overline{D}}+\frac{\overline{\overline{\tau}}_{t}}{\rho} \quad (108)$$

Specific kinetic energy balance equation (107) reads in compact form

$$\frac{D}{Dt}\left(\frac{\vec{W}^{2}}{2}\right)=\vec{W}\cdot\left(\vec{\nabla}\cdot\frac{\overline{\overline{P}}}{\rho}\right) \qquad \left(\mathrm{W}\cdot\mathrm{kg}^{-1}\right) \quad (109)$$

As the relative flow is assumed to be <u>incompressible</u>, the left hand side of equation (109) reads

$$\begin{aligned}\frac{D}{Dt}\left(\frac{\vec{W}^{2}}{2}\right)&=\frac{\partial}{\partial t}\left(\frac{\vec{W}^{2}}{2}\right)+\left(\vec{W}\cdot\vec{\nabla}\right)\frac{\vec{W}^{2}}{2}=\frac{\partial}{\partial t}\left(\frac{\vec{W}^{2}}{2}\right)+\vec{\nabla}\cdot\left[\frac{\vec{W}^{2}}{2}\vec{W}\right]-\frac{\vec{W}^{2}}{2}\underbrace{\vec{\nabla}\cdot\vec{W}}_{=0}\\&=\frac{\partial}{\partial t}\left(\frac{\vec{W}^{2}}{2}\right)+\vec{\nabla}\cdot\left[\frac{\vec{W}^{2}}{2}\vec{W}\right]\end{aligned} \quad (110)$$

And (109) is written as

$$\frac{\partial}{\partial t}\left(\frac{\vec{W}^{2}}{2}\right)+\vec{\nabla}\cdot\left[\frac{\vec{W}^{2}}{2}\vec{W}\right]=\vec{W}\cdot\left(\vec{\nabla}\cdot\frac{\overline{\overline{P}}}{\rho}\right) \qquad \left(\mathrm{W}\cdot\mathrm{kg}^{-1}\right) \quad (111)$$

By introducing the tensor components, a divergence term can be made apparent in the left hand side of (111):

$$W_i\frac{\partial P_{ij}}{\partial X_j}=\frac{\partial W_iP_{ij}}{\partial X_j}-\frac{\partial W_i}{\partial X_j}P_{ij} \quad (112)$$

However symmetry property of $\overline{\overline{P}}$ yields $P_{ij}=P_{ji}$ therefore

$$\frac{\partial W_iP_{ij}}{\partial X_j}=\frac{\partial W_iP_{ji}}{\partial X_j}=\frac{\partial P_{ji}W_i}{\partial X_j} \quad (113)$$

And substituting (113) into (112) yields

$$W_i\frac{\partial P_{ij}}{\partial X_j}=\frac{\partial P_{ji}W_i}{\partial X_j}-\frac{\partial W_i}{\partial X_j}P_{ij} \quad (114)$$

Or in symbolic notation

$$\vec{W}\cdot\left(\vec{\nabla}\cdot\overline{\overline{P}}\right)=\vec{\nabla}\cdot\left(\overline{\overline{P}}\cdot\vec{W}\right)-\left(\vec{\nabla}\otimes\vec{W}\right):\overline{\overline{P}} \tag{115}$$

The scalar relation (115) remains unchanged by transposition which leads to:

$$\left(\vec{\nabla}\otimes\vec{W}\right):\overline{\overline{P}}=\left[\left(\vec{\nabla}\otimes\vec{W}\right):\overline{\overline{P}}\right]^t \tag{116}$$

Owing the symmetry property of $\overline{\overline{P}}$

$$\left[\left(\vec{\nabla}\otimes\vec{W}\right):\overline{\overline{P}}\right]^t=\left(\vec{\nabla}\otimes\vec{W}\right)^t:\overline{\overline{P}}=\overline{\overline{D}}:\overline{\overline{P}} \tag{117}$$

And then the following relation stands

$$\left(\vec{\nabla}\otimes\vec{W}\right):\overline{\overline{P}}=\frac{1}{2}\left[\left(\vec{\nabla}\otimes\vec{W}\right)+\left(\vec{\nabla}\otimes\vec{W}\right)^t\right]:\overline{\overline{P}}=\overline{\overline{D}}:\overline{\overline{P}} \tag{118}$$

Leading to write (111) as

$$\underbrace{\frac{\partial}{\partial t}\left(\frac{\vec{W}^2}{2}\right)+\vec{\nabla}\cdot\left[\frac{\vec{W}^2}{2}\vec{W}\right]}_{\text{Change of relative specific kinetic energy}}=\underbrace{\vec{\nabla}\cdot\left(\frac{\overline{\overline{P}}}{\rho}\cdot\vec{W}\right)}_{\text{External contribution}}-\underbrace{\left(\overline{\overline{D}}:\frac{\overline{\overline{P}}}{\rho}\right)}_{\text{Internal contribution}} \qquad \left(\mathrm{W}\cdot\mathrm{kg}^{-1}\right) \tag{119}$$

The change of relative specific kinetic energy is due to both external contribution, the divergence term, and internal contribution, the tensor scalar product.

By substituting the total stress tensor $\overline{\overline{P}}$ definition (108), (119) yields

$$\begin{aligned}\frac{D}{Dt}\left(\frac{\vec{W}^2}{2}\right)&=\frac{\partial}{\partial t}\left(\frac{\vec{W}^2}{2}\right)+\vec{\nabla}\cdot\left(\frac{\vec{W}^2}{2}\vec{W}\right)\\&=\vec{\nabla}\cdot\left(\left\{-\left(\frac{p}{\rho}+gZ-\frac{\vec{U}^2}{2}\right)\overline{\overline{I}}+2\nu\overline{\overline{D}}+\frac{\overline{\overline{\tau_t}}}{\rho}\right\}\cdot\vec{W}\right)\\&\quad-\left(\left\{-\left(\frac{p}{\rho}+gZ-\frac{U^2}{2}\right)\overline{\overline{I}}+2\nu\overline{\overline{D}}+\frac{\overline{\overline{\tau_t}}}{\rho}\right\}:\overline{\overline{D}}\right)\end{aligned} \qquad \left(\mathrm{W}\cdot\mathrm{kg}^{-1}\right) \tag{120}$$

The divergence term of (120) left hand side corresponding to external contribution of relative specific energy reads:

$$\vec{\nabla}\cdot\left[\left\{-\left(\frac{p}{\rho}+gZ-\frac{U^2}{2}\right)\overline{\overline{I}}\right\}\cdot\vec{W}\right]=-\vec{\nabla}\cdot\left\{\left(\frac{p}{\rho}+gZ-\frac{\vec{U}^2}{2}\right)\vec{W}\right\}$$

While the tensor scalar product corresponding to external contribution to energy dissipation reads

$$\begin{aligned}-\left(\left\{-\left(\frac{p}{\rho}+gZ-\frac{U^2}{2}\right)\overline{\overline{I}}+2\nu\overline{\overline{D}}+\frac{\overline{\overline{\tau_t}}}{\rho}\right\}:\overline{\overline{D}}\right)&=\left(\frac{p}{\rho}+gZ-\frac{\vec{U}^2}{2}\right)\overline{\overline{I}}:\overline{\overline{D}}-2\nu\overline{\overline{D}}:\overline{\overline{D}}-\frac{\overline{\overline{\tau_t}}}{\rho}:\overline{\overline{D}}\\&=\left(\frac{p}{\rho}+gZ-\frac{\vec{U}^2}{2}\right)\underbrace{\left(\vec{\nabla}\cdot\vec{C}\right)}_{\substack{=0\\ \text{for incompressible flow}}}-2\nu\overline{\overline{D}}:\overline{\overline{D}}-\frac{\overline{\overline{\tau_t}}}{\rho}:\overline{\overline{D}}\end{aligned}$$

For incompressible flow, the static pressure is not involved in the energy dissipation!

Finally, the balance (120) of relative specific kinetic energy reads

$$\begin{aligned}\frac{D}{Dt}\left(\frac{\vec{W}^2}{2}\right)&=\frac{\partial}{\partial t}\left(\frac{\vec{W}^2}{2}\right)+\vec{\nabla}\cdot\left(\frac{\vec{W}^2}{2}\vec{W}\right)\\&=-\vec{\nabla}\cdot\left(\left\{\frac{p}{\rho}+gZ-\frac{\vec{U}^2}{2}\right\}\vec{W}\right)+\vec{\nabla}\cdot\left(\left\{2\nu\overline{\overline{D}}+\frac{\overline{\overline{\tau}}_t}{\rho}\right\}\cdot\vec{W}\right)-2\nu\overline{\overline{D}}:\overline{\overline{D}}-\frac{\overline{\overline{\tau}}_t}{\rho}:\overline{\overline{D}}\end{aligned}\qquad(121)$$

Local total specific rothalpy balance equation

The local total specific rothalpy can be made apparent in the relative specific kinetic energy balance expression (121), yielding

$$\begin{aligned}\vec{\nabla}\cdot\left(\left\{\underbrace{\frac{p}{\rho}+gZ-\frac{\vec{U}^2}{2}+\frac{\vec{W}^2}{2}}_{\text{Local total specific rothalpy}}\right\}\vec{W}\right)&=-2\nu\overline{\overline{D}}:\overline{\overline{D}}-\frac{\overline{\overline{\tau}}_t}{\rho}:\overline{\overline{D}}\\&\quad-\vec{\nabla}\cdot\left(\left\{2\nu\overline{\overline{D}}+\frac{\overline{\overline{\tau}}_t}{\rho}\right\}\cdot\vec{W}\right)-\frac{\partial}{\partial t}\left(\frac{\vec{W}^2}{2}\right)\end{aligned}\qquad\left(\mathrm{W\cdot kg^{-1}}\right)\quad(122)$$

Thus, the net flux of the local total specific energy of the relative flow is balanced by *i)* internal specific energy dissipation rate due to viscosity and turbulence, *ii)* both viscous and turbulent stress work per unit of time and *iii)* a contribution of mean relative flow unsteadiness, if any.

In the case of inviscid flow in steady relative motion, local total specific rothalpy balance equation (122) simply yields

$$\vec{\nabla}\cdot\left[\left(\frac{p}{\rho}+gZ-\frac{\vec{U}^2}{2}+\frac{\vec{W}^2}{2}\right)\vec{W}\right]=0\qquad\left(\mathrm{W\cdot kg^{-1}}\right)\quad(123)$$

The local total specific rothalpy remains constant in the case of inviscid flow in steady relative motion.

1.3 Runner Impeller Global Power Transfer

Turbine Runner Hydraulic Power balance

By taking into account the power transfer between the flow and the runner P_t and the rate of energy internal dissipation P_{r_b} by both viscosity and turbulent production, the hydraulic power balance (31) applied to the turbine runner flow passages defined by the control volume V, see Figure 35 bounded by $\partial V = A_1 \cup \Sigma_b \cup A_{\bar{1}}$ the runner blade to blade channel walls Σ_b and the high and low energy fluid sections A_1, $A_{\bar{1}}$, respectively, yields:

$$\begin{aligned}\underbrace{-\int_{A_1}\left\{\frac{p}{\rho}+gZ+\frac{\vec{C}^2}{2}\right\}\rho\vec{C}_1\cdot\vec{n}_1 dA_1}_{A_1\text{ Mean flow power}}&=\underbrace{\int_{A_{\bar{1}}}\left\{\frac{p}{\rho}+gZ+\frac{\vec{C}^2}{2}\right\}\rho\vec{C}_{\bar{1}}\cdot\vec{n}_{\bar{1}} dA_{\bar{1}}}_{A_{\bar{1}}\text{ Mean flow power}}+P_t+P_{r_b}\\&\quad\underbrace{-\int_{A_1\cup A_{\bar{1}}}\left[\rho\left\{2\nu\overline{\overline{D}}+\frac{\overline{\overline{\tau}}_t}{\rho}\right\}\cdot\vec{C}\right]\cdot\vec{n}dA}_{\text{Net power budget of both viscous and turbulent stresses}}\\&\quad+\underbrace{\int_V\frac{\partial}{\partial t}\frac{\vec{C}^2}{2}\rho dV}_{\text{Time change of mean flow kinetic energy}}\end{aligned}\qquad(124)$$

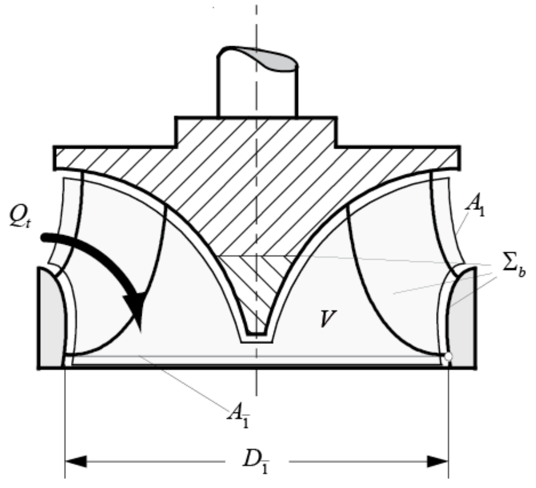

Figure 35 – Control volume for the balance of angular momentum in the runner

The change of hydraulic power of the mean flow through the runner-impeller is due to:

1. the power transfer between the flow and the runner P_t;
2. the rate of energy internal dissipation P_{r_b} by both viscosity and turbulent production;
3. the net power budget of both viscous and turbulent stresses;
4. the rate of the mean flow kinetic energy change.

Therefore, rearranging (124) to make apparent the balance of the power transfer between the flow and the runner P_t and the rate of energy internal dissipation P_{r_b} yields:

$$P_t + P_{r_b} = -\int_{A_1 \cup A_{\bar{1}}} \left\{ \frac{p}{\rho} + gZ + \frac{\vec{C}^2}{2} \right\} \rho \vec{C}_{\bar{1}} \cdot \vec{n}_{\bar{1}} dA_{\bar{1}} + \int_{A_1 \cup A_{\bar{1}}} \left[\rho \left\{ 2\nu \overline{\overline{D}} + \frac{\overline{\overline{\tau}}_t}{\rho} \right\} \cdot \vec{C} \right] \cdot \vec{n} dA - \int_V \frac{\partial}{\partial t} \frac{\vec{C}^2}{2} \rho dV \qquad (125)$$

Expanding the 1st term of (125) right hand side yields

$$P_t + P_{r_b} = -\int_{A_1 \cup A_{\bar{1}}} \left(\frac{p}{\rho} + gZ \right) \rho \vec{C} \cdot \vec{n} dA - \int_{A_1 \cup A_{\bar{1}}} \frac{\vec{C}^2}{2} \rho \vec{C} \cdot \vec{n} dA + \int_{A_1 \cup A_{\bar{1}}} \rho \left[\left\{ 2\nu \overline{\overline{D}} + \frac{\overline{\overline{\tau}}_t}{\rho} \right\} \cdot \vec{C} \right] \cdot \vec{n} dA - \int_V \frac{\partial}{\partial t} \frac{\vec{C}^2}{2} \rho dV \qquad (126)$$

Runner Total Specific Rothalpy Balance

Furthermore, the runner total specific rothalpy balance is achieved by integrating equation (122) over the control volume V bounded by $\partial V = A_1 \cup \Sigma_B \cup A_{\bar{1}}$ and by applying the divergence theorem. Then, the specific total rothalpy conservation yields the following global balance equation

$$\int_{\partial V} \left(\frac{p}{\rho} + gZ - \frac{\vec{U}^2}{2} + \frac{\vec{W}^2}{2} \right) \vec{W} \cdot \vec{n} dA = \int_{\partial V} \left(\left\{ 2\nu \overline{\overline{D}} + \frac{\overline{\overline{\tau}}}{\rho} \right\} \cdot \vec{W} \right) \cdot \vec{n} dA - \int_V \left\{ +2\nu \overline{\overline{D}} : \overline{\overline{D}} + \frac{\overline{\overline{\tau}}}{\rho} : \overline{\overline{D}} \right\} dV - \int_V \frac{\partial}{\partial t} \frac{\vec{W}^2}{2} dV \qquad (127)$$

At the runner wall Σ_b and at A_1 and $A_{\bar{1}}$ fluid section, the kinematic conditions $\vec{W}\cdot\vec{n}_\Sigma = 0$ and $\vec{W}\cdot\vec{n} = \vec{C}\cdot\vec{n}$ stand, respectively, therefore (127) is rearranged to yield

$$\begin{aligned}\int\limits_{A_1\cup A_{\bar{1}}} \left(\frac{p}{\rho}+gZ\right)\vec{C}\cdot\vec{n}dA = &-\int\limits_{A_1\cup A_{\bar{1}}}\left(-\frac{\vec{U}^2}{2}+\frac{\vec{W}^2}{2}\right)\vec{C}\cdot\vec{n}dA \\ &+\int\limits_{\partial V}\left(\left\{2\nu\bar{\bar{D}}+\frac{\bar{\bar{\tau}}}{\rho}\right\}\cdot\vec{W}\right)\cdot\vec{n}dA \\ &-\int\limits_{V}\left\{+2\nu\bar{\bar{D}}:\bar{\bar{D}}+\frac{\bar{\bar{\tau}}}{\rho}:\bar{\bar{D}}\right\}dV - \int\limits_{V}\frac{\partial}{\partial t}\frac{\vec{W}^2}{2}dV\end{aligned} \qquad (128)$$

Hydraulic Power Transfer to the Turbine Runner

Substituting (128) into (126) yields

$$\begin{aligned}P_t + P_{r_b} = &+\int\limits_{A_1\cup A_{\bar{1}}}\left(-\frac{\vec{U}^2}{2}+\frac{\vec{W}^2}{2}\right)\vec{C}\cdot\vec{n}dA - \int\limits_{A_1\cup A_{\bar{1}}}\frac{\vec{C}^2}{2}\rho\vec{C}\cdot\vec{n}dA \\ &+\int\limits_{V}\left\{+2\nu\bar{\bar{D}}:\bar{\bar{D}}+\frac{\bar{\bar{\tau}}}{\rho}:\bar{\bar{D}}\right\}dV \\ &+\int\limits_{A_1\cup A_{\bar{1}}}\rho\left[\left\{2\nu\bar{\bar{D}}+\frac{\bar{\bar{\tau}}_t}{\rho}\right\}\cdot\vec{C}\right]\cdot\vec{n}dA - \int\limits_{\partial V}\left(\left\{2\nu\bar{\bar{D}}+\frac{\bar{\bar{\tau}}}{\rho}\right\}\cdot\vec{W}\right)\cdot\vec{n}dA \\ &-\int\limits_{V}\frac{\partial}{\partial t}\frac{\vec{C}^2}{2}\rho dV + \int\limits_{V}\frac{\partial}{\partial t}\frac{\vec{W}^2}{2}dV\end{aligned} \qquad (129)$$

Or by rearranging the right hand side of (129)

$$\begin{aligned}P_t + P_{r_b} = &\int\limits_{A_1\cup A_{\bar{1}}}\left(-\frac{\vec{C}^2}{2}-\frac{\vec{U}^2}{2}+\frac{\vec{W}^2}{2}\right)\rho\vec{C}\cdot\vec{n}dA + \int\limits_{A_1\cup A_{\bar{1}}}\rho\left(\left\{2\nu\bar{\bar{D}}+\frac{\bar{\bar{\tau}}_t}{\rho}\right\}\cdot\left(\vec{C}-\vec{W}\right)\right)\cdot\vec{n}dA \\ &+\int\limits_{V}\left\{+2\nu\bar{\bar{D}}:\bar{\bar{D}}+\frac{1}{\rho}\bar{\bar{\tau}}_t:\bar{\bar{D}}\right\}\rho dV - \int\limits_{V}\frac{\partial}{\partial t}\frac{\vec{C}^2}{2}\rho dV\end{aligned} \qquad (130).$$

Using (104) to substitute $\vec{W} = \vec{C} - \vec{U}$ in (130) yields

$$\begin{aligned}P_t + P_{r_b} = &-\int\limits_{A_1\cup A_{\bar{1}}}\left(\vec{C}\cdot\vec{U}\right)\rho\vec{C}\cdot\vec{n}dA + \int\limits_{A_1\cup A_{\bar{1}}}\rho\left(\left\{2\nu\bar{\bar{D}}+\frac{\bar{\bar{\tau}}_t}{\rho}\right\}\cdot\vec{U}\right)\cdot\vec{n}dA \\ &+\int\limits_{V}\rho\left\{2\nu\bar{\bar{D}}:\bar{\bar{D}}+\frac{\bar{\bar{\tau}}_t}{\rho}:\bar{\bar{D}}\right\}dV - \int\limits_{V}\frac{\partial}{\partial t}\frac{\vec{C}^2}{2}\rho dV\end{aligned} \qquad (131)$$

where the identity $\vec{W}^2 = \vec{C}^2 - 2\vec{C}\cdot\vec{U} + \vec{U}^2$ was used.

Therefore, by introducing the power dissipation by both viscosity and turbulence, (24), the net hydraulic power budget at the limits A_1 and $A_{\bar{1}}$ of the runner blade to blade flow passages reads:

$$\begin{aligned} P_t + P_{r_b} = &- \int\limits_{A_1 \cup A_{\bar{1}}} \left(\vec{C} \cdot \vec{U}\right) \rho \vec{C} \cdot \vec{n} dA + \int\limits_{A_1 \cup A_{\bar{1}}} \left(\left\{\overline{\overline{\tau}} + \overline{\overline{\tau}}_t\right\} \cdot \vec{U}\right) \cdot \vec{n} dA \\ &+ \int\limits_V \left(\Phi + \Pi\right) \rho dV - \int\limits_V \frac{\partial}{\partial t} \frac{\vec{C}^2}{2} \rho dV \end{aligned} \qquad (132)$$

1.4 Resulting moment of flow action on the runner

The integration of the relative flow angular momentum equation applied to the turbine runner flow passages defined by the control volume V, see Figure 35 bounded by $\partial V = A_1 \cup \Sigma_b \cup A_{\bar{1}}$ the runner blade to blade channel walls Σ_b and the high and low energy fluid sections A_1, $A_{\bar{1}}$, respectively, yields:

$$\begin{aligned} \int_V \frac{\partial}{\partial t}\left(\vec{X} \times \rho \vec{W}\right) dV + \int_{\partial V} \left(\vec{X} \times \rho \vec{W}\right) \vec{W} \cdot \vec{n} dA = &- \int_V \vec{X} \times \left(2\vec{\omega} \times \rho \vec{W}\right) dV - \int_V \vec{X} \times \left(\vec{\omega} \times \left(\vec{\omega} \times \rho \vec{X}\right)\right) dV \\ &- \int_{A_1 \cup A_{\bar{1}}} \vec{X} \times \left(p + \rho g Z\right) \vec{n} dA + \int_{A_1 \cup A_{\bar{1}}} \vec{X} \times \left(\left\{\overline{\overline{\tau}} + \overline{\overline{\tau}}_t\right\} \cdot \vec{n}\right) dA \\ &\underbrace{- \int_{\Sigma_b} \vec{X} \times \left(p + \rho g Z\right) \vec{n} dA + \int_{\Sigma_b} \vec{X} \times \left(\left\{\overline{\overline{\tau}} + \overline{\overline{\tau}}_t\right\} \cdot \vec{n}\right) dA}_{-\vec{T}_t} \end{aligned} \qquad (133)$$

The resulting moment $\vec{T}_t$ of the flow action on the runner blade-to-blade channel walls Σ_b is made apparent in (133) as:

$$-\vec{T}_t = \int\limits_{\Sigma_b} \vec{X} \times \left(-p - \rho g Z\right) \vec{n} dA + \int\limits_{\Sigma_b} \vec{X} \times \left(\left\{\overline{\overline{\tau}} + \overline{\overline{\tau}}_t\right\} \cdot \vec{n}\right) dA \qquad (134)$$

Therefore, substituting (134) into (133) yields the resulting moment of flow action on the runner

$$\begin{aligned} \vec{T}_t = &- \int\limits_V \vec{X} \times \rho \frac{\partial \vec{W}}{\partial t} dV - \int\limits_{\partial V} \left(\vec{X} \times \rho \vec{W}\right) \vec{W} \cdot \vec{n} dA \\ &- \int\limits_V \vec{X} \times \left(2\vec{\omega} \times \rho \vec{W}\right) dV - \int\limits_V \vec{X} \times \left(\vec{\omega} \times \left(\vec{\omega} \times \rho \vec{X}\right)\right) dV \\ &- \int\limits_{A_1 \cup A_{\bar{1}}} \vec{X} \times \left(p + \rho g Z\right) \vec{n} dA + \int\limits_{A_1 \cup A_{\bar{1}}} \vec{X} \times \left(\left\{\overline{\overline{\tau}} + \overline{\overline{\tau}}_t\right\} \cdot \vec{n}\right) dA \end{aligned} \qquad (135)$$

1.5 Power Transferred to the Runner

The flow transferred power to the runner $P_t = \vec{T}_t \cdot \vec{\omega}$ is obtained from the scalar product of the resulting moment $\vec{T}_t$ with $\vec{\omega}$

$$\begin{aligned}\vec{\omega}\cdot\vec{T}_t = P_t = \rho Q_t E_t \\ &= -\int_V \vec{\omega}\cdot\left(\vec{X}\times\rho\frac{\partial\vec{W}}{\partial t}\right)dV - \int_{\partial V}\vec{\omega}\cdot\left(\vec{X}\times\rho\vec{W}\right)\vec{W}\cdot\vec{n}dA \\ &-\int_V \vec{\omega}\cdot\left(\vec{X}\times\left(2\vec{\omega}\times\rho\vec{W}\right)\right)dV - \int_V \vec{\omega}\cdot\left(\vec{X}\times\left(\vec{\omega}\times\left(\vec{\omega}\times\rho\vec{X}\right)\right)\right)dV \\ &- \int_{A_1\cup A_{\bar{1}}}\vec{\omega}\cdot\left(\vec{X}\times\left(p+\rho gZ\right)\vec{n}\right)dA + \int_{A_1\cup A_{\bar{1}}}\vec{\omega}\cdot\left(\vec{X}\times\left(\left\{\overline{\overline{\tau}}+\overline{\overline{\tau}}_t\right\}\cdot\vec{n}\right)\right)dA\end{aligned} \quad (136)$$

The symmetry property of the triple product $\vec{A}\cdot\left(\vec{B}\times\vec{C}\right)=\vec{B}\cdot\left(\vec{C}\times\vec{A}\right)=\vec{C}\cdot\left(\vec{A}\times\vec{B}\right)$ yields the following identities:

$$\vec{\omega}\cdot\left(\vec{X}\times\rho\frac{\partial\vec{W}}{\partial t}\right)=\vec{X}\cdot\left(\rho\frac{\partial\vec{W}}{\partial t}\times\vec{\omega}\right)=\rho\frac{\partial\vec{W}}{\partial t}\cdot\left(\vec{\omega}\times\vec{X}\right)=\rho\frac{\partial\vec{W}}{\partial t}\cdot\vec{U} \quad (137);$$

$$\vec{\omega}\cdot\left(\vec{X}\times\rho\vec{W}\right)=\vec{X}\cdot\left(\rho\vec{W}\times\vec{\omega}\right)=\rho\vec{W}\cdot\left(\vec{\omega}\times\vec{X}\right)=\rho\vec{W}\cdot\vec{U} \quad (138);$$

$$\vec{\omega}\cdot\left(\vec{X}\times\left(2\vec{\omega}\times\rho\vec{W}\right)\right)=\left(2\vec{\omega}\times\rho\vec{W}\right)\cdot\vec{U} \quad (139);$$

$$\vec{\omega}\cdot\left(\vec{X}\times\left(\vec{\omega}\times\left(\vec{\omega}\times\rho\vec{X}\right)\right)\right)=\left(\vec{\omega}\times\left(\vec{\omega}\times\rho\vec{X}\right)\right)\cdot\vec{U}=\left(\vec{\omega}\times\rho\vec{U}\right)\cdot\vec{U} \quad (140);$$

$$\vec{\omega}\cdot\left(\vec{X}\times\left(p+\rho gZ\right)\vec{n}\right)=\left(p+\rho gZ\right)\vec{n}\cdot\vec{U} \quad (141);$$

and

$$\vec{\omega}\cdot\left(\vec{X}\times\left(\left\{\overline{\overline{\tau}}+\overline{\overline{\tau}}_t\right\}\cdot\vec{n}\right)\right)=\left(\left\{\overline{\overline{\tau}}+\overline{\overline{\tau}}_t\right\}\cdot\vec{n}\right)\cdot\vec{U} \quad (142).$$

Therefore, the flow power transferred to the runner simply reads

$$\begin{aligned}P_t &= -\int_V \rho\frac{\partial\vec{W}}{\partial t}\cdot\vec{U}dV - \int_{\partial V}\left(\rho\vec{W}\cdot\vec{U}\right)\vec{W}\cdot\vec{n}dA \\ &-\int_V\left(2\vec{\omega}\times\rho\vec{W}\right)\cdot\vec{U}dV - \int_V\rho\underbrace{\left(\vec{\omega}\times\vec{U}\right)\cdot\vec{U}dV}_{=0} \\ &- \int_{A_1\cup A_{\bar{1}}}\left(p+\rho gZ\right)\underbrace{\vec{n}\cdot\vec{U}}_{=0}dA + \int_{A_1\cup A_{\bar{1}}}\left(\left\{\overline{\overline{\tau}}+\overline{\overline{\tau}}_t\right\}\cdot\vec{n}\right)\cdot\vec{U}dA\end{aligned} \quad (143)$$

On cylindrical surface A_1 and $A_{\bar{1}}$, the outward normal vector $\vec{n}$ is embedded in the meridional plane, *i.e.* $\vec{n}_1\cdot\vec{U}_1=0$ and $\vec{n}_{\bar{1}}\cdot\vec{U}_{\bar{1}}=0$, therefore the pressure acting on cylindrical surfaces A_1 and $A_{\bar{1}}$ does not contribute to the resulting moment:

$$\int_{A_1}\left(p+\rho gZ\right)_1\vec{n}_1\cdot\vec{U}_1 dA_1 = 0 \text{ and } \int_{A_{\bar{1}}}\left(p+\rho gZ\right)_{\bar{1}}\vec{n}_{\bar{1}}\cdot\vec{U}_{\bar{1}}dA_{\bar{1}}=0 \quad (144)$$

Furthermore, as $\vec{W}=\vec{C}-\vec{U}$, the first surface integral term of the right hand term of (143) can be expressed as

$$-\int_{\partial V}\rho\vec{W}\cdot\vec{U}\vec{W}\cdot\vec{n}dA = -\int_{\partial V}\rho\left(\vec{C}\cdot\vec{U}\right)\vec{W}\cdot\vec{n}dA + \int_{\partial V}\rho\left(\vec{U}\cdot\vec{U}\right)\vec{W}\cdot\vec{n}dA \quad (145)$$

Therefore, the divergence theorem yields the following integral transformation

$$-\int_{\partial V} \rho \vec{W} \cdot \vec{U} \vec{W} \cdot \vec{n} dA = -\int_{\partial V} \rho \left(\vec{C} \cdot \vec{U} \right) \vec{W} \cdot \vec{n} dA + \int_V \vec{\nabla} \cdot \rho \left(\vec{U}^2 \vec{W} \right) dV \tag{146}$$

and with the identity $\vec{\nabla} \vec{U}^2 = 2\vec{U} \times \vec{\omega}$, it reads

$$-\int_{\partial V} \rho \vec{W} \cdot \vec{U} \vec{W} \cdot \vec{n} dA = -\int_{\partial V} \rho \left(\vec{C} \cdot \vec{U} \right) \vec{W} \cdot \vec{n} dA + \int_V \left(2\vec{\omega} \times \rho \vec{W} \right) \cdot \vec{U}\, dV \tag{147}$$

After substitution in (143), the two Coriolis acceleration terms cancel each other and the transferred power equation (143) simply reads

$$P_t = -\int_{\partial V} \rho \left(\vec{C} \cdot \vec{U} \right) \vec{W} \cdot \vec{n} dA + \int_{A_1 \cup A_{\bar{1}}} \left(\left\{ \bar{\bar{\tau}} + \bar{\bar{\tau}}_t \right\} \cdot \vec{n} \right) \cdot \vec{U} dA - \int_V \rho \frac{\partial \vec{W}}{\partial t} \cdot \vec{U} dV \tag{148}$$

By making apparent $\vec{C}$ the absolute flow velocity on the cylindrical surfaces A_1 et $A_{\bar{1}}$ the following relation holds

$$\vec{C} \cdot \vec{n} = \underbrace{\vec{U} \cdot \vec{n}}_{=0 \text{ on } A_1 \text{ and } A_{\bar{1}}} + \vec{W} \cdot \vec{n} = \vec{W} \cdot \vec{n} \tag{149}$$

Both relative and absolute flow velocity vectors are featuring the same meridional component.

Therefore, the final expression for P_t the transferred power reads

$$P_t = -\int_{A_1 \cup A_{\bar{1}}} \left(\vec{C} \cdot \vec{U} \right) \rho \vec{C} \cdot \vec{n} dA + \int_{A_1 \cup A_{\bar{1}}} \left(\left\{ \bar{\bar{\tau}} + \bar{\bar{\tau}}_t \right\} \cdot \vec{n} \right) \cdot \vec{U} dA - \int_V \rho \frac{\partial \vec{W}}{\partial t} \cdot \vec{U} dV \tag{150}$$

1.6 Power Dissipation in the Turbine Runner

Substituting the transferred power expression (150) of P_t into the hydraulic power budget (132) yields

$$\begin{aligned} +P_{r_b} = &+ \int_{A_1 \cup A_{\bar{1}}} \left(\left\{ \bar{\bar{\tau}} + \bar{\bar{\tau}}_t \right\} \cdot \vec{U} \right) \cdot \vec{n} dA - \int_{A_1 \cup A_{\bar{1}}} \left(\left\{ \bar{\bar{\tau}} + \bar{\bar{\tau}}_t \right\} \cdot \vec{n} \right) \cdot \vec{U} dA \\ &+ \int_V \left(\Phi + \Pi \right) \rho dV - \int_V \frac{\partial}{\partial t} \frac{\vec{C}^2}{2} \rho dV + \int_V \rho \frac{\partial \vec{W}}{\partial t} \cdot \vec{U} dV \end{aligned} \tag{151}$$

Owing to the symmetry properties of both the viscous and turbulent stress tensors the following identify stands

$$\begin{aligned} &\left(\left\{ \bar{\bar{\tau}} + \bar{\bar{\tau}}_t \right\} \cdot \vec{U} \right) \cdot \vec{n} = \left(\left\{ \bar{\bar{\tau}} + \bar{\bar{\tau}}_t \right\} \cdot \vec{n} \right) \cdot \vec{U} \\ &\left(\tau_{ij} + \tau_{tij} \right) U_j n_i = \left(\tau_{ij} + \tau_{tij} \right) n_j U_i \\ &\qquad = \left(\tau_{ji} + \tau_{t\,ji} \right) U_i n_j = \left(\tau_{ij} + \tau_{tij} \right) U_j n_i \end{aligned} \tag{152}$$

Therefore, the 1st and the 2nd terms of the right hand side of (151) cancel each other and it simply reads

$$P_{r_b} = + \int_V \left(\Phi + \Pi \right) \rho dV - \int_V \frac{\partial}{\partial t} \frac{\vec{C}^2}{2} \rho dV + \int_V \rho \frac{\partial \vec{W}}{\partial t} \cdot \vec{U} dV \tag{153}$$

Therefore, the dissipated power in the runner by turbulence and viscosity is expressed as

$$P_{r_b} = +\int_V (\Phi + \Pi)\rho dV - \int_V \frac{\partial}{\partial t}\frac{\vec{C}^2}{2}\rho dV + \int_V \rho \frac{\partial \vec{W}}{\partial t}\cdot \vec{U} dV \tag{154}$$

$$-\frac{\partial}{\partial t}\frac{\vec{C}^2}{2} + \frac{\partial \vec{W}}{\partial t}\cdot \vec{U} = ???$$

$$\pm P_{rb} = \int_V \rho \left\{ +2\nu \overline{\overline{D}} : \overline{\overline{D}} + \frac{1}{\rho}\overline{\overline{\tau}}_t : \overline{\overline{D}} \right\} dV \tag{155}$$

1.7 Global Euler Equation

Local form of the global Euler equation

From the transferred power formula expressed in the previous section, the transferred specific energy is defined as

$$E_t = \frac{P_t}{\rho \cdot Q_t} = -\int_{A_1 \cup A_{\bar{1}}} \vec{C}\cdot\vec{U}\frac{\vec{C}\cdot\vec{n}dA}{Q_t} + \frac{1}{Q_t}\int_{A_1 \cup A_{\bar{1}}} \frac{\left(\overline{\overline{\tau}} + \overline{\overline{\tau}}_t\right)\cdot\vec{n}}{\rho}\cdot\vec{U}dA \tag{156}$$

This formula can be expressed in a local form by considering any particular streamline, for example, the transferred specific energy is defined by using the outer, external, streamline between the points $1e$ and $\bar{1}e$.

$$E_t = k_{Cu1e}\left(\vec{C}_{1e}\cdot\vec{U}_{1e}\right) - k_{Cu\bar{1}e}\left(\vec{C}_{\bar{1}e}\cdot\vec{U}_{\bar{1}e}\right) \tag{157}$$

As the Euler equation is defined for the mean flow, the local form uses the following flow velocity distribution coefficients

$$k_{Cu1e} = \frac{\int_{A_1}\left(\vec{C}\cdot\vec{U}\right)\vec{C}\cdot\vec{n}dA}{Q_t\left(\vec{C}_{1e}\cdot\vec{U}_{1e}\right)} \quad \text{and} \quad k_{Cu\bar{1}e} = \frac{\int_{A_{\bar{1}}}\left(\vec{C}\cdot\vec{U}\right)\vec{C}\cdot\vec{n}dA}{Q_t\left(\vec{C}_{\bar{1}e}\cdot\vec{U}_{\bar{1}e}\right)} \tag{158}$$

to take into account the influence of the spatial velocity distribution.

In a same way, flow velocity distribution coefficients for the meridional components can define as well:

$$k_{Cm1e} \times Cm_{1e} = \frac{Q_t}{A_1} \quad \text{and} \quad k_{Cm\bar{1}e} \times Cm_{\bar{1}e} = \frac{Q_t}{A_{\bar{1}}} \tag{159}$$

Reference Case

A reference case can be defined by assuming that *i)* at the turbine runner inlet, both distributions of tangential and meridional components of the flow velocity are uniform and *ii)* at the runner outlet the distribution of meridional component of the flow velocity is uniform and that tangential component distribution is corresponding to a solid body rotation of the flow.

At the inlet the assumption of uniform flow distributions yields for the tangential component

$$k_{Cu1e} = \frac{\int_{A_1}\left(\vec{C}\cdot\vec{U}\right)\vec{C}\cdot\vec{n}\,dA}{Q_t\left(\vec{C}_{1e}\cdot\vec{U}_{1e}\right)} = \frac{\left(\vec{C}_{1e}\cdot\vec{U}_{1e}\right)\overbrace{\int_{A_1}\vec{C}\cdot\vec{n}\,dA}^{Q_t}}{Q_t\left(\vec{C}_{1e}\cdot\vec{U}_{1e}\right)}$$

Therefore, the condition for an uniform distribution of Cu_{1e}, the turbine runner inlet tangential component is:

$$k_{Cu1e} = 1$$

and for the meridional component

$$k_{Cm1e} = \frac{-\int_{A_1} \vec{C} \cdot \vec{n}\, dA}{A_1 Cm_{1e}} = \frac{Q_t}{A_1 Cm_{1e}}$$

which yields

$$k_{Cm1e} = 1 .$$

At the outlet assuming an uniform flow distribution of velocity meridional component and, for the tangential component, a solid body rotation of the flow, *i.e.* the tangential velocity Cu being a linear function of the radius R like the rotation velocity U, the following relations read

$$Cm_{\bar{1}e} = \frac{Q_t}{A_{\bar{1}}} , \quad \frac{Cu}{Cu_{\bar{1}e}} = \frac{R}{R_{\bar{1}e}} \quad \text{and} \quad \frac{U}{U_{\bar{1}e}} = \frac{R}{R_{\bar{1}e}}$$

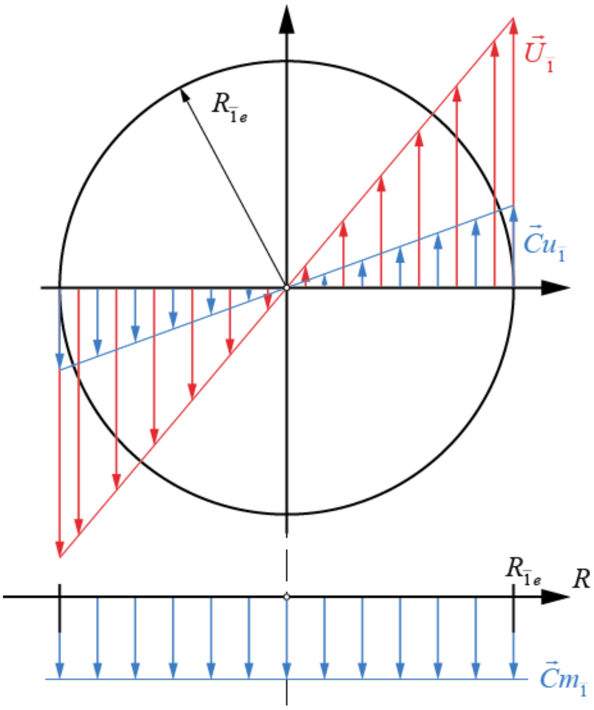

Figure 36 – Velocity components profile at the outlet of the discharge cone

Therefore, the distribution coefficient is computed as

$$k_{Cu\bar{1}e} = \frac{\int_{A_{\bar{1}}} \left(\vec{C} \cdot \vec{U}\right) \cdot \vec{C} \cdot \vec{n} dA}{Q_t \left(\vec{C}_{\bar{1}e} \cdot \vec{U}_{\bar{1}e}\right)} = \frac{Cm_{\bar{1}e}}{Q_t} \frac{1}{R^2_{\bar{1}e}} \int_{A_{\bar{1}}} R^2 dA = \frac{Cm_{\bar{1}e}}{Q_t} \frac{1}{R^2_{\bar{1}e}} \int_0^{R_{\bar{1}e}} 2\pi R^3 dR$$

$$= 2\pi \frac{Cm_{\bar{1}e}}{Q_t} \frac{1}{R^2_{\bar{1}e}} \frac{R^4_{\bar{1}e}}{4} = \frac{\pi R^2_{\bar{1}e} Cm_{\bar{1}e}}{Q_t} \times \frac{1}{2}$$

Which yields

$$k_{Cu\bar{1}e} = \frac{1}{2} \text{ and } k_{Cm\bar{1}e} = 1$$

2 HYDRAULIC CHARACTERISTICS

2.1 Turbine Mode

Euler equation

In this section, an analysis of the specific energy transfer through the runner is performed by neglecting the fluxes of Reynolds and viscous stresses between 1 and $\bar{1}$ runner fluid sections. Therefore

$$E_t = k_{Cu1e} \times U_{1e} Cu_{1e} - k_{Cu\bar{1}e} \times U_{\bar{1}e} Cu_{\bar{1}e} \tag{160}$$

Examples of velocity diagrams for different specific speed and for the best efficiency operating condition (assuming $Cu_{\bar{1}e} = 0$ at BEP) are provided in Figure 37.

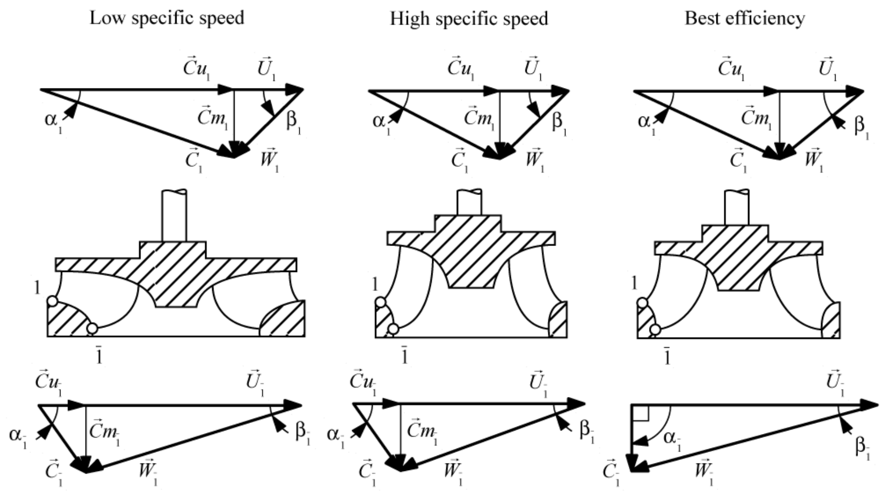

Figure 37 - Velocity diagrams at turbine inlet and outlet, for different operating points

From the velocity diagram, the tangential component of absolute flow velocity Cu depends on the meridional component Cm, absolute flow angle α_1 and relative flow angle $\beta_{\bar{1}}$, which is related to the blade angle at runner outlet.

Therefore, the following relations stands

$$Cu_{1e} = \frac{Cm_{1e}}{\tan \alpha_{1e}} \quad \text{and} \quad Cu_{\bar{1}e} = U_{\bar{1}e} - \frac{Cm_{\bar{1}e}}{\tan \beta_{\bar{1}e}} \tag{161}$$

Moreover, the absolute velocity meridional component can also be expressed as a function of the runner discharge Q_t and distribution coefficient k_{Cm}.

$$Cm_{1e} = \frac{Q_t}{k_{Cm1e} \cdot A_1} \quad \text{and} \quad Cm_{\bar{1}e} = \frac{Q_t}{k_{Cm\bar{1}e} \cdot A_{\bar{1}}} \tag{162}$$

Therefore, the specific energy transferred in the runner depends only on the absolute flow angle, blade angle at runner outlet, the discharge and the rotational speed (because $U_{\bar{1}e} = \omega \cdot R_{\bar{1}e}$).

Indeed substituting (161) and (162) into (160) yields

$$
\begin{aligned}
E_t &= k_{Cu1e} \times U_{1e} \times \frac{Cm_{1e}}{\tan\alpha_{1e}} - k_{Cu\bar{1}e} \times U_{\bar{1}e}\left(U_{\bar{1}e} - \frac{Cm_{\bar{1}e}}{\tan\beta_{\bar{1}e}}\right) \\
&= k_{Cu1e} \times U_{1e} \times \frac{1}{\tan\alpha_{1e}} \times \frac{Q_t}{k_{Cm1e}A_1} - k_{Cu\bar{1}e} \times U_{\bar{1}e}\left(U_{\bar{1}e} - \frac{1}{\tan\beta_{\bar{1}e}} \times \frac{Q_t}{k_{Cm\bar{1}e}A_{\bar{1}}}\right)
\end{aligned} \tag{163}
$$

To finally obtain the relation

$$
E_t = -k_{Cu\bar{1}e} \times U_{\bar{1}e}^{\ 2} + k_{Cu\bar{1}e}\left[\frac{k_{Cu1e}}{k_{Cu\bar{1}e}}\frac{k_{Cm\bar{1}e}}{k_{Cm1e}}\frac{R_{1e}}{R_{\bar{1}e}}\frac{A_{\bar{1}}}{A_1}\frac{1}{\tan\alpha_{1e}} + \frac{1}{\tan\beta_{\bar{1}e}}\right] \times U_{\bar{1}e} \times \frac{Q_t}{k_{Cm\bar{1}e}\cdot A_{\bar{1}}} \tag{164}
$$

To ease the use of the above equation (164), the following runner dimensionless geometrical parameters are introduced

$$
r_{1e} = \frac{R_{1e}}{R_{\bar{1}e}} \text{ and } a_1 = \frac{A_1}{A_{\bar{1}}} \tag{165}
$$

Therefore (164) yields simply

$$
E_t = -k_{Cu\bar{1}e} \times U_{\bar{1}e}^{\ 2} + \left[\frac{k_{Cu1e}}{k_{Cu\bar{1}e}}\frac{k_{Cm\bar{1}e}}{k_{Cm1e}} \times \frac{r_{1e}}{a_1} \times \frac{1}{\tan\alpha_{1e}} + \frac{1}{\tan\beta_{\bar{1}e}}\right] \times U_{\bar{1}e} \times \frac{Q_t}{k_{Cm\bar{1}e}\cdot A_{\bar{1}}} \tag{166}
$$

E_t, the specific energy transferred to the runner is a linear law of Q_t, the discharge traversing the runner blades passage and a quadratic law of $U_{\bar{1}e}$ the runner speed.

$$
E_t \geq 0 \ \text{ for } \frac{Q_t}{U_{\bar{1}e}\cdot A_{\bar{1}\,t}} \geq \frac{k_{Cm\bar{1}e}k_{Cu\bar{1}e}}{\frac{k_{Cu1e}}{k_{Cu\bar{1}e}}\frac{k_{Cm\bar{1}e}}{k_{Cm1e}} \times \frac{r_{1e}}{a_1} \times \frac{1}{\tan\alpha_{1e}} + \frac{1}{\tan\beta_{\bar{1}e}}}
$$

$$
E_{t\max} = \ \text{ for } \frac{Q_t}{U_{\bar{1}e}\cdot A_{\bar{1}\,t}} \geq \frac{k_{Cm\bar{1}e}k_{Cu\bar{1}e}}{\frac{k_{Cu1e}}{k_{Cu\bar{1}e}}\frac{k_{Cm\bar{1}e}}{k_{Cm1e}} \times \frac{r_{1e}}{a_1} \times \frac{1}{\tan\alpha_{1e}} + \frac{1}{\tan\beta_{\bar{1}e}}}
$$

And is positive for The specific en

Or by introducing both the discharge and specific energy coefficients, respectively

$$
\varphi_{t\bar{1}} = \frac{Q_t}{A_{\bar{1}}U_{\bar{1}e}} \text{ and } \psi_{t\bar{1}} = \frac{2E_t}{U_{\bar{1}e}^{\ 2}} \tag{167}
$$

The following non dimensional form is obtained

$$
\psi_t = -2k_{Cu\bar{1}e} + \left[\frac{k_{Cu1e}}{k_{Cu\bar{1}e}} \times \frac{k_{Cm\bar{1}e}}{k_{Cm1e}} \times \frac{r_{1e}}{a_1} \times \frac{1}{\tan\alpha_{1e}} + \frac{1}{\tan\beta_{\bar{1}e}}\right] \times \frac{\varphi_{t\bar{1}}}{k_{Cm\bar{1}e}} \tag{168}
$$

or

$$
E_t = \left\{-1 + \left[\frac{k_{Cu1e}}{k_{Cu\bar{1}e}} \times \frac{k_{Cm\bar{1}e}}{k_{Cm1e}} \times \frac{r_{1e}}{a_1} \times \frac{1}{\tan\alpha_{1e}} + \frac{1}{\tan\beta_{\bar{1}e}}\right] \times \frac{Q_t}{k_{Cm\bar{1}e}\cdot A_{\bar{1}}} \times \frac{1}{U_{\bar{1}e}}\right\} \times k_{Cu\bar{1}e} \times U_{\bar{1}e}^{\ 2} \tag{169}
$$

Or as a function of $Cm_{\bar{1}e}$ the meridional component of the absolute flow velocity at $\bar{1}e$ point

$$
E_t = \left\{-1 + \left[\frac{k_{Cu1e}}{k_{Cu\bar{1}e}} \times \frac{k_{Cm\bar{1}e}}{k_{Cm1e}} \times \frac{r_{1e}}{a_1} \times \frac{1}{\tan\alpha_{1e}} + \frac{1}{\tan\beta_{\bar{1}e}}\right] \times \frac{Cm_{\bar{1}e}}{U_{\bar{1}e}}\right\} \times k_{Cu\bar{1}e} \times U_{\bar{1}e}^{\ 2} \tag{170}
$$

$$
\begin{aligned}
E_t &= -k_{Cu\bar{1}e} \times U_{\bar{1}e}^{\ 2} + \left[\frac{k_{Cu1e}}{k_{Cm1e}} \frac{r_{1e}}{a_1} \frac{1}{\tan \alpha_{1e}} + \frac{k_{Cu\bar{1}e}}{k_{Cm\bar{1}e}} \frac{1}{\tan \beta_{\bar{1}e}} \right] \times U_{\bar{1}e} \times k_{Cm\bar{1}e} \times Cm_{\bar{1}e} \\
E_t &= \left\{ -U_{\bar{1}e} + \left[\frac{k_{Cm\bar{1}e}}{k_{Cm1e}} \times \frac{A_{\bar{1}}}{A_1} \times \frac{k_{Cu1e}}{k_{Cu\bar{1}e}} \times \frac{R_{1e}}{R_{\bar{1}e}} \times \frac{1}{\operatorname{tg} \alpha_{1e}} + \frac{1}{\operatorname{tg} \beta_{\bar{1}e}} \right] Cm_{\bar{1}e} \right\} \times k_{Cu\bar{1}e} U_{\bar{1}e} \\
U_{\bar{1}e}^{\max} &= \frac{1}{2} \left[\frac{k_{Cm\bar{1}e}}{k_{Cm1e}} \times \frac{A_{\bar{1}}}{A_1} \times \frac{k_{Cu1e}}{k_{Cu\bar{1}e}} \times \frac{R_{1e}}{R_{\bar{1}e}} \times \frac{1}{\operatorname{tg} \alpha_{1e}} + \frac{1}{\operatorname{tg} \beta_{\bar{1}e}} \right] Cm_{\bar{1}e} \\
&= \frac{Cm_{\bar{1}e}}{\varphi_t^{\max}} \\
E_t^{\max} &= \left\{ -U_{\bar{1}e}^{\max} + 2U_{\bar{1}e}^{\max} \right\} \times k_{Cu\bar{1}e} U_{\bar{1}e}^{\max} \\
E_t^{\max} &= k_{Cu\bar{1}e} U_{\bar{1}e}^{\max 2} \\
U_{\bar{1}e} &= U_{\bar{1}e}^{\max} = \sqrt{\frac{E_t^{\max}}{k_{Cu\bar{1}e}}} = Cste \\
\psi_t &= -2 \times k_{Cu_{\bar{1}e}} + 2 \times k_{Cu_{\bar{1}e}} \left[\frac{k_{Cm_{\bar{1}e}}}{k_{Cm_{1e}}} \times \frac{A_{\bar{1}}}{A_1} \times \frac{k_{Cu_{1e}}}{k_{Cu_{\bar{1}e}}} \times \frac{R_{1e}}{R_{\bar{1}e}} \times \frac{1}{\operatorname{tg} \alpha_{1e}} + \frac{1}{\operatorname{tg} \beta_{\bar{1}e}} \right] \varphi_t \\
\psi_t &= -2 \times k_{Cu_{\bar{1}e}} \left(-1 + 2 \times \frac{\varphi_t}{\varphi_t^{\max}} \right)
\end{aligned}
\tag{171}
$$

Deviation factors to the reference case

The flow distribution factors can be expressed as deviation from the aforementioned reference case, where, at <u>the inlet section</u> of the turbine runner A_1, both meridional and tangential components are considered as uniform distribution and, at the outlet section $A_{\bar{1}}$, are considered uniform and corresponding to a solid body rotation for the meridional and the tangential components, respectively. Therefore flow distribution factors can be written as function of deviation factors c_u, $c_{\bar{u}}$, c_m and $c_{\bar{m}}$

$$
\begin{aligned}
k_{Cu1e} &= 1 + c_u \\
k_{Cu\bar{1}e} &= \frac{1}{2} \times \left(1 + c_{\bar{u}}\right) \\
k_{Cm1e} &= 1 + c_m \\
k_{Cm\bar{1}e} &= 1 + c_{\bar{m}}
\end{aligned}
\quad \text{or} \quad
\begin{aligned}
c_u &= k_{Cu1e} - 1 \\
c_{\bar{u}} &= 2k_{Cu\bar{1}e} - 1 \\
c_m &= k_{Cm1e} - 1 \\
c_{\bar{m}} &= k_{Cm\bar{1}e} - 1
\end{aligned}
\tag{172}
$$

Therefore, for the reference case of uniform flow distribution for both meridional and tangential components at the inlet section of the turbine runner A_1, definitions (172) yield $c_m = c_u = 0$ and for the outlet section $A_{\bar{1}}$, corresponding to an uniform flow distribution and a solid body rotation for the meridional and the tangential components, respectively, definitions (172) yield $c_{\bar{m}} = c_{\bar{u}} = 0$ as well.

However, for a general case, equation (164) simply reads

$$
E_t = -\frac{1 + c_{\bar{u}}}{2} \times U_{\bar{1}e}^{\ 2} + \left(\frac{1 + c_u}{1 + c_m} \times \frac{r_{1e}}{a_1} \times \frac{1}{\tan \alpha_{1e}} + \frac{1}{2} \times \frac{1 + c_{\bar{u}}}{1 + c_{\bar{m}}} \times \frac{1}{\tan \beta_{\bar{1}e}} \right) \times \left(1 + c_{\bar{m}}\right) \times Cm_{\bar{1}e} \times U_{\bar{1}e}
$$

and with $U_{\bar{1}e}$ in common factor

$$E_t = \left\{ -U_{\bar{1}e} + 2\left(\frac{1+c_u}{1+c_{\bar{u}}} \times \frac{1+c_{\bar{m}}}{1+c_m} \frac{r_{1e}}{a_1} \times \frac{1}{\tan\alpha_{1e}} + \frac{1}{2} \times \frac{1}{\tan\beta_{\bar{1}e}} \right) \times Cm_{\bar{1}e} \right\} \times \frac{1+c_{\bar{u}}}{2} \times U_{\bar{1}e} \quad (173)$$

Or by making apparent the traversing discharge $Q_t = \left(1+c_{\bar{m}}\right) \times Cm_{\bar{1}e} \times A_{\bar{1}}$

$$E_t = \left\{ -U_{\bar{1}e} + 2\left(\frac{1}{1+c_m} \times \frac{1+c_u}{1+c_{\bar{u}}} \times \frac{r_{1e}}{a_1} \times \frac{1}{\tan\alpha_{1e}} + \frac{1}{2} \times \frac{1}{1+c_{\bar{m}}} \times \frac{1}{\tan\beta_{\bar{1}e}} \right) \times \frac{Q_t}{A_{\bar{1}}} \right\} \times \frac{1+c_{\bar{u}}}{2} \times U_{\bar{1}e}$$

(174)

Introducing the same definitions for the flow distribution factors, equation (160) yields

$$E_t = \left(1+c_u\right) \times U_{1e} Cu_{1e} - \frac{1}{2}\left(1+c_{\bar{u}}\right) \times U_{\bar{1}e} Cu_{\bar{1}e} \quad (175)$$

For the reference case ($c_m = c_{\bar{m}} = c_u = c_{\bar{u}} = 0$) equation (173) yields

$$E_t = \left\{ -U_{\bar{1}e} + 2\left(\frac{r_{1e}}{a_1} \times \frac{1}{\tan\alpha_{1e}} + \frac{1}{2} \times \frac{1}{\tan\beta_{\bar{1}e}} \right) \times Cm_{\bar{1}e} \right\} \times \frac{U_{\bar{1}e}}{2} \quad (176)$$

Or as a function of Q_t

$$E_t = \left\{ -U_{\bar{1}e} + 2\left(\frac{r_{1e}}{a_1} \times \frac{1}{\tan\alpha_{1e}} + \frac{1}{2} \times \frac{1}{\tan\beta_{\bar{1}e}} \right) \times \frac{Q_t}{A} \right\} \times \frac{U_{\bar{1}e}}{2} \quad (177)$$

and for equation (175) as well

$$E_t = U_{1e} Cu_{1e} - \frac{1}{2} \times U_{\bar{1}e} Cu_{\bar{1}e} \quad (178)$$

From equations (173) and (174) it can be observed a linear relationship between E_t the specific energy transferred to the runner and either $Cm_{\bar{1}e}$ the meridional component or Q_t the traversing discharge. The transferred specific energy in the runner is plotted in Figure 38 by varying the discharge while the rotational speed is kept constant.

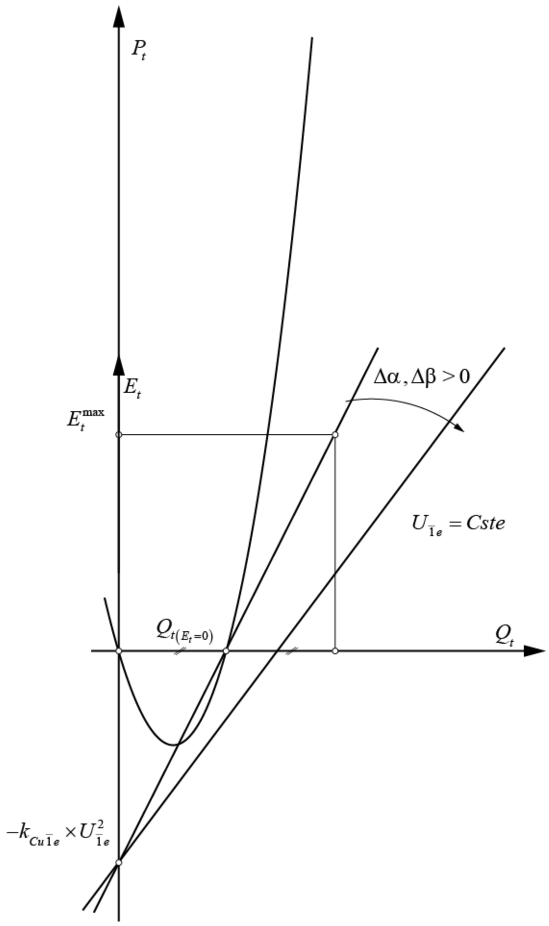

Figure 38 - Hydraulic characteristic of a turbine runner for a constant rotational speed

If either the guide vane or the blades opening values are increasing, corresponding to $\Delta\alpha$ or $\Delta\beta$ increases, the slope of the line $E_t\left(Q_t\right)$ is decreasing.

Moreover, the condition $E_t\left(Q_t\right) \geq 0$ yields

$$\frac{Cm_{\bar{1}e}}{U_{\bar{1}e}} \geq \frac{1}{2} \times \frac{1}{\left(\frac{1+c_u}{1+c_{\bar{u}}} \times \frac{1+c_{\bar{m}}}{1+c_m} \frac{r_{1e}}{a_1} \times \frac{1}{\tan\alpha_{1e}} + \frac{1}{2} \times \frac{1}{\tan\beta_{\bar{1}e}}\right)} \qquad (179)$$

The relation $E_t\left(U_{\bar{1}e}\right)$ while Q_t or $Cm_{\bar{1}e} = Cm_{\bar{1}e}^{\max}$ are kept constant is a parabolic law, see Figure 39, with the following roots:

$$U_{\bar{1}e} = 0 \text{ and } U_{\bar{1}e} = 2\left(\frac{1+c_{\bar{m}}}{1+c_m} \times \frac{1+c_u}{1+c_{\bar{u}}} \times \frac{r_{1e}}{a_1} \times \frac{1}{\tan\alpha_{1e}} + \frac{1}{2} \times \frac{1}{\tan\beta_{\bar{1}e}}\right) \times Cm_{\bar{1}e}^{\max}. \qquad (180)$$

Therefore $E_t\left(U_{\bar{1}e}\right)$ exhibits a maximum value for

$$U_{\bar{1}e}^{\max} = \left(\frac{1+c_{\bar{m}}}{1+c_m} \times \frac{1+c_u}{1+c_{\bar{u}}} \times \frac{r_{1e}}{a_1} \times \frac{1}{\tan\alpha_{1e}} + \frac{1}{2} \times \frac{1}{\tan\beta_{\bar{1}e}}\right) \times Cm_{\bar{1}e}^{\max} \qquad (181)$$

which is corresponding to $Q_t = 2 \times Q_{t(E_t=0)}$, see condition (179).

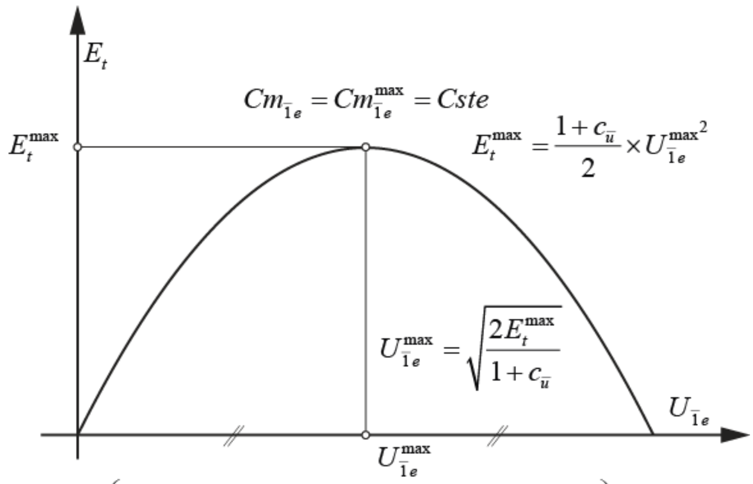

$$U_{\bar{1}e}^{\max} = \left(\frac{1+c_{\bar{m}}}{1+c_m} \times \frac{1+c_u}{1+c_{\bar{u}}} \times \frac{r_{1e}}{a_1} \times \frac{1}{\tan\alpha_{1e}} + \frac{1}{2} \times \frac{1}{\tan\beta_{\bar{1}e}} \right) \times Cm_{\bar{1}e}^{\max}$$

Figure 39 Hydraulic characteristic of a turbine runner for a constant discharge

By making apparent $U_{\bar{1}e}^{\max}$, equation (173) yields

$$E_t = \left\{ -U_{\bar{1}e} + 2U_{\bar{1}e}^{\max} \times \frac{Cm_{\bar{1}e}}{Cm_{\bar{1}e}^{\max}} \right\} \times \frac{1+c_{\bar{u}}}{2} \times U_{\bar{1}e} \tag{182}$$

and the maximum value of E_t reached for $U_{\bar{1}e}^{\max}$ and $Cm_{\bar{1}e}^{\max}$ is

$$E_t^{\max} = \frac{1+c_{\bar{u}}}{2} \times U_{\bar{1}e}^{\max\,2} \tag{183}$$

Which yields

$$U_{\bar{1}e}^{\max} = \sqrt{\frac{2E_t^{\max}}{1+c_{\bar{u}}}} \tag{184}$$

Considering now the rotating speed being kept constant $U_{\bar{1}e} = U_{\bar{1}e}^{\max}$ and substituting the expression (184) in (182) simply yields

$$E_t = E_t^{\max} \left(-1 + 2 \times \frac{Cm_{\bar{1}e}}{Cm_{\bar{1}e}^{\max}} \right) \tag{185}$$

E_t , $Cm_{\bar{1}e}$ linear relationship (185) is reported in Figure 40

Equation (182) can be also cast in dimensionless form

$$\frac{2E_t}{U_{\bar{1}e}^{\max\,2}} = \left(1+c_{\bar{u}}\right) \left\{ -1 + 2 \times \frac{Cm_{\bar{1}e}}{Cm_{\bar{1}e}^{\max}} \right\} \tag{186}$$

Or by introducing $\psi_{t\bar{1}e}$ and $\varphi_{t\bar{1}e}$ the energy and discharge coefficients respectively

$$\psi_{t\bar{1}e} = \frac{2E_t}{U_{\bar{1}e}^2} \quad \text{and} \quad \varphi_{t\bar{1}e} = \frac{Cm_{\bar{1}e}}{U_{\bar{1}e}}$$

Equation (186) simply yields the following dimensionless linear relation between $\psi_{t\bar{1}e}$ and $\varphi_{t\bar{1}e}$

$$\psi_{t\bar{1}e} = \left(1+c_{\bar{u}}\right) \left(-1 + 2 \times \frac{\varphi_{t\bar{1}e}}{\varphi_{t\bar{1}e}^{\max}} \right) \tag{187}$$

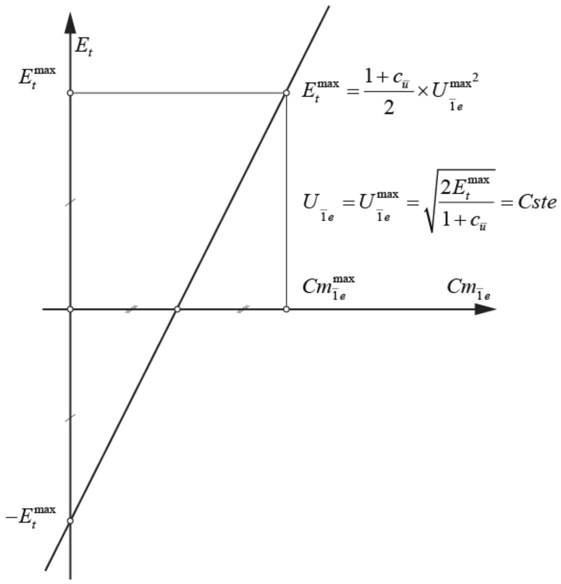

Figure 40 E_t , $Cm_{\bar{1}e}$ *characteristic of a turbine runner at constant rotating speed*

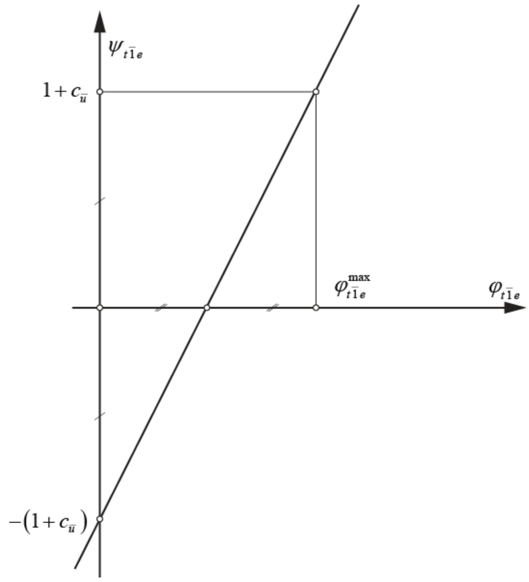

Figure 41 E_t , $Cm_{\bar{1}e}$ *characteristic of a turbine runner at constant rotating speed*

Turbine runner inlet velocity triangles for E_t maximum value

For the operating condition corresponding to the maximum value $E_t^{\max}$ reached for $U_{\bar{1}e}^{0}$ and $Cm_{\bar{1}e}^{0}$ equations (181) and (184) yield the following relation between α_{1e}^{0} the absolute flow velocity angle at the turbine runner inlet and $\beta_{\bar{1}e}$ the relative flow velocity angle at the runner outlet

$$\tan\alpha_{1e}^{\max} = \frac{Cm_{\bar{1}e}^{\max}}{\sqrt{\frac{2E_t^{\max}}{1+c_{\bar{u}}}}} \left(\frac{\frac{1+c_{\bar{m}}}{1+c_m} \times \frac{1+c_u}{1+c_{\bar{u}}} \times \frac{r_{1e}}{a_1}}{1 - \frac{1}{2} \times \frac{1}{\tan\beta_{\bar{1}e}} \times \frac{Cm_{\bar{1}e}^{\max}}{\sqrt{\frac{2E_t^{\max}}{1+c_{\bar{u}}}}}} \right) \tag{188}$$

Therefore, $Cm_{1e}^{\max}$ the flow velocity meridional component at the inlet is given

$$Cm_{1e}^{\max} = \frac{1+c_{\bar{m}}}{1+c_m} \times \frac{1}{a_1} Cm_{\bar{1}e}^{\max} \tag{189}$$

And $Cu_{1e}^{\max}$ the flow velocity tangential component at the inlet is given

$$Cu_{1e}^{\max} = \frac{Cm_{1e}^{\max}}{\tan \alpha_{1e}^{\max}} \tag{190}$$

by substituting (198) and (189), equation (190) yields

$$Cu_{1e}^{\max} = \frac{1}{r_{1e}} \left(1 - \frac{1}{2} \times \frac{1}{\tan \beta_{\bar{1}e}} \times \frac{Cm_{\bar{1}e}^{\max}}{\sqrt{2E_t^{\max}}} \right) \times \frac{1+c_{\bar{m}}}{1+c_m} \times \sqrt{2E_t^{\max}} \tag{191}$$

Finally the rotating velocity is

$$U_{1e}^{\max} = r_{1e} \times U_{\bar{1}e}^{\max} = r_{1e} \times \sqrt{\frac{2E_t^{\max}}{1+c_{\bar{u}}}} \tag{192}$$

For the reference case flow distributions equations (189), (191) and (192) yield

The relative flow velocity angle at the runner inlet is given by the following trigonometric relationship

$$\tan \beta = \frac{Cm}{U_{1e} - Cu} \tag{193}$$

which yields

$$\tan \beta_{1e}^{\max} = \frac{\frac{1+c_{\bar{m}}}{1+c_m} \times \frac{1}{a_1} Cm_{\bar{1}e}^{\max}}{r_{1e} U_{\bar{1}e} -} \tag{194}$$

Or by making apparent $U_{\bar{1}e}^{\max}$ and $Cm_{\bar{1}e}^{\max}$

$$\tan \beta_{1e}^{\max} = \frac{\frac{Cm_{\bar{1}e}^{\max}}{a_1}}{r_1 U_{\bar{1}e}^{\max} - \frac{1}{r_{1e}} \left(1 - \frac{1}{2} \times \frac{1}{\tan \beta_{\bar{1}e}} \times \frac{Cm_{\bar{1}e}^{\max}}{\sqrt{2E_t^{\max}}} \right) \times \frac{1+c_{\bar{m}}}{1+c_m} \times \sqrt{2E_t^{\max}}} \tag{195}$$

By further substituting the expression (184) of $U_{\bar{1}e}^{\max}$, equation (195) yields

$$\tan \beta_{1e}^{\max} = \frac{\frac{1}{r_1 a_1} \frac{Cm_{\bar{1}e}^{\max}}{\sqrt{\frac{2E_t^{\max}}{1+c_{\bar{u}}}}}}{1 - \frac{1}{\tan \alpha_{1e}^{\max}} \frac{1}{r_1 a_1} \frac{Cm_{\bar{1}e}^{\max}}{\sqrt{\frac{2E_t^{\max}}{1+c_{\bar{u}}}}}} \tag{196}$$

For the reference case flow distributions equations (189), (191) and (192) yield

$$U_{1e}^{\max} = r_{1e} \times U_{\bar{1}e}^{\max} = r_{1e} \times \sqrt{2E_t^{\max}} \tag{197}$$

$$\tan \alpha_{1e}^{\max} = \frac{Cm_{\bar{1}e}^{\max}}{\sqrt{2E_t^{\max}}} \left(\frac{\frac{r_{1e}}{a_1}}{1 - \frac{1}{2} \times \frac{1}{\tan \beta_{\bar{1}e}} \times \frac{Cm_{\bar{1}e}^{\max}}{\sqrt{2E_t^{\max}}}} \right) \tag{198}$$

$$Cm_{1e}^{\max} = \frac{Cm_{\bar{1}e}^{\max}}{a_1} \tag{199}$$

$$Cu_{1e}^{\max} = \frac{1}{r_{1e}} \left(1 - \frac{1}{2} \times \frac{1}{\tan \beta_{\bar{1}e}} \times \frac{Cm_{1e}^{\max}}{\sqrt{2E_t^{\max}}} \right) \times \sqrt{2E_t^{\max}} \tag{200}$$

$$\tan \beta_{1e}^{\max} = \frac{\frac{1}{r_1 a_1} \times \frac{Cm_{\bar{1}e}^{\max}}{\sqrt{2E_t^{\max}}}}{1 - \frac{1}{\tan \alpha_{1e}^{\max}} \times \frac{1}{r_1 a_1} \times \frac{Cm_{\bar{1}e}^{\max}}{\sqrt{2E_t^{\max}}}} \tag{201}$$

For $U_{\bar{1}e} = U_{\bar{1}e}^{0}$ and In this section, an analysis of the specific energy evolution through the runner is performed by neglecting the fluxes of Reynolds and viscous stresses between 1 and $\bar{1}$.

$$E_t = k_{Cu1e} \times U_{1e} Cu_{1e} - k_{Cu\bar{1}e} \times U_{\bar{1}e} Cu_{\bar{1}e} \tag{202}$$

Therefore, for a selected traversing discharge the maximum specific energy transfer will be achieved for the rotating speed value given by (181).

For the case $a = \bar{a} = b = \bar{b} = 0$, (182) and (181) are simply written as

$$E_{t\max} = \frac{U_{\bar{1}e}^{\max\ 2}}{2} \text{ for } U_{\bar{1}e}^{\max} = \left[\frac{A_{\bar{1}}}{A_1} \times \frac{R_{1e}}{R_{\bar{1}e}} \times \frac{1}{\tan \alpha_{1e}} + \frac{1}{2} \times \frac{1}{\tan \beta_{\bar{1}e}} \right] \times \frac{Q_t}{A_{\bar{1}}} \tag{203}$$

For axial outlet flow

$$E_{t\max} = \frac{U_{\bar{1}e}^{\max\ 2}}{2} \text{ for } \tan \alpha_{1e} = 2 \times \frac{A_{\bar{1}}}{A_1} \times \frac{R_{1e}}{R_{\bar{1}e}} \times \tan \beta_{\bar{1}e} \tag{204}$$

Relations (182) and (181) or for the case $a = \bar{a} = b = \bar{b} = 0$ relations (203) give the conditions for the absolute flow angle α_{1e} and relative flow angle $\beta_{\bar{1}e}$ to be fulfilled for achieving a maximum specific energy transfer.

In other words, for selecting a turbine runner suited to a given specific energy E and unit discharge Q we should assume a given energy and discharge efficiency values η_e and η_q respectively to evaluate the corresponding E_t and Q_t values by the following relations

$$E_t = \eta_e \times E \text{ and } Q_t = \eta_q \times Q \tag{205}$$

Which impose to select a rotating speed value which fulfills the following relations

$$\eta_e \times E = \frac{1+\bar{a}}{2} \times \left(U_{\bar{1}e}^{\max} \right)^2 \text{ and } \frac{\eta_q \times Q}{A_{\bar{1}}} = 2 \times \frac{U_{\bar{1}e}}{k}$$

Or

$$U_{\bar{1}e}=\sqrt{\frac{2\times\eta_e\times E}{1+\bar{a}}}\quad\text{and}\quad k=\frac{2}{\sqrt{1+\bar{a}}}\times\frac{\sqrt{\eta_e}}{\eta_q}\times\frac{A_{\bar{1}}\sqrt{2E}}{Q}$$

For the condition of maximum transfer we can introduce the energy and discharge coefficients.

$$\psi_t=1+\bar{a}\quad\text{and}\quad \varphi_t=\frac{1+\bar{a}}{\frac{1+a}{1+b}\times\frac{A_{\bar{1}}}{A_1}\times\frac{R_{1e}}{R_{\bar{1}e}}\times\frac{1}{\tan\alpha_{1e}}+\frac{1}{2}\times\frac{1+\bar{a}}{1+\bar{b}}\times\frac{1}{\tan\beta_{\bar{1}e}}}$$

And the specific speed

$$\psi_t=1+\bar{a}\quad\text{and}\quad \nu=\frac{\varphi^{\frac{1}{2}}}{\psi^{\frac{3}{4}}}=\frac{\left(1+\bar{a}\right)^{\frac{1}{2}}}{\left(1+\bar{a}\right)^{\frac{3}{4}}}\times\frac{1}{\left(\frac{1+a}{1+b}\times\frac{A_{\bar{1}}}{A_1}\times\frac{R_{1e}}{R_{\bar{1}e}}\times\frac{1}{\tan\alpha_{1e}}+\frac{1}{2}\times\frac{1+\bar{a}}{1+\bar{b}}\times\frac{1}{\tan\beta_{\bar{1}e}}\right)^{\frac{1}{2}}}$$

Which yields

$$\nu^2=\frac{1}{\left(1+\bar{a}\right)^{\frac{1}{2}}}\times\frac{1}{\frac{1+a}{1+b}\times\frac{A_{\bar{1}}}{A_1}\times\frac{R_{1e}}{R_{\bar{1}e}}\times\frac{1}{\tan\alpha_{1e}}+\frac{1}{2}\times\frac{1+\bar{a}}{1+\bar{b}}\times\frac{1}{\tan\beta_{\bar{1}e}}}$$

Or

$$\frac{1+a}{1+b}\times\frac{A_{\bar{1}}}{A_1}\times\frac{R_{1e}}{R_{\bar{1}e}}\times\frac{1}{\tan\alpha_{1e}}=\frac{1}{\left(1+\bar{a}\right)^{\frac{1}{2}}\times\nu^2}-\frac{1}{2}\times\frac{1+\bar{a}}{1+\bar{b}}\times\frac{1}{\tan\beta_{\bar{1}e}}$$

For the case $a=\bar{a}=b=\bar{b}=0$ we simply get

$$\frac{A_{\bar{1}}}{A_1}\times\frac{R_{1e}}{R_{\bar{1}e}}\times\frac{1}{\tan\alpha_{1e}}=\frac{1}{\nu^2}-\frac{1}{2}\times\frac{1}{\tan\beta_{\bar{1}e}}$$

Or

$$1\times\frac{A_{\bar{1}}}{A_1}\times\frac{R_{1e}}{R_{\bar{1}e}}\times\frac{1}{\tan\alpha_{1e}}=\frac{1}{\nu^2}-\frac{1}{2}\times\frac{1}{\tan\beta_{\bar{1}e}}$$

$$P_t=\rho\cdot Q_t\cdot E_t=E_t=-\rho Q_t\cdot\left(1+a\right)\cdot\frac{U_{\bar{1}e}{}^2}{2}\ +\left[\frac{R_{1e}}{R_{\bar{1}e}}\frac{1+b}{\tan\alpha_{1e}}+\frac{1+c}{\tan\beta_{\bar{1}e}}\right]\frac{\rho Q_t^2\cdot U_{\bar{1}e}}{A_{\bar{1}}}$$

Therefore, the driving torque acting on the shaft is given by

$$T_t=\frac{P_t}{\omega}=-\rho\cdot Q_t\cdot\left(1+a\right)\omega\cdot R_{\bar{1}}{}^2\ +\left[\frac{R_1}{R_{\bar{1}}}\frac{1+b}{\tan\alpha_1}+\frac{1+c}{\tan\beta_{\bar{1}}}\right]\frac{\rho\cdot Q^2{}_t\cdot R_{\bar{1}}}{A_{\bar{1}}}$$

As the evolutions of power and torque depend on both rotational speed and discharge, these formulas are given on Figure 42 for both a constant rotational speed and for a constant discharge.

For a given rotational speed, the machine needs a discharge greater than Q_0 in order to generate power.

For a given discharge, the machine produces a maximum power for an optimal rotational speed

$$\omega_{opt}=\frac{1}{2}\left(\frac{R_{1e}}{R_{\bar{1}e}}\frac{A_{\bar{1}}}{A_1}\frac{1}{\tan\alpha_{1e}}+\frac{1}{\tan\beta_{\bar{1}e}}\right)\frac{Q_t}{A_{\bar{1}}\cdot R_{\bar{1}}}$$

Therefore, the value of maximum power and energy read:

$$P_{t,\max} = \rho \cdot Q_t \cdot U_{\bar{1}}^{\,2} \quad \text{and so} \quad E_{t,\max} = U_{\bar{1}}^{\,2}$$

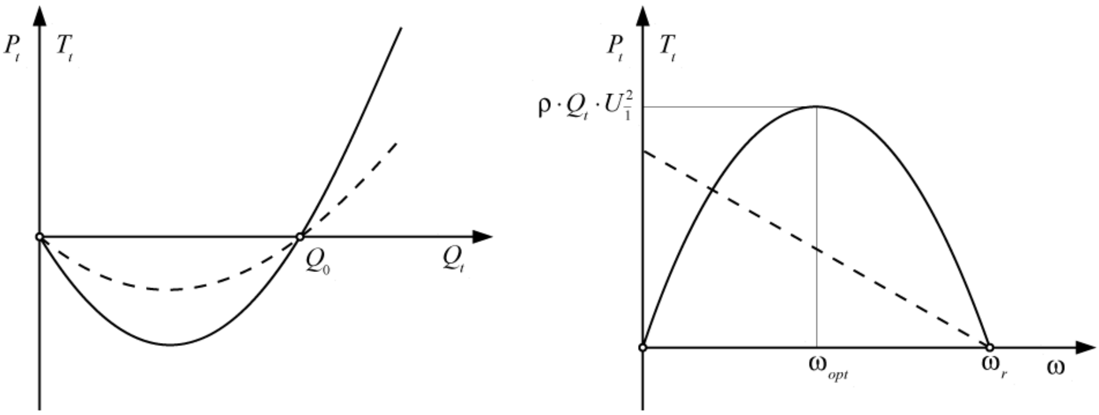

Figure 42 - Evolutions of transferred power (filled) and torque (dashed) in a turbine runner for a given rotational speed (left) and discharge (right)

From the torque formula, the runaway speed reads

$$\omega_r = \left(\frac{R_1}{R_{\bar{1}}} \frac{A_{\bar{1}}}{A_1} \frac{1}{\tan \alpha_1} + \frac{1}{\tan \beta_{\bar{1}}} \right) \frac{Q_t}{A_{\bar{1}} \cdot R_{\bar{1}}}$$

2.2 Pump Mode

In this section, a uniform distribution of velocities at pump outlet and an axial flow at the pump inlet are assumed

$$k_{Cu} = 0, \quad k_{Cm} = 0, \quad \alpha_{\bar{1}} = \frac{\pi}{2} \quad \text{and} \quad Cu_{\bar{1}} = 0 \quad \text{so} \quad E_t = Cu_1 \cdot U_1$$

The Figure 43 provides examples of velocity triangle for different specific speed and for the maximum power operating condition.

From the velocity triangle, the tangential component of absolute velocity Cu depends on the meridional component Cm and relative flow angle β_1, which is related to the blade angle at runner outlet.

$$Cu_1 = U_1 - \frac{Cm_1}{\tan \beta_1}$$

Moreover, the meridional component of absolute velocity can also be expressed as a function of the impeller discharge Q_t, which is defined negative in pump mode.

$$Cm_1 = -\frac{Q_t}{A_1}$$

Therefore, the transferred specific energy in the impeller depends only on the blade angle at outlet, discharge and rotational speed (because $U_1 = -\omega \cdot R_1$ with $\omega < 0$ in pump mode).

$$E_t = U_1^{\,2} + \frac{1}{\tan \beta_1} \frac{Q_t \cdot U_1}{A_1}$$

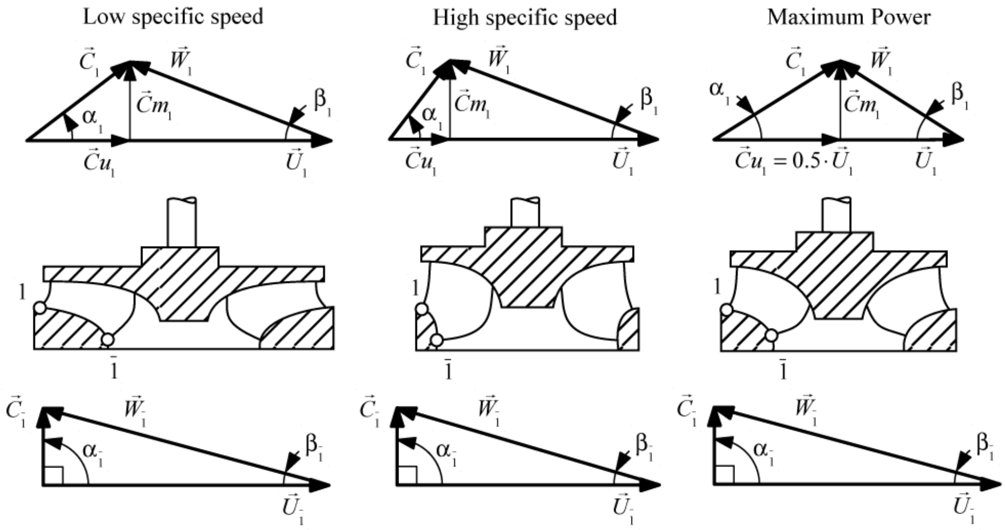

Figure 43 - Velocity triangles at pump inlet and outlet, for different operating points

The evolution of transferred specific energy in the impeller is given in Figure 44 for a constant rotational speed.

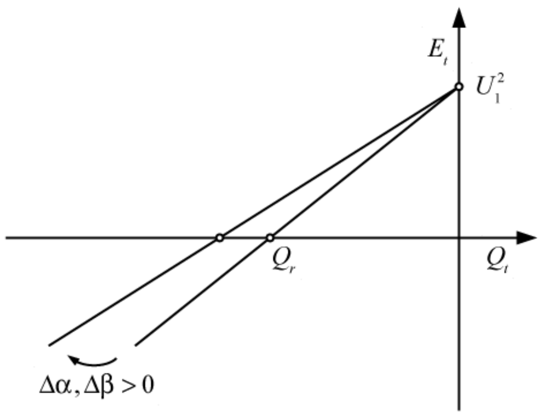

Figure 44 - Hydraulic characteristic of a pump impeller for a given rotational speed

The transferred power formula is deduced from the specific energy

$$P_t = \rho \cdot Q_t \cdot E_t = \rho \cdot Q_t \cdot U_1^2 \ + \frac{1}{\tan\beta_1} \frac{\rho \cdot Q_t^2 \cdot U_1}{A_1}$$

Therefore, the torque on the shaft is given by

$$T_t = \frac{P_t}{\omega} = \rho \cdot Q_t \cdot \omega \cdot R_1^2 \ + \frac{1}{\tan\beta_1} \frac{\rho \cdot Q_t^2 \cdot R_1}{A_1}$$

As the evolutions of power and torque depend on both rotational speed and discharge, these formulas are given on Figure 45 for a constant rotational speed and for a constant discharge.

For a given discharge, the machine needs a rotational speed greater than ω_0 in order to store energy.

For a given rotational speed, the machine store a maximum power for an optimal discharge

$$Q_{opt} = \frac{1}{2} \cdot U_1 \cdot A_1 \cdot \tan\beta_1$$

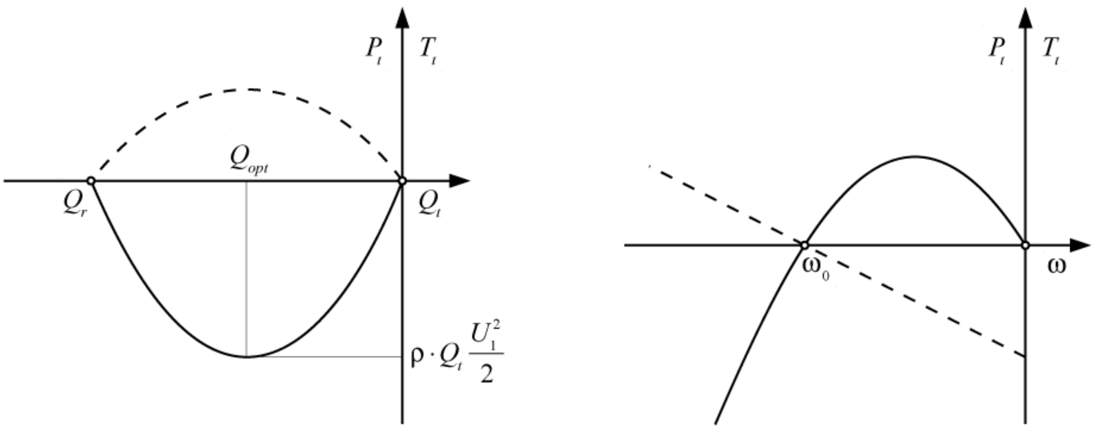

Figure 45 - Evolutions of transferred power (filled) and torque (dashed) in a pump impeller for a given rotational speed (left) and discharge (right)

Therefore, the value of maximum power and energy read

$$P_{t,\max} = \rho \cdot Q_t \cdot \frac{U_1^{\,2}}{2} \quad \text{and so} \quad E_{t,\max} = \frac{U_1^{\,2}}{2}$$

From the torque formula, the runaway discharge is deduced as

$$Q_r = U_1 \cdot A_1 \cdot \tan \beta_1$$

VII REFERENCES

[1] R.L. Panton, *"Incompressible Flow"*, Wiley Interscience, 4th Edition, 2013.

[2] H. Tennekes and J. Lumley, "*A First Course in Turbulence"*, the MIT Press, 1972.

[3] L. F. Moody, *"Friction Factors for Pipe Flow"*, ASME Transactions, vol. 66, pp. 671–684, 1944.

[4] ASME, The Guide to Hydropower Mechanical Design, H. P. Books, 1996.

[5] BOHL, W., *Stromungsmaschinen 1*, Vogel, 1988.

[6] BOHL, W., *Stromungsmaschinen 2*, Vogel, 1988.

[7] BRENNEN, C., *Hydrodynamics of pumps*, Concepts ETI, 1994.

[8] CEI, Norme internationale: turbines hydrauliques, pompes d'accumulation et pompes-turbines. Essais de reception sur modele, CEI, 1999.

[9] COMOLET, R., Mécanique expérimentale des fluides : Tome 2, Dynamique des fluides réels, turbomachines, Paris : Masson, 1994.

[10] FRANC, J.-P., AVELLAN, F., *La cavitation : mécanismes physiques et aspects industriels*, Presses universitaires de Grenoble PUG, 1995.

[11] GULICH, J., Kreiselpumpen : Handbuch fur Entwicklung, Anlagenplanung und Betrieb, Springer, 2003.

[12] HENRY, P., Turbomachines hydrauliques : choix illustré de réalisations marquantes, Presses polytechniques et universitaires romandes, 1992.

[13] HOLZENBERGER, K. and JUNG, K., Centrifugal Pump Lexicon - Updated 3rd edition, KSB, 1990.

[14] PFLEIDERER, C. and PETERMANN H., Strömung Maschinen, Springer-Verlag Berlin and Heidelberg GmbH & Co. K, 7 unveränderte Auflage, 2004.

[15] RAABE, J., Hydraulische Maschinen und Anlagen, VDI Verlag, 1989.

[16] RAABE, J., *Hydropower*, VDI Verlag, 1985.

[17] SEDILLE, M., Turbomachines hydrauliques et thermiques, Masson, 1967,

[18] SIEKMANN, H., Strömungslehre für den Maschinenbau : Technik und Beispiele, Springer, 2002.

[19] SIEKMANN, H., *Strömungslehre: Grundlagen*, Springer, 2000.

[20] STEPANOFF, A., Pompes centrifuges et pompes hélices, Dunod, 1961.

[21] SULZER, *Sulzer centrifugal pump handbook*, Elsevier Advanced Technology, 1998.

[22] TURTON, R., *Principles of turbomachinery*, E. & F. N. Spon, 1984.

[23] VIVIER, L., Turbines hydrauliques et leur régulation, Albin Michel, 1966.

Aris, R., 1989. Vectors, tensors, and the basic equations of fluid mechanics, Dover ed. ed, Dover books on engineering. Dover Publications, New York.

Bureau International des Poids et Mesures (Ed.), 2006. Le système international d'unités (SI) =: The international system of units (SI), 8. éd. ed. BIPM, Sèvres.

Charle Pusterle, 1991. Analyse vectorielle des champs: méthodes pour la physique, Enseignement de la physique. Masson, Paris [etc.

Churchill, S.W., 1977. Friction-Factor Equation Spans All Fluid-Flow Regimes. Chem. Eng. N. Y. 84, 91–92.

Comolet, R., 1994. Mécanique expérimentale des fluides - T. 2 Dynamique des fluides réels. Turbomachines. Masson.

IEC, 1999. Hydraulic turbines, storage pumps and pump-turbines - model acceptance tests, 2. éd. ed, Norme internationale / Commission Electrotechnique Internationale. IEC, Geneva.

Idel'cik, I.E., 1999. Memento des Pertes de Charge. Direction des Etudes et Recherches d'Electricité.

Miller, D.S., 1978. Internal flow systems, BHRA fluid engineering series. BHRA Fluid Engineering, Cranfield, Bedfordshire?

Moody, L.F., 1944. Friction Factors for Pipe Flow. ASME Trans. 671–684.

Panton, R.L., 2013. Incompressible flow, Fourth edition. ed. Wiley, Hoboken, New Jersey.

Pont-à-Mousson, 1989. Formulaire. Technique et documentation Lavoisier.

Prandtl, L., 1933. Recent results of turbulence research (Technical Memorandum No. 720). National Advisory Committee for Aeronautics, Washington.

Schlichting, H., Gersten, K., 2000. Boundary-layer theory, 8th rev. and enl. ed. ed. Springer, Berlin ; New York.

Tennekes, H., Lumley, J.L., 1972. A First Course in Turbulence. MIT Press.

Thompson, A., Taylor, B.N., 2008. Guide for the Use of the International System of Units (SI) NIST Special Pubilcation 811. National Institute of Standards and Technology.

White, F.M., 2009. Fluid mechanics. McGraw-Hill, New York, NY.